Journal of Research of the National Bureau of Standards Vol. 48, No. 5, May 1952 Research Paper 2322

Influence of Temperature and Moisture on the Electrical Properties of Leather

Charles E. Weir

Apparent, or bulk, dielectric constants and power factors of chrome and vegetable leather and untanned hide are reported for moisture contents up to 30 percent, at temperatures of 23° C, 0° C, and −70° C over the frequency range 0.75 to 96 kilocycles. Dielectric constants of fibers determined on dry material at 3 kilocycles and 22° C are: chrome 5.4; vegetable 6.4; and kangaroo tendon 5.1. Apparent direct-current resistivity decreases from values $>10^{16}$ ohm-cm when dry to values $<10^{9}$ ohm-cm at 30-percent moisture. Apparent dielectric constant decreases with frequency and temperature at all moisture contents, the frequency dependence increasing with moisture content. Apparent power factors generally exhibit similar behavior. At −70° C at high moisture contents, a diffuse absorption maximum observed may be due to ice or to permanent dipoles of collagen which are freed by moisture. Observed behavior is interpreted as probably arising from a combination of interfacial polarization at surfaces existing in the fibrous leather and dipolar polarization. Results indicate electrical measurements in this frequency range are probably not reliable for precise quantitative moisture analyses.

1. Introduction

Adsorption of moisture by hygroscopic materials generally causes a marked change in the electrical properties (conductivity, dielectric constant, and power factor) of such substances. This effect is generally attributed to the high dielectric constant and conductivity of the adsorbed moisture as compared to the much lower values exhibited by the dry adsorbate. In view of the large electrical effects produced by the moisture and the rapidity, relative simplicity, and nondestructive nature of electrical measurements, such determinations have been proposed as methods for quantitative moisture determinations [3, 14, 41].[1] Unfortunately, the materials of particular interest in this connection are usually powders or fibrous materials that possess large adsorption surface areas and, therefore, the results of electrical measurements are not easily interpreted because of the complex physical structure of the specimens. Recently, interest has arisen in application of dielectric measurements for the determination of moisture in leather [27].

This report describes the results of critical studies of the effects of moisture and temperature on the dielectric constant and power factor of leather in the audio and low intermediate frequency range.

In most measurements dealing with a porous material such as leather, two experimental values are recognized, a "real" value associated with the fibers alone, and an "apparent" value that refers to the bulk material including the air in the interstices. To avoid confusion between the former and the real part of the complex dielectric constant, the term "fiber dielectric constant" will be used instead. Apparent values as used are understood to refer to the bulk material.

[1] Figures in brackets indicate the literature references at the end of this paper.

2. Experimental Method

2.1. Electric Apparatus

Measurements of capacitance and resistance were obtained with a shielded resistance-capacitance bridge containing a Wagner-earthing circuit. The bridge is shown schematically in figure 1. A detailed discussion of this bridge has been published previously [29]. High-stability input signals in the frequency range 0.75 to 96 kc were provided by a variable frequency oscillator. Bridge balance was ascertained through direct use of earphones at all frequencies as high as 12 kc, while at higher frequencies a regenerative, all-wave receiver was used to detect and amplify the output signals.

Fiber dielectric constants were determined by the immersion method [42, 45] in a completely shielded, cylindrical, guard-ring condenser. This condenser was constructed of heavy brass, and all surfaces were given a fine machine finish. The guard was located near the top of the condenser below an opening fitted with a reservoir that was used as an overflow. A second opening at the bottom of the condenser was fitted to permit introduction of liquids and suspensions. The capacitance of the empty condenser was 40.22 $\mu\mu$f, a value that was reproducible to within ± 0.01 $\mu\mu$f.

All measurements with this condenser were carried out at 22.2° C at a frequency of 3 kc in the following manner: The condenser was filled with a suitable solution of ethylene dichloride in benzene. Choice of these liquids resulted from previous studies [26] indicating negligible interaction between leather and liquid. The solution was then circulated through the condenser by using the two openings until a stable and reproducible value of capacitance was obtained. Upon attainment of equilib-

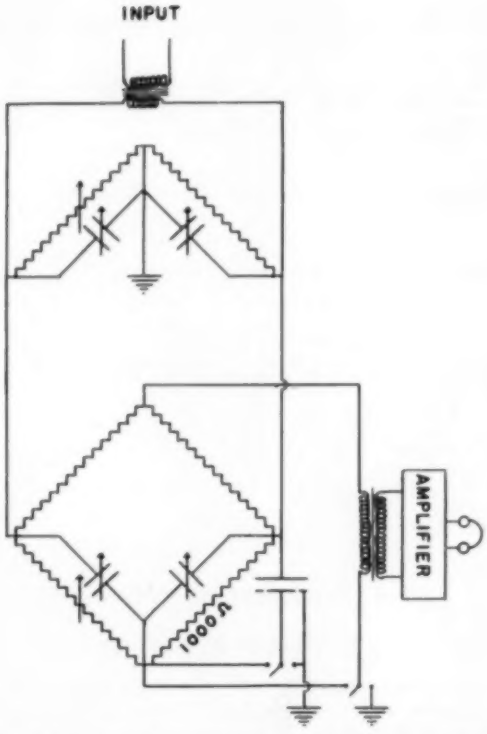

FIGURE 1.—*Capacitance-resistance bridge used for measurements of dielectric constant and power factor.*

rium, a suspension of finely ground dry leather or collagen was made up by using a portion of the excess liquid, and this suspension was introduced so as to displace the liquid in the condenser. A change in capacitance upon introducing the suspension was indicative of inequality of liquid and solid dielectric constants. The composition of the solution was varied until the dielectric constant of the suspended material was closely bracketed between values for two solutions. The usual method of linear interpolation to determine dielectric constants by the immersion method [11] was difficult to apply with this apparatus as the finely ground solid material used to minimize anisotropic effects tended to settle out or surface slowly and render the suspension nonuniform.

Measurements of apparent dielectric constant were made by using a shielded, parallel-plate, guard-ring condenser. Electrodes were made of heavy brass plates ½ in. thick, which were given a fine machine finish. The measuring electrode was 5¾ in. in diameter, and the normal (empty) plate separation was approximately 0.04 in. The air capacitance was approximately 37 $\mu\mu$f. This condenser was used at all frequencies in the range studied and at temperatures varying between +20° to −70° C. At lowest frequencies balance was obtained to a precision of ±0.15 $\mu\mu$f and ±0.002 ohm, whereas at highest frequencies balance was obtained to within ±0.01 $\mu\mu$f and ±0.001 ohm.

The condenser was equipped with two sets of three projecting ears spaced at angles of 120° on its periphery, one set on the top or movable plate, the other directly below on the frame of the condenser. These ears were used to measure the plate spacing, measurements being made to the nearest 0.0001 in. by means of micrometers. Such measurements were made at the conclusion of electrical studies on each specimen. Three set screws mounted in the top plate, equidistant between the ears, permitted resetting the empty condenser to the same spacing measured when the test specimen was in the condenser. The spacings were reproduced to within ±0.0002 in. at each ear, and the average of the three settings was reproduced to ±0.0001 in. Measurements on the empty condenser under these conditions were used to determine the air capacitance—assumed equal to the vacuum capacitance. In all measurements the top plate of the condenser, which weighed 15 lb, was loaded with an additional 20 lb to improve the contact between specimen and plates.

The real part of the dielectric constant, designated as ϵ', was obtained as the ratio of the capacitance of the condenser containing the specimen to that of the empty condenser with the same plate separation. The power factor, designated as cos ϕ, was obtained from the relationship

$$\cos\phi = 1/\sqrt{1+(R_p\omega C_p)^2},$$

where R_p is the equivalent parallel resistance of the condenser containing the specimen, C_p it's capacitance, and ω the angular frequency. The empty condenser exhibited no losses in this frequency range, therefore all losses observed were associated with the test specimens.

2.2. Test Specimens

Finely ground specimens of kangaroo tail tendon, chrome hydraulic-packing leather, and vegetable crust leather were used in suspension studies. All specimens were degreased and washed after an initial grinding and then reground. Specimens were dried by exhaustive evacuation at a pressure of less than 1 mm of mercury for at least 72 hr.

Disks 6¼ in. in diameter of chrome hydraulic-packing leather, vegetable crust leather, and unhaired cowhide were split to a uniform thickness of approximately 4±0.02 mm by removing portions of grain and flesh layers on a band-knife splitting machine. The disks were degreased, washed, and dried exhaustively in vacuum.

Initial measurements were made on dry specimens, which were then permitted to adsorb moisture from the air to obtain moisture contents as high as approximately 15 percent. For higher moisture contents specimens were exposed to vapors existing above suitable saturated salt solutions or water. Moisture contents below approximately 10 percent

were obtained by short (a few minutes to as much as 1 hr) exposures to conditioned air. Uniform moisture distribution was unlikely under these circumstances, but no appreciable change in capacitance or resistance that might be attributed to redistribution of adsorbed moisture was noted during measurements that required as long a period as 48 hr. Above 10 percent of moisture, exposures to conditioned atmospheres were conducted for at least 18 hr. Despite the longer exposures, appreciable variations in both capacitance and resistance were noted in periods of less than 1 hr. Moisture contents were obtained by weighing specimens in a sealed container made of polyethylene film and are based on the dry weight of the specimen. At low moisture contents specimens gained and at high moisture contents lost moisture during introduction and removal from the condenser. Therefore, weights were obtained before and after study, and the average of the two weights was taken to represent the moisture content during measurement. In most instances change in weight noted corresponded to less than 0.1 percent of moisture.

2.3. Effect of Temperature

All measurements below room temperature were made in a double-walled insulated container. The parallel-plate condenser and its external loading weight were placed in the innermost container, which was then covered. An ice-water bath, or a dry ice-acetone bath was placed in the outer container to obtain the desired low temperature. Temperatures were measured with a copper-constantan thermocouple mounted inside the condenser. The reference junction of this thermocouple was maintained at 0° C. Measurements on specimens were generally made after exposure to the desired temperature for 6 hr, and although thermal equilibrium was usually not attained in this time, the change in temperature during the time required for measurements was negligible.

3. Results

3.1. Dielectric Constants of Dry Leather and Collagen Fibers

The results of measurements of dielectric constants of leather and collagen fibers by the immersion method are given in table 1.

Duplicate measurements on each specimen are designated as run 1 and run 2. Following run 1, specimens were exposed to conditioned air at 72° F and 50-percent relative humidity for 14 days, then redried in vacuum and the dielectric constants redetermined. Data obtained on the second measurement are referred to as run 2. The agreement between these duplicates indicates that the drying technique employed is reasonably reproducible or that very low moisture contents have little effect on the dielectric properties. The data in table 1 were obtained by bracketing the unknown dielectric constants between solutions differing by not more than 0.15 unit in ϵ'. The values given are considered to be accurate to within ± 0.05 unit in ϵ'.

TABLE 1. *Dielectric constants of dry collagen and leather fibers*

Temperature 22.25° C, frequency 3.0 kc

Material	ϵ'		
	Run 1	Run 2	Avg
Kangaroo tendon collagen	5.12	5.12	5.12
Hydraulic chrome leather	5.37	5.41	5.39
Vegetable leather	6.30	6.30	6.25

The value for collagen is about the same as the value reported by Errera and Sack [11] on wool—5.4 at 8 kc—as well as in general accord with data of Kremen [26] ($\epsilon'=4.2$ for untanned hide, and $\epsilon'=4.6$ for chrome leather at 11 Mc). It is to be noted that chrome leather exhibits a value of ϵ' slightly higher than that of collagen, but considerably lower than vegetable leather. These data agree with the order reported by Kremen on chrome leather and hide. The values reported here and by Kremen are considerably larger than those calculated from the indices of refraction at optical frequencies of approximately 1.5 as observed by Marriot [30] and Newman [37]. This fact was also mentioned by Errera and Sack [11] in connection with nylon, silk, and wool.

3.2. Apparent Dielectric Constant and Power Factor

a. Effect of Moisture

Measurements on chrome, vegetable, and untanned leather disks of various moisture contents are given in tables 2, 3, and 4, while a portion of the data on chrome leather is shown in figures 2 and 3.

The following behavior is noted in the data of tables 2, 3, and 4: ϵ' increases with increasing moisture content at all frequencies; ϵ' decreases with increasing frequency at all moisture contents, the frequency dependence being least for dry material and greatest for moisture contents of 15 percent or more; $\cos\phi$ increases with increased moisture content; $\cos\phi$ appears to be relatively frequency independent until high moisture levels are reached, that is, 15 percent or more; $\cos\phi$ decreases strongly with increasing frequency at higher moisture levels.

For moisture contents below approximately 15 percent, all measured capacitances and resistances appeared to be independent of time, being reproducible to within 0.1 percent after several hours. At moisture contents greater than 15 percent, definite time dependence was noted, the effect being an increased capacitance and in most instances a decreased power factor at a constant frequency with increasing time. Such effects caused no appreciable error in the measured values, because the changes occurring during the hour required for measurement were generally much less than 1 percent.

b. Direct-Current Resistance

To ascertain the resistivity of the test specimens and the magnitude of corrections to the effective a-c

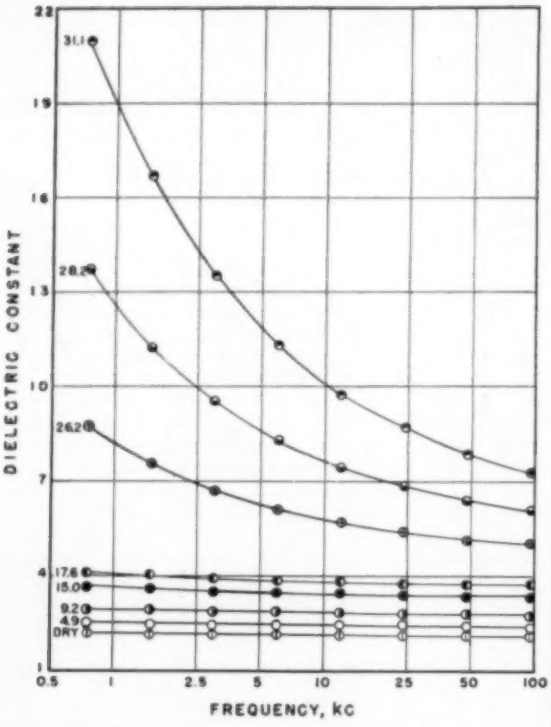

FIGURE 2. *Effect of moisture on dielectric constant of chrome leather at 22.3° C.*

◓, 31.1 percent H_2O; ◒, 28.2 percent H_2O; ⊕, 26.2 percent H_2O; ◐, 17.6 percent H_2O; ●, 15.0 percent H_2O; ◑, 9.2 percent H_2O; ○, 4.9 percent H_2O; ⊖, dry.

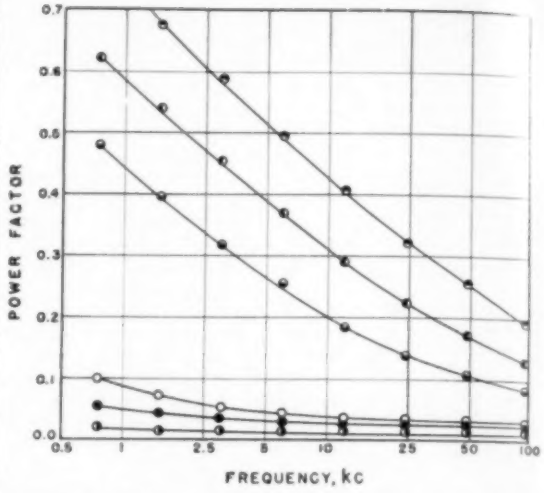

FIGURE 3. *Effect of moisture on power factor of chrome leather at 22.3° C.*

◓, 31.1 percent H_2O; ◐, 28.2 percent H_2O; ◒, 26.2 percent H_2O; ○, 17.6 percent H_2O; ●, 15.0 percent H_2O; ◑, dry.

resistance of the condenser containing the specimen, d-c resistance measurements were carried out on chrome and vegetable leathers immediately following the dielectric measurements. A commercially available megohm bridge containing a guard circuit was used in these studies, all measurements being conducted at room temperature (20° to 25° C) with an applied voltage of 500 vdc. The results of these measurements, calculated in terms of resistivities, are shown graphically in figure 4.

TABLE 2. *Apparent dielectric constant and power factor of hydraulic-packing chrome-tanned leather at 22.25° C*

Frequency	Dry		2.63% H_2O		4.91% H_2O		7.28% H_2O		9.23% H_2O		15.03% H_2O	
	ϵ'	cos ϕ	ϵ'	cos ϕ	ϵ'	cos ϕ	ϵ'	cos ϕ	ϵ'	cos ϕ	ϵ'	cos ϕ
kc												
0.75	2.19	0.0182	2.46	0.0110	2.50	0.0154	2.74	0.0163	2.94	0.0226	3.63	0.0546
1.5	2.18	.0136	2.45	.0153	2.49	.0147	2.72	.0174	2.92	.0185	3.59	.0404
3.0	2.16	.0136	2.44	.0153	2.48	.0148	2.70	.0171	2.89	.0181	3.54	.0329
6.0	2.15	.0140	2.42	.0160	2.47	.0157	2.68	.0173	2.87	.0177	3.50	.0289
12.0	2.14	.0139	2.40	.0173	2.45	.0167	2.66	.0166	2.84	.0185	3.46	.0265
24.0	2.13	.0140	2.38	.0179	2.43	.0179	2.64	.0187	2.82	.0191	3.43	.0250
48.0	2.11	.0138	2.36	.0187	2.41	.0191	2.62	.0202	2.80	.0203	3.39	.0252
96.0	2.10	.0132	2.34	.0185	2.39	.0196	2.60	.0208	2.77	.0212	3.35	.0251

Frequency	17.56% H_2O		26.2% H_2O		28.2% H_2O		31.1% H_2O		17.65% H_2O	
	ϵ'	cos ϕ	ϵ'	cos ϕ	ϵ'	cos ϕ	ϵ'	cos ϕ	ϵ'	cos ϕ
0.75	4.11	0.0690	8.75	0.479	13.74	0.621	21.00	0.743	4.60	0.1270
1.5	4.01	.0714	7.56	.397	11.25	.540	16.69	.675	4.44	.0918
3.0	3.94	.0538	6.60	.319	9.52	.455	13.52	.589	4.34	.0650
6.0	3.87	.0429	6.11	.255	8.30	.368	11.32	.495	4.25	.0529
12.0	3.82	.0361	5.71	.183	7.44	.280	9.77	.407	4.18	.0431
24.0	3.77	.0322	5.41	.138	6.84	.221	8.64	.323	4.11	.0365
48.0	3.72	.0305	5.19	.107	6.41	.171	7.84	.254	4.06	.0338
96.0	3.68	.0293	5.03	.085	6.11	.130	7.30	.193	4.01	.0305

TABLE 3. *Apparent dielectric constant and power factor of vegetable tanned crust leather at 22.5° C*

Frequency	Dry		2.32% H_2O		4.31% H_2O		6.85% H_2O		9.98% H_2O		12.17% H_2O	
	ϵ'	cos ϕ	ϵ'	cos ϕ	ϵ'	cos ϕ	ϵ'	cos ϕ	ϵ'	cos ϕ	ϵ'	cos ϕ
kc												
0.75	2.12	0.0095	2.26	0.0204	2.45	0.0153	2.87	0.0309	3.61	0.0526	3.84	0.0972
1.5	2.12	.0151	2.25	.0150	2.43	.0183	2.84	.0231	3.56	.0421	3.75	.0763
3.0	2.11	.0142	2.24	.0161	2.42	.0169	2.82	.0210	3.52	.0335	3.67	.0538
6.0	2.10	.0144	2.23	.0160	2.41	.0168	2.80	.0204	3.48	.0294	3.62	.0420
12.0	2.09	.0141	2.22	.0164	2.39	.0175	2.79	.0201	3.44	.0266	3.56	.0346
24.0	2.07	.0137	2.20	.0168	2.37	.0182	2.76	.0204	3.41	.0246	3.52	.0297
48.0	2.06	.0132	2.19	.0173	2.36	.0191	2.74	.0215	3.37	.0246	3.48	.0277
96.0	2.05	.0124	2.18	.0169	2.34	.0192	2.74	.0220	3.34	.0236	3.47	.0253

	13.67% H_2O		15.3% H_2O		17.8% H_2O		22.7% H_2O		25.5% H_2O		27.4% H_2O	
	ϵ'	cos ϕ	ϵ'	cos ϕ	ϵ'	cos ϕ	ϵ'	cos ϕ	ϵ'	cos ϕ	ϵ'	cos ϕ
0.75	4.19	0.1432	4.82	0.2200	6.31	0.329	10.36	0.396	14.35	0.480	15.40	0.602
1.5	4.01	.1042	4.51	.1642	5.61	.266	9.46	.302	12.80	.422	14.12	.474
3.0	3.90	.0772	4.30	.1196	5.09	.211	7.95	.306	10.88	.407	12.62	.412
6.0	3.81	.0575	4.15	.0870	4.84	.154	6.83	.318	9.00	.390	10.78	.398
12.0	3.75	.0449	4.05	.0658	4.63	.113	6.21	.255	7.65	.344	9.03	.379
24.0	3.70	.0369	3.99	.0505	4.49	.0824	5.64	.191	6.75	.280	7.69	.331
48.0	3.64	.0325	3.91	.0415	4.38	.0626	5.34	.141	6.15	.216	6.76	.272
96.0	3.60	.0301	3.86	.0343	4.31	.0478	5.14	.0996	5.80	.153	6.22	.200

TABLE 4. *Apparent dielectric constant and power factor of untanned hide at 22.25° C*

Frequency	Dry		2.83% H_2O		5.64% H_2O		8.52% H_2O		11.3% H_2O	
	ϵ'	cos ϕ	ϵ'	cos ϕ	ϵ'	cos ϕ	ϵ'	cos ϕ	ϵ'	cos ϕ
kc										
0.75	1.91	0.0132	2.04	0.0119	2.23	0.0182	2.47	0.0205	2.79	0.0256
1.5	1.90	.0135	2.03	.0153	2.22	.0180	2.46	.0224	2.76	.0251
3.0	1.88	.0129	2.02	.0159	2.21	.0180	2.44	.0202	2.73	.0241
6.0	1.87	.0132	2.00	.0161	2.19	.0182	2.42	.0206	2.71	.0238
12.0	1.86	.0124	1.99	.0164	2.18	.0190	2.40	.0212	2.68	.0249
24.0	1.85	.0117	1.97	.0168	2.15	.0196	2.37	.0219	2.65	.0253
48.0	1.84	.0112	1.96	.0173	2.13	.0208	2.35	.0234	2.60	.0267
96.0	1.83	.0101	1.94	.0163	2.12	.0206	2.33	.0232	2.58	.0248

	14.9% H_2O		19.7% H_2O		31.7% H_2O		40.3% H_2O	
	ϵ'	cos ϕ	ϵ'	cos ϕ	ϵ'	cos ϕ	ϵ'	cos ϕ
0.75	3.27	0.0261	4.33	0.0757	10.58	0.578	19.80	0.897
1.5	3.24	.0245	4.24	.0572	10.29	.428	16.52	.810
3.0	3.22	.0234	4.17	.0445	7.80	.388	13.81	.707
6.0	3.18	.0236	4.12	.0360	6.94	.309	11.60	.563
12.0	3.16	.....	4.06	.0335	6.35	.235	10.02	.478
24.0	3.12	.0247	4.01	.0322	5.95	.171	8.86	.367
48.0	3.09	.0265	3.95	.0328	5.69	.126	8.04	.274
96.0	3.05	.0265	3.90	.0316	5.51	.0911	7.50	.192

It will be noted that the resistivities are rather high, even at higher moisture contents. The magnitude of these values is such that at room temperature no significant correction for d-c resisistivity is required, since a-c resistivities were invariably much less than the d-c values. It was also observed that the resistance was independent of time at low moisture contents, but at higher moisture levels a time dependent drift of resistance to higher values was noted.

c. Effect of Temperature and Moisture

To obtain further information on the phenomena responsible for the observed behavior of ϵ' and cos ϕ at room temperature, as well as data on the temperature dependence of these quantities, measurements were made at room temperature and at approximately 0° C and −70° C. As noted previously, thermal equilibrium was generally not attained at reduced temperatures so that measurements were conducted with a very slowly decreasing temperature, the actual temperature being measured thermoelectrically. Prior to each measurement at a reduced temperature, a set of data was obtained at room temperature, in order to ascertain any hysteresis effect resulting from a previous cooling. In general, measurements were conducted at 0° C before cooling to −70° C, but in some instances this order was reversed because the experiments indicated that hysteresis effects did not affect the general nature of the results. The results of these experiments are given in tables 5, 6, and 7, the sets of data obtained at room temperature being given in the columns to the left of the succeeding data obtained at reduced temperatures.

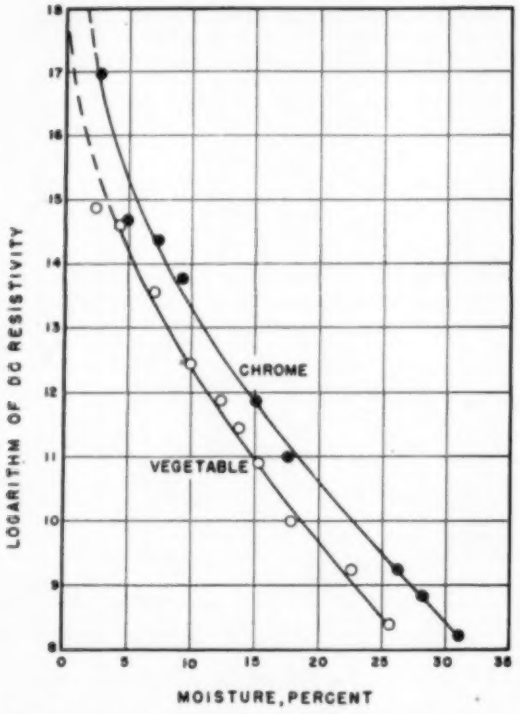

FIGURE 4. *Effect of moisture on d-c resistance at 22° C.*

○, Chrome leather; ●, vegetable leather.

Apparent dielectric constants shown in these tables were obtained by use of the air capacitance of the condenser as measured at room temperature, since it was not feasible to measure the plate separation while the condenser was subjected to low temperatures. A measure of the error involved in this procedure may be obtained by manipulations of the equation for the capacitance of a parallel plate condenser and use of the coefficients of thermal expansion of brass [17] and leather [47]. For the experimental quantities involved here such calculations indicate an error of 1.4 percent in capacitance for a temperature change of 100 deg C. The corresponding error in ϵ' is also 1.4 percent. As the expansivity of leather in air is probably smaller than the expansivity used in the calculation [47], the probable error is expected to be less than 1.4 percent. Such an error will in no way affect the following conclusions drawn from these data: ϵ' decreases with decreasing temperature at all frequencies and moisture contents, and is strongly temperature dependent at high moisture levels; ϵ' decreases with increasing frequency at all temperatures and moisture contents; cos ϕ generally decreases with decreasing temperature at a fixed frequency for very low and very high moisture contents, being strongly temperature dependent at higher moisture levels.

At intermediate moisture contents cos ϕ may increase or decrease with decreasing temperature depending on frequency and temperature.

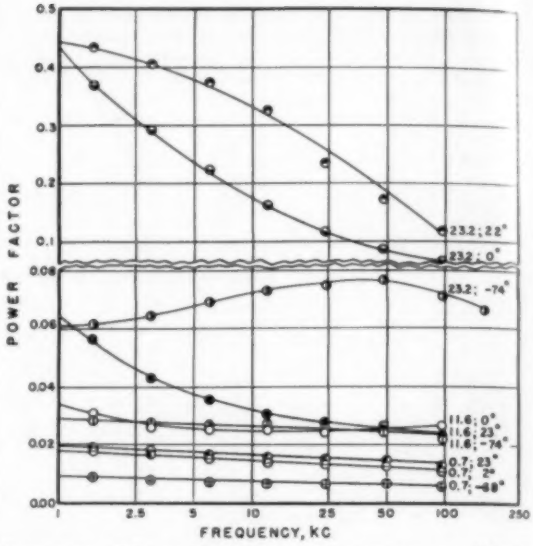

FIGURE 5. *Effects of moisture and temperature on dielectric constant of vegetable leather.*

23.2 percent H_2O: ◓, 22°C; ◒, 0°C; ◑, −74°C. 0.7 percent H_2O: ●, 23°C; ○, 2°C; ◐, −68°C.

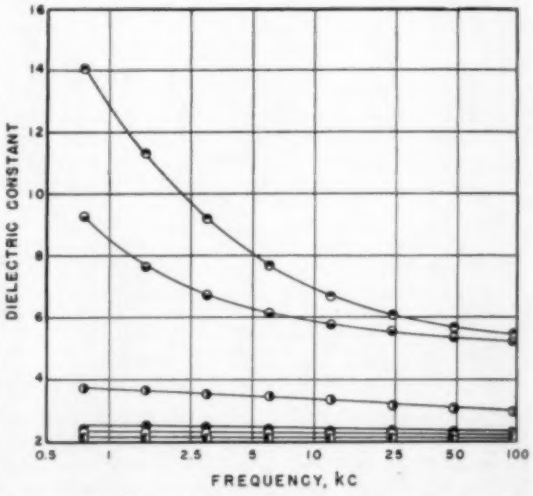

FIGURE 6. *Effects of moisture and temperature on power factor of vegetable leather.*

23.2 percent H_2O: ◓, 22°C; ◒, 0°C; ◑, −74°C. 11.6 percent H_2O: ●, 23°C; ○, 0°C; ◐, −71° C. 0.7 percent H_2O: ◐, 23° C; ⊖, 2° C; ⊕, −68° C.

At low temperatures and high moisture contents cos ϕ (as well as ϵ'') exhibits a somewhat broadened but unmistakable absorption maximum for hide and vegetable leathers, and such a maximum would appear to be present in chrome leather at higher moisture contents. Representative data are shown in figures 5 and 6.

TABLE 5. *Effect of temperature and moisture on apparent dielectric constant and power factor of hide collagen*

Frequency	Dry hide							
	20.5° C		−70.0° C		22.0° C		2° C	
	ϵ'	cos ϕ	ϵ'	cos ϕ	ϵ'	cos ϕ	ϵ'	cos ϕ
kc								
0.75	1.88	0.00976	1.74	0.00198	1.88	0.00912	1.84	0.0155
1.5	1.88	.0155	1.71	.00365	1.88	.0137	1.84	.0113
3.0	1.87	.0153	1.71	.00400	1.87	.0148	1.83	.0139
6.0	1.86	.0147	1.70	.00473	1.86	.0145	1.82	.0130
12.0	1.84	.0140	1.70	.00474	1.85	.0140	1.81	.0123
24.0	1.83	.0133	1.70	.00441	1.84	.0133	1.80	.0112
48.0	1.82	.0130	1.69	.00429	1.83	.0127	1.79	.0105
96.0	1.81	.0113	1.69	.00377	1.82	.0113	1.78	.0093
	16.0% H_2O							
	22.5° C		−68° C		23.0° C		2° C	
	ϵ'	cos ϕ	ϵ'	cos ϕ	ϵ'	cos ϕ	ϵ'	cos ϕ
0.75	3.27	0.0286	2.42	0.0281	3.22	0.0291	3.03	0.0208
1.5	3.24	.0263	2.40	.0259	3.19	.0286	3.01	.0243
3.0	3.21	.0249	2.37	.0291	3.15	.0263	2.99	.0237
6.0	3.18	.0251	2.33	.0303	3.12	.0256	2.95	.0241
12.0	3.14	.0252	2.30	.0319	3.08	.0249	2.93	.0255
24.0	3.10	.0263	2.26	.0323	3.05	.0263	2.89	.0263
48.0	3.07	.0279	2.22	.0313	3.01	.0279	2.86	.0283
96.0	3.03	.0277	2.18	.0326	2.97	.0279	2.83	.0282
	37.1% H_2O							
	22.3° C		−74.7° C		22.1° C		0° C	
	ϵ'	cos ϕ	ϵ'	cos ϕ	ϵ'	cos ϕ	ϵ'	cos ϕ
0.75	19.20	0.775	4.07	0.0720	19.60	0.825	11.70	0.610
1.5	14.96	.701	3.97	.0735	15.11	.747	9.79	.502
3.0	12.60	.614	3.83	.0854	12.22	.650	8.58	.385
6.0	9.90	.520	3.69	.0953	10.20	.535	7.79	.283
12.0	8.54	.412	3.52	.1078	8.90	.413	7.29	.200
24.0	7.66	.305	3.34	.1178	8.06	.300	6.95	.141
48.0	7.08	.221	3.15	.1275	7.50	.215	6.69	.106
96.0	6.74	.153	2.98	.0617	7.15	.148	6.51	.0805

TABLE 6. *Effect of temperature and moisture on apparent dielectric constant and power factor of chrome leather*

Frequency	2.6% H_2O							
	23.7° C		−71.0° C		20.0° C		2.3° C	
	ϵ'	cos ϕ	ϵ'	cos ϕ	ϵ'	cos ϕ	ϵ'	cos ϕ
kc								
0.75	2.47	0.0134	2.15	0.00637	2.46	0.0178	2.39	0.00920
1.5	2.45	.0135	2.14	.0100	2.44	.00920	2.38	.0133
3.0	2.44	.0144	2.13	.0107	2.43	.0134	2.37	.0151
6.0	2.43	.0153	2.12	.00986	2.41	.0142	2.35	.0136
12.0	2.41	.0163	2.11	.00905	2.39	.0158	2.34	.0168
24.0	2.39	.0169	2.10	.00825	2.38	.0163	2.31	.0168
48.0	2.38	.0179	2.09	.00781	2.36	.0172	2.29	.0169
96.0	2.36	.0157	2.08	.00700	2.34	.0167	2.28	.0155
	9.8% H_2O							
	22.5° C		−68° C		22.3° C		2.5° C	
	ϵ'	cos ϕ	ϵ'	cos ϕ	ϵ'	cos ϕ	ϵ'	cos ϕ
0.75	3.11	0.0201	2.54	0.0261	3.11	0.0182	3.00	0.0148
1.5	3.09	.0172	2.52	.0245	3.09	.0177	2.98	.0168
3.0	3.08	.0168	2.52	.0230	3.08	.0167	2.96	.0169
6.0	3.06	.0170	2.47	.0226	3.06	.0169	2.94	.0174
12.0	3.03	.0177	2.45	.0224	3.03	.0177	2.92	.0184
24.0	3.01	.0183	2.42	.0213	3.01	.0182	2.89	.0193
48.0	2.98	.0197	2.39	.0211	2.98	.0197	2.87	.0210
96.0	2.96	.0199	2.37	.0192	2.96	.0198	2.84	.0211

TABLE 6. *Effect of temperature and moisture on apparent dielectric constant and power factor of chrome leather*—Con.

	21.5% H_2O							
	25° C		−65° C		24° C		2° C	
	ϵ'	cos ϕ	ϵ'	cos ϕ	ϵ'	cos ϕ	ϵ'	cos ϕ
0.75	6.53	0.347	3.58	0.0309	6.31	0.314	5.05	0.137
1.5	5.89	.227	3.53	.0327	5.77	.237	4.86	.0985
3.0	5.46	.199	3.48	.0340	5.42	.172	4.71	.0741
6.0	5.16	.143	3.43	.0368	5.17	.126	4.63	.0593
12.0	4.96	.105	3.36	.0395	5.00	.0945	4.54	.0494
24.0	4.81	.0792	3.30	.0439	4.86	.0727	4.45	.0429
48.0	4.69	.0640	3.23	.0500	4.75	.0603	4.37	.0401
96.0	4.60	.0520	3.15	.0518	4.65	.0500	4.31	.0364
	30.6% H_2O							
	23.0° C		−73.0° C		20.0° C		1.0° C	
	ϵ'	cos ϕ	ϵ'	cos ϕ	ϵ'	cos ϕ	ϵ'	cos ϕ
0.75	25.80	0.784	4.78	0.0495	22.75	0.787	13.90	0.607
1.5	19.18	.725	4.69	.0498	17.70	.715	11.54	.514
3.0	15.14	.639	4.58	.0559	14.25	.622	9.91	.419
6.0	12.44	.544	4.46	.0649	11.84	.527	8.74	.325
12.0	11.87	.407	4.32	.0894	10.17	.430	7.95	.254
24.0	9.37	.348	4.15	.0883	8.99	.335	7.40	.191
48.0	8.45	.271	3.95	.1032	8.15	.260	6.96	.149
96.0	7.96	.198	3.76	.1057	7.58	.188	6.67	.115

TABLE 7. *Effect of temperature and moisture on apparent dielectric constant and power factor of vegetable leather*

Frequency	Dry							
	23° C		−68° C		23° C		2° C	
	ϵ'	cos ϕ	ϵ'	cos ϕ	ϵ'	cos ϕ	ϵ'	cos ϕ
kc								
0.75	2.41	0.0198	2.14	0.00712	2.41	0.0191	2.31	0.0195
1.5	2.39	.0173	2.14	.00832	2.39	.0186	2.31	.0171
3.0	2.38	.0163	2.13	.00730	2.38	.0163	2.30	.0148
6.0	2.36	.0159	2.13	.00669	2.37	.0161	2.28	.0139
12.0	2.34	.0152	2.12	.00676	2.35	.0154	2.27	.0132
24.0	2.33	.0149	2.12	.00638	2.33	.0149	2.25	.0126
48.0	2.31	.0143	2.11	.00639	2.32	.0144	2.24	.0121
96.0	2.30	.0129	2.10	.00592	2.30	.0130	2.23	.0108
	11.6% H_2O							
	23° C		−71° C		18° C		0° C	
	ϵ'	cos ϕ	ϵ'	cos ϕ	ϵ'	cos ϕ	ϵ'	cos ϕ
0.75	3.56	0.0755	2.55	0.0319	3.70	0.0660	3.40	0.0377
1.5	3.49	.0564	2.52	.0279	3.63	.0498	3.37	.0301
3.0	3.43	.0429	2.49	.0273	3.57	.0383	3.34	.0264
6.0	3.38	.0359	2.46	.0267	3.52	.0333	3.30	.0256
12.0	3.34	.0307	2.43	.0268	3.49	.0298	3.26	.0250
24.0	3.31	.0275	2.40	.0255	3.44	.0276	3.23	.0249
48.0	3.27	.0267	2.37	.0254	3.41	.0274	3.20	.0265
96.0	3.23	.0237	2.32	.0236	3.37	.0261	3.16	.0262
	23.2% H_2O							
	22° C		−74° C		23° C		0° C	
	ϵ'	cos ϕ	ϵ'	cos ϕ	ϵ'	cos ϕ	ϵ'	cos ϕ
0.75	14.06	0.417	3.68	0.0572	13.00	0.493	9.25	0.427
1.5	10.35	.435	3.60	.0610	10.27	.471	7.63	.369
3.0	9.20	.406	3.47	.0644	8.50	.416	6.74	.292
6.0	7.65	.373	3.40	.0660	7.29	.346	6.14	.223
12.0	6.69	.327	3.29	.0729	6.55	.268	5.76	.162
24.0	6.06	.253	3.18	.0746	6.06	.196	5.53	.117
48.0	5.66	.171	3.07	.0764	5.75	.143	5.35	.0869
96.0	5.42	.119	2.97	.0709	5.55	.100	5.21	.0645
160.0			2.90	.0680				

4. Discussion

4.1 Electrical Properties of Collagen and Leather

The data obtained here are quite similar to results that have been reported for other fibrous materials, some of which might not be expected to be electrically comparable. With due consideration to the frequencies involved, values of dielectric constants of leather and collagen fibers are of the same order as values of silk and wool [11] as previously noted, as well as values on cellulose [7] obtained by Dakin. Earlier values on cellulose [4, 9, 43] are slightly different but of the same general order. The higher values for vegetable leather reported here are to be expected, since the appreciable amount of incorporated vegetable tannin probably has a higher dielectric constant than collagen, as shown by measurements of Knoke [25]. The reported dielectric constant of dry gelatin, 2.68 at 512 kc [13], appears to be less than might be expected in view of its being derived from collagen.

Resistivity data are likewise similar to results previously reported on cellulose products that have been extensively studied in view of their widespread electrical applications. However, results obtained here for leather exhibit no linear relationship between logarithm of resistance and any simple function of moisture content as has been reported for textiles and cotton [34, 36, 46]. This divergence may be associated with the greater adsorptive capacity of leather for moisture.

Apparant or bulk dielectric constants of moist leather have been reported by Compton [6], who used a bridge method at 1 kc. His experimental values are much larger than those reported here at comparable moisture contents. This fact, together with his extremely high values of dielectric constant—ϵ' as high as 4980, will be discussed later. Neither Compton nor Kremen [26, 27] investigated the effects of temperature or frequency on ϵ' and neither studied power losses, although Compton concluded that resistance measurements made during his measurements showed such little concordance that their use did not seem justified.

The data obtained here are similar in many respects to previous reports of effects of adsorbed vapors on the electrical properties of other porous materials [1, 8, 22, 23, 24, 31, 35, 44]. In view of the similarities in results and the characteristics of the materials, the interpretations of the present data will be patterned to some extent along the lines of the conclusions of previous workers [8, 12, 13, 22, 34, 35, 38, 43], who have emphasized the importance of considering interfacial polarization in electrical measurements on nonhomogeneous materials of this type.

Leather must possess a large adsorption surface area by virtue of its fibrous structure. This area has been calculated by Kanagy [20] from adsorption data. Since the fibers are composed of submicroscopic fibrils and moisture appears to penetrate the fibers, it would appear that the fibrillar surface area must play a role in these data. The filaments that make up the fibrils may also be involved, but qualitatively the conclusions reached here will be independent of the units involved. There are probably three phases present in moist leather—the leather substrate, which may contain combined or dissolved moisture; a surface layer of adsorbed moisture; and the surrounding air. The interface between any two of these phases is an obvious source of Maxwell-Wagner polarization effects. The behavior of such types of interfacial polarization has been considered in detail and developed quantitatively for simple systems by other workers [32, 38, 39]. In leather the vast number of these interfaces present, the complexity of the interconnections of the physical matrix, and the unknown conductivities and dielectric constants of the phases involved present a problem that permits no quantitative analysis. The only facts available are that the dielectric constants of the three phases are quite different in bulk form, while the conductivity of the air will be much less than that of either the moist substrate or the adsorbed moisture layer. Wagner [39] has shown that a necessary condition for minimizing interfacial effects is that

$$\sigma_1 \epsilon_1' = \sigma_2 \epsilon_2',$$

where σ and ϵ' are conductivity and dielectric constant, respectively, and the subscripts refer to the phases that form the interface. In the present situation it is extremely improbable that such a relationship will hold at the three possible interfaces at all moisture contents studied.

A somewhat different type of polarization, known as electrode polarization, may exist at the discontinuity between specimens and the condenser plates. In the present experiments no differentiation between electrode polarization and the interfacial polarization existing within the specimen is possible, and the electrode polarization will be considered as lumped with the interfacial effects.

The other important type of polarization arises as a result of the numerous permanent dipoles present in the basic protein by virtue of its amino acid composition. These dipoles will represent sources of Debye polarization, an effect that is qualitatively similar to interfacial polarization. The extreme difficulty in distinguishing between these two phenomena has been emphasized previously [32, 38].

The qualitative interpretation of the data in tables 2 to 7 appears to require at least two polarization processes, one being freely operative only at very low frequencies at high moisture contents and in all probability associated with interfacial effects, the other being effective up to much higher frequencies and probably arising from dipolar effects. The relative importance of these two effects is determined by the moisture content of the specimen.

The strong absorption region at low frequencies predominates at moisture contents above approximately 15 percent, except at low temperatures. This dielectric absorption is attributed to interfacial polarization phenomena. The rapid decrease of ϵ' and cos ϕ with increasing frequency and decreasing temperature may be logically attributed to this

effect. The dependence of capacitance and resistance on time at a constant frequency is suggestive of charging currents and therefore of polarization at a discontinuity. The data of Compton [6], who worked in this frequency range, can be interpreted to a large extent as arising from interfacial effects. The specimens used by Compton in all probability had a much lower resistivity than those prepared here. This increased conductivity permits a larger charging current and an apparent increase in dielectric constant [39]. Thus Compton's dielectric constants at comparable moisture contents and frequency vary from at least three to several hundred times the present values. The extremely high values of ϵ' reported by Compton—ϵ' as high as 4980 on chrome leather containing only 26 percent of moisture—can be logically interpreted only on the basis of interfacial effects arising from appreciable conductivity in the test specimens. For the foregoing reasons it is believed that at high moisture contents the present data are obtained on the descending slope of a large interfacial power absorption region that persists to very low frequencies.

At low moisture contents—that is, below approximately 15 percent of moisture—the electrical behavior is quite different. In this region it would appear that the data is obtained in a region between two dielectric absorption maxima, the interfacial region at low frequencies, which diminishes in importance with decreased moisture content, and a second dielectric absorption region with a maximum at high frequencies far beyond the experimental range of frequency. This second dielectric absorption maximum would account for the increased losses with increasing frequency observed in this moisture range, as well as the increase in loss observed on decreasing the temperature. This latter effect arises as a result of the analogy between frequency and temperature, a reduction in temperature being experimentally equivalent to increasing the frequency of the measurements or to shifting the dielectric relaxation effects to lower frequencies.

At high moisture contents at −70° C the interfacial effects have virtually disappeared as a result of reduced conductivity at low temperatures [39], but a distinct dielectric absorption maximum in $\cos \phi$ appears in two specimens in the experimental frequency range—the corresponding maximum in ϵ'' appears for all three specimens. This dielectric absorption maximum is not observed under similar conditions for dry leather or at low moisture contents, so that the moisture appears to be largely responsible for the observed effect. Since a dielectric absorption maximum has been indicated at high frequencies at room temperature, this maximum may have been shifted to the experimental frequency range by the temperature reduction. However, since a similar effect is not observed at lower moisture contents, it would be necessary to assume that the frequency of the absorption maximum is dependent on moisture content. It is also possible that this dielectric absorption maximum is attributable to ice, which is known to exhibit such a maximum in this frequency range, but at a somewhat higher temperature [10, 33, 40].

As a result of the foregoing considerations, the following general picture may be given. In the dry condition in this frequency range, leather may be considered to have a dielectric behavior that is characterized by a moderate power absorption with slight frequency dependence. As the moisture content of the leather increases, two dielectric absorption maxima—one at very high, the other at very low frequencies—appear and increase in magnitude with increasing moisture content. The high-frequency maximum grows the more rapidly at low moisture contents, and at very low moisture contents largely determines the behavior of the leather. As moisture is added the low frequency, or interfacial effect, grows at an increasing rate, and in the moisture range 5 to 15 percent, losses due to both types of dielectric absorption are determining factors. In this moisture range the data may be pictured as being taken in the trough between the two dielectric absorption maxima. As the moisture content rises above about 15 percent, the rate of growth of the interfacial region accelerates tremendously, and at high moisture contents the enormous size of the power absorption arising from interfacial effects completely overshadows the smaller but probably still important maximum at higher frequencies. The source of the low-frequency losses has been attributed to interfacial charging phenomena, and it remains to consider the causes of the losses at higher frequencies. The high-frequency absorption may be due to dipolar polarization or to a different type of interfacial phenomenon. Since dipoles are known to be present in the protein, it would seem that the power absorption may be due to such causes. The increasing importance of this absorption with increasing moisture content, noted at low moisture contents but probably occurring even at high moisture contents, may be considered as due to increased mobility of the existing dipoles conferred by the imbibed moisture. The dipoles in the dry material may be thought of as being largely immobilized by the compact molecular structure of dry collagen with correspondingly large restraining forces. Since the compact structure relaxes in the presence of moisture, these bound dipoles may be freed to some extent, the degree of freedom increasing with increasing moisture content.

The interpretation of these data given in the foregoing implies a somewhat different role of moisture in the low and high-moisture ranges, with a gradual shift of the effect centering at approximately 15 percent of moisture. This behavior is clearly shown by ϵ' and $\cos \phi$ in the tabular data. The gradual transition region occurs at lower moisture contents in vegetable leather than in chrome leather or in hide, and may be directly related to that moisture content range in which the slope of the heat of adsorption curve is undergoing its greatest change [20]. The apparent difference in effects of moisture in the low- and high-moisture range may be considered to be due to the decreased binding energy of the moisture

with increasing moisture content. Such concepts have been advanced previously [1, 35].

This difference in behavior of moisture in the two moisture ranges may be related to concepts of "bound water", which have been discussed by numerous workers [2, 15, 16, 18, 19], and with particular reference to leather by Compton [6], Kremen [28], and Cheshire and Holmes [5]. These latter workers conclude that between 30 and 50 percent of moisture on a hide substance basis can be considered as bound water. The present studies were conducted principally in the range of moisture contents in which these workers would consider all moisture present to be bound.

The present data show that the moisture present in small amounts produces a markedly different effect than that present in large quantities. Below a rather ill-defined transition region centering at about 15 percent of moisture, the principal effect is the enhancement of the high-frequency dielectric absorption, while interfacial polarization is effected to a rather small degree. In this range the moisture might be considered to be mainly intimately associated with the protein, probably by means of chemical forces through hydrogen bonding. Relatively little moisture is therefore available to act electrically as one might expect water to behave.

At the higher moisture contents the effect of moisture on the high-frequency dielectric absorption is masked by the rapid growth of the interfacial polarization. In this range the principal effect appears to be on the surface of the structural units involved, so that conducting layers are rapidly built up to produce the interfacial effects observed. In this range the moisture produces electrical results that might be expected of water.

It is possible, therefore, to distinguish between these two essentially different roles of moisture, even in the range in which all moisture has been considered to be bound. It must be concluded that there is considerable difference in binding of the so-called bound water.

5. Determination of Moisture in Leather by Electrical Methods

From the data obtained in these studies it follows that in this frequency range electrical methods cannot be expected to yield precise results in quantitative analyses for moisture. To test this conclusion an experiment was performed on similar specimens of commercial, fat-liquored, chrome upper leather that were cut from corresponding areas of different hides of the same tannage. All specimens were cut from similar positions in the shoulder region, and were selected for uniformity of thickness over the area of the test piece. Following initial measurements, the specimens were degreased and rerun to ascertain the effects of inequalities in grease content. The results of these measurements are given in table 8.

Thickness measurements are the average of 15 determinations distributed uniformly over the area of the test specimen. These measurements were made to the nearest 0.001 in. Condenser plate separations are the average of three measurements made as described previously, and are accurate to the nearest 0.0001 in. Differences noted in ϵ' and cos ϕ are real, since the experimental capacitances and resistances involved were measured to at least four significant figures.

TABLE 8. *Reproducibility of electrical data on specimens from different hides of the same tannage* [a]

σ for ϵ' commercial = 0.10; σ for ϵ' degreased = 0.13

Specimen	Commercial leather				Degreased leather			
	Thickness	Condenser plate separation	ϵ'	cos ϕ	Thickness	Condenser plate separation	ϵ'	cos ϕ
	in.	*in.* [b]			*in.*	*in.* [b]		
1	0.093	1.1057	3.29	0.0275	0.094	1.1079	3.26	0.0521
2	.094	1.1040	3.35	.0356	.094	1.1071	3.18	.0485
3	.094	1.1059	3.43	.0382	.094	1.1075	3.41	.0805
4	.090	1.1078	3.18	.0269	.092	1.1037	3.10	.0448
5	.094	1.1060	3.42	.0444	.095	1.1087	3.38	.0599

[a] Measurements at 3 kc.
[b] Measured from arbitrary zero.

Variations noted in ϵ' and cos ϕ indicate that use of these quantities to characterize or measure the moisture content would be subject to considerable uncertainty in an arbitrary piece of leather. Measurements of moisture contents of these specimens have not been made, since all specimens were subjected to identical treatments throughout, and experience in this laboratory has shown that a moisture content of approximately 12 percent with a variation of less than approximately 1 percent may be expected for such specimens from the same location of different hides of the same tannage. Since some differences in apparent density or fiber orientation exist, the variations observed in ϵ' and cos ϕ are not considered excessive.

It is concluded, therefore, that in this frequency range electrical methods are not expected to produce precise quantitative determinations of moisture in leather. Although this conclusion is reached largely as a result of data accumulated using alternating currents, it is believed that the same considerations apply to direct-current measurements. This extension of the conclusions appears to be valid as a result of observations made previously concerning behavior of the direct-current resistance of specimens containing moderate amounts of moisture. For rapid, nondestructive estimates of moisture content, particularly for control work, such methods may be adequate, provided the effects of temperature and salt content are recognized and controlled.

The author is indebted to C. G. Malmberg and A. A. Maryott for use of the capacitance bridge that made these measurements possible, as well as for the stimulating discussions directed toward this problem.

6. References

[1] G. Argue and O. Maass, Can. J. Research **13B,** 156 (1935).
[2] D. R. Briggs, J. Phys. Chem. **36**, 367 (1932).
[3] E. F. Burton and Arnold Pitt, Can. J. Research **1,** 155 (1929).

[4] A. Campbell, Proc. Roy. Soc. (London) **78A,** 196 (1907).
[5] A. Cheshire and N. L. Holmes, J. Int. Soc. Leather Trades Chem. **26,** 237 (1942).
[6] E. D. Compton, J. Am. Leather Chem. Assoc. **39,** 74 (1944).
[7] T. W. Dakin, Annual Report 1950; Conference on Electrical Insulation Nat. Acad. Sci., Nat. Research Council (March 15, 1951).
[8] T. W. Dakin and R. W. Auxier, Ind. Eng. Chem. **37,** 268 (1945).
[9] H. A. DeLuca and W. B. Campbell, Can. J. Research **16,** 273 (1938).
[10] M. J. Errera, J. Phys. Radium **5,** 304 (1924).
[11] M. J. Errera and Sack, Ind. Eng. Chem. **35,** 712 (1943).
[12] H. Fricke and H. J. Curtis, J. Phys. Chem. **41,** 729 1937).
[13] H. Fricke and E. Parker, J. Phys. Chem. **44,** 716 (1940).
[14] S. D. Gardiner, J. Soc. Chem. Ind. **62,** 75 (1943).
[15] R. A. Gortner, Outlines of biochemistry (John Wiley & Sons, Inc., New York, N. Y., 1938).
[16] W. F. Hampton and J. H. Mennie, Can. J. Research **10,** 452 (1934).
[17] Handbook of chemistry and physics, 30 ed. (Chemical Rubber Publishing Co., Cleveland, Ohio).
[18] W. R. Horn and J. H. Mennie, Can. J. Research **12,** 702 (1935).
[19] I. D. Jones and R. A. Gortner, J. Phys. Chem. **36,** 387 (1932).
[20] J. R. Kanagy, J. Research NBS **44,** 31 (1950) RP2056.
[21] J. R. Kanagy, J. Research NBS **38,** 119 (1947) RP1763.
[22] G. King, Trans. Faraday Soc. **43,** 601 (1947).
[23] G. King, Nature **158,** 134 (1946).
[24] G. T. Kohman, Ind. Eng. Chem. **31,** 807 (1939).
[25] S. Knoke, Z. Elektrochem. **43,** 749 (1937).
[26] S. S. Kremen, Dissertation, University of Cincinnati (1949).
[27] S. S. Kremen, J. Am. Leather Chem. Assoc. **44,** 774 (1949).
[28] S. S. Kremen and R. M. Lollar, J. Am. Leather Chem. Assoc. **46,** 34 (1951).
[29] C. G. Malmberg and A. A. Maryott, J. Research NBS **45,** 299 (1950) RP2137.
[30] R. H. Marriott, J. Int. Soc. Leather Trades Chem. **19,** 133 (1935).
[31] R. McIntosh, H. S. Johnson, N. Hollies, and L. McCleod, Can. J. Research **25B,** 566 (1947).
[32] S. O. Morgan, Trans. Electrochem. Soc. **65,** 109 (1934).
[33] E. J. Murphy, Trans. Electrochem. Soc. **65,** 133 (1934).
[34] E. J. Murphy, J. Phys. Chem. **33,** 200 (1929).
[35] E. J. Murphy and H. H. Lowry, J. Phys. Chem. **34,** 598 (1930).
[36] E. J. Murphy and A. C. Walker, J. Phys. Chem. **32,** 1761 (1928).
[37] S. B. Newman, private communication.
[38] H. H. Race, Trans. Am. Inst. Elec. Engrs. **52,** 682 (1933).
[39] H. Schering, Die Isolierstoffe der Electrotechnik, chapt. I by K. W. Wagner (Julius Springer, Berlin, 1924).
[40] C. P. Smyth and C. S. Hitchcock, J. Am. Chem. Soc. **54,** 4631 (1932).
[41] J. L. Spencer-Smith, J. Textile Inst. **26,** T336 (1935).
[42] H. Starke, Verhandl. deut. physik Ges. **15,** 69 (1896).
[43] W. N. Stoops, J. Am. Chem. Soc. **56,** 1480 (1934).
[44] J. Tausz and H. Rumm, Kolloid-Beihefte **39,** 58 (1934).
[45] H. Vollmar, Z. Elektrochem. **50,** 150 (1944).
[46] A. C. Walker, J. Text. Inst. **24,** T145 (1933).
[47] C. E. Weir, J. Research NBS **41,** 279 (1948) RP1924.

WASHINGTON, December 13, 1951.

Journal of Research of the National Bureau of Standards Vol. 48, No. 5, May 1952 Research Paper 23 3

Synthesis of Mica

Alvin Van Valkenburg and Robert G. Pike

A synthetic fluorophlogopite mica ($KMg_3AlSi_3O_{10}F_2$), in which the (OH) ions that are normally found in normal micas were completely replaced by fluorine, has been synthesized. This material has essentially the same physical and electrical properties as natural phlogopite mica, except with somewhat lower flexibility. To grow large, usable sheets of mica, it is necessary to obtain preferred crystal orientation, which depends primarily on controlled thermal gradients, batch composition, and rate of cooling. Platinum crucibles were found to be the best material for holding the batch during the melt. Data on the physical, electrical, thermal, and chemical properties of the synthetic mica are given.

1. Introduction

"Mica" is a general term used to describe a series of silicate minerals that are characterized physically by a perfect basal cleavage and yield with ease thin, tough laminas. Commercially, the two most widely used micas in the electrical industry are the muscovite and phlogopite types. These are important because of their high dielectric strength, thin laminas, high resistance to heat, flexibility, and low unit cost. No substitute has yet been found for these minerals. Because of the strategic importance of the better grades of mica and the failure of domestic supplies to meet our needs, the possibility of the development of a synthetic mica to replace natural mica in wartime has been of great interest.

Claims for the synthesis of mica date back to about 1880. A summary of the work of early investigators is given in F. W. Clarke's "Data of geochemistry", U. S. Geological Survey Bulletin 770, 1924. J. H. L. Vogt [1][1] analyzed slags from copper smelting in Sweden and reported a magnesium mica, which may have been a phlogopite. Fouqué and Lévey [2] synthesized a mica trachyte by heating a powdered granitic glass with water under pressure; scales of mica were reported. C. Doelter [3], P. Hautefeville [4], L. P. de Saint-Gilles, and K. Chrustschoft [5] used fluorine compounds in fusing various silicates, both natural and artificial, and obtained micas. Later, D. P. Grigor'ev [6] in his systematic studies on the synthesis of micas demonstrated the importance of fluorine in the structure of micas.

A synthetic fluorine phlogopite mica is not a unique product, as many natural phlogopite micas contain fluorine as a partial replacement for hydroxyl. This substitution can be readily accomplished because the ionic radius of fluorine, 1.33 A, is approximately the same as that of the (OH) ion, 1.40 A. Their respective volumes are fluorine 9.86 and (OH) 11.48A^3. F^{-1} and $(OH)^{-1}$ each have 2K and 8L electrons, but F^{-1} has one nucleus with a charge of +9, and $(OH)^{-1}$ possesses two nuclear charges, +8 and +1, respectively. The unique feature of the synthetic fluorine phlogopite is that fluorine ions completely replace the hydroxyl ions.

[1] Figures in brackets indicate the literature references at the end of this paper.

One of the first patents on a process for producing synthetic mica by fluorination was issued in 1919 to the German industrial company of Siemens & Halske, German patent DRP No. 367,537. Subsequent patents were issued to both German and American companies, but no attempts were made to commercialize them. At the conclusion of World War II the successful synthesis of a fluorine mica in Germany in laboratory melts as large as 100 kg was reported. Active work on mica synthesis had begun in 1938 by the Siemens-Schuchert concern in Berlin and was continued under the leadership of V. Middel until late 1944. In 1941, laboratory research on the properties and crystallization of synthetic mica was also started at the Kaiser-Wilhelm Institute fur Silikatforschung and continued through most of the war. The German work demonstrated that a synthetic fluorine phlogopite mica with a composition of $K_4Mg_{12}Al_4Si_{12}O_{40}F_8$ could be readily crystallized from a melt. Although the Germans were successful in crystallizing a fluorine mica, apparently development never reached the state of fabrication of the mica into shapes for commercial articles.

Data on the electrical properties of synthetic mica obtained at the conclusion of World War II indicated only that synthetic fluorine phlogopite had electric constants equal to or better than that of natural phlogopite.

When it became known that it was possible to synthesize a fluorine phlogopite mica, the Department of the Navy, through the Bureau of Ships and the Office of Naval Research, and the Department of the Army, through the Signal Corps, planned a joint synthetic-mica program. Research contracts were negotiated with the U. S. Bureau of Mines at Norris, Tenn., the Colorado School of Mines at Golden, Colo., and the National Bureau of Standards at Washington, D. C. These three groups have been working on the various problems involved in the synthesis of mica, exchanging ideas, and at joint meetings discussing technical data.

The synthetic-mica research program at the National Bureau of Standards is part of a broad program of fundamental research on fluorine-type artificial minerals. The general purpose of the mica program is to determine the laws governing the growth of this mineral and to compare the physical,

electrical, and chemical properties of the synthetic mica with those of its natural analogue. Exploratory experiments were initiated in November 1946 and continued with Bureau appropriations, as personnel and funds allowed, until early in 1947, when funds of the Office of Technical Services, Department of Commerce, permitted greater activity on the project. On June 30, 1947, funds from this source were discontinued. Thereafter, this work was supported by the Office of Naval Research.

2. Experimental Work

As a starting point in the mica-synthesis program, the first experiments were patterned after the German work as reported in the Fiat publications. A mica batch, with a composition corresponding to the German formula published in the Office of Military Government Fiat Report 746, was prepared The batch was adjusted to give a final composition of:

	Percentage by weight
Al_2O_3	11. 6
MgO	32. 6
SiO_2	30. 7
K_2SiF_6	25. 1

A 1-g sample of batch material was placed in a sealed platinum-foil envelope and heated to 1,450 °C for 10 minutes. The charge was then cooled at a controlled rate of 3 deg/min to 1,300° C, after which the furnace was cooled rapidly to room temperature. The sample had completely crystallized, forming small interlocking mica crystals up to 3 mm in diameter. Individual crystals cleaved readily into thin flexible flakes. Impurities in the form of irregular white patches or cloudy surfaces occurred in thin layers parallel to the cleavage directions. This preliminary experiment demonstrated that synthetic fluophlogopite mica, with a composition similar to the natural phlogopite mica, could be readily crystallized from a melt. Additional experiments indicated that the major problems involved in growing mica were: composition of batch; control of losses by volatilization to prevent melts from changing composition; composition of crucible; attainment of uniform and controlled thermal gradients within melts to give a preferred orientation to growing crystals; prevention of excessive seed crystal formation at the beginning of crystallization.

2.1. Composition and Melting Point

Phase determinations were made on a batch consisting of:

	Percentage by weight
Al_2O_3	11. 79
MgO	27. 99
SiO_2	34. 74
K_2SiF_6	25. 48

This composition, which approximates the ideal phlogopite formula $KMg_3AlSi_3O_{10}F_2$ with the exception of an excess of F_2, yielded the best crystals. In preparing the batch materials prior to the melting operation, care must be taken to eliminate water vapor and CO_2 from the raw ingredients, as the presence of these in the batch may cause premature breakdown of the fluorinating compound, releasing fluorine probably as silicon fluorides at temperatures well below the melting point of the batch. The fluorine thus released escapes from the crucible. A batch was prepared by calcining gibbsite ($Al_2O_3.3H_2O$), magnesium carbonate ($MgCO_3$), and silicic acid (SiO_2) at a temperature of 1,000° C for a period of several hours, usually an overnight operation. After calcination, the fluorine compound (K_2SiF_6) was added and the batch placed immediately in the furnace for melting and crystallization. The batch materials were of "C. P." grade.

Microcline, which is a natural-occurring feldspar, has a composition of $KAlSi_2O_8$ and is therefore a possible fluorophlogopite batch material. By adding 2 moles of MgO and 1 mole of MgF_2 to 1 mole of microcline, one should have the composition of a fluorophlogopite. Unfortunately, microcline or its chemical analogue, orthoclase, is rarely found in the pure state. Sodium, which is usually present in amounts up to 3 percent in microcline, apparently prevents good crystallization of fluorophlogopite. Several attempts were made to produce a mica from a microcline feldspar with the addition of MgO and MgF_2. These were mostly failures, as the resulting melts contained abundant amounts of glass and orthosilicates. Occasionally small mica flakes were observed under the microscope.

Efforts were made to determine the temperature of crystallization and the primary phase in melts having the composition of the normal fluorophlogopite. Both the soak-quench technique and differential thermal analysis were used. Preliminary soak-quench experiments, using 0.3-g samples, were found to be unsatisfactory presumably because of excessive volatilization losses in such small samples. Experiments with samples of about 2.5 g gave much better reproducibility. Charges in sealed platinum envelopes were heated to at least 1,400° C, well above the liquidus of this composition, cooled at rates of about 1 deg/min to the desired temperature and quenched in water. Because the centers of the melts cooled too slowly to freeze to glass, the conditions of the charges immediately adjacent to the platinum envelopes were used as the criteria. Using this method, the melting temperature was determined to be about 1,345° C, and the primary phase was found to be fluorophlogopite. When compositions were carefully controlled, water vapor and carbon dioxide removed from the batch by precalcining, and the charge protected from excessive volatilization, the crystallization of fluorophlogopite took place on cooling without the intermediate crystallization of any other solid phase.

The procedure and apparatus used for obtaining differential heating and cooling curves are the same

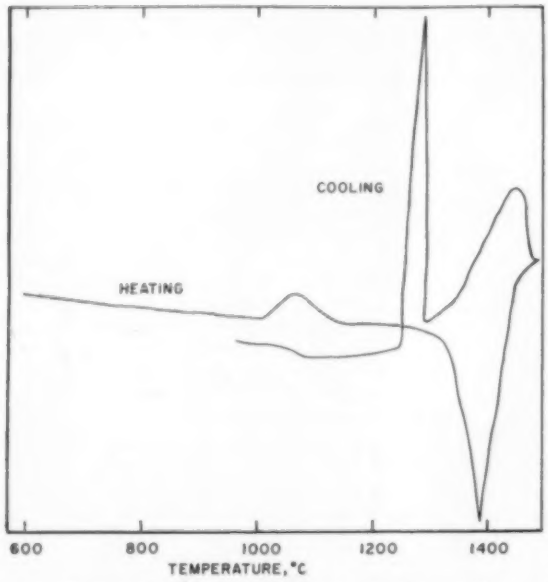

FIGURE 1.—*Differential thermal curve of synthetic fluorophlogopite.*

as those described by Newman and Wells [7]. Differential thermal analyses were made on a sample of clear, homogeneous, synthetic, fluorophlogopite flakes, which were carefully selected to avoid impurities. After the first run, only one thermal effect was noted on heating and one on cooling, evidently associated with melting and crystallization. As in the case of most silicates, the effects were not abrupt and the temperatures of the beginning of the endothermal effect on heating and of the exothermal effect on cooling were greatly influenced by such factors as size of charge, rate of temperature change, etc. The curve obtained from the first run of three obtained on the same sample is shown in figure 1. The exothermic hump on heating, beginning at about 1,025°, is unexplained. It was absent in later runs on the same sample. The exothermic effect on cooling, beginning immediately after reversal of the furnace, is characteristic of the method and occurs before temperature change and heat flow have become uniform. The large endothermic effect on heating, starting at about 1,325°, is associated with melting, and the large exothermic effect on cooling, beginning at about 1,280°, is associated with crystallization. These heat effects may vary in temperature over a range of 30 deg, due to differences in rates of temperature change and uncontrollable experimental conditions.

2.2. Control of Volatility

In early crystallization experiments in which carbon or platinum crucibles were used without adequate means of controlling volatilization, such impurities as minerals of the fluorohumite group

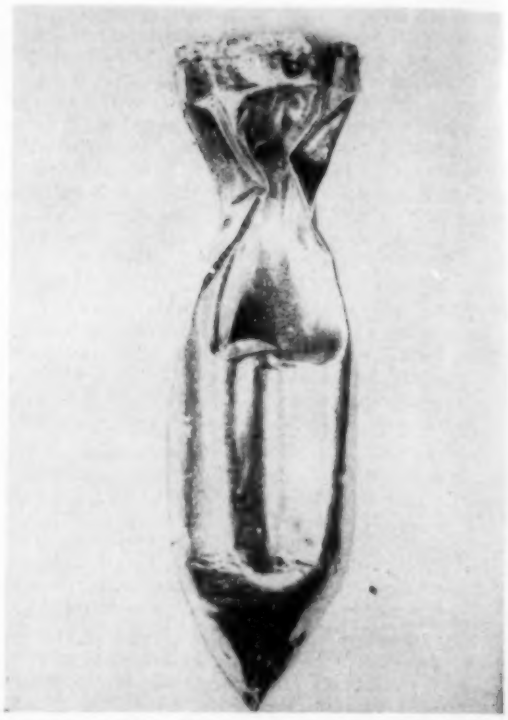

FIGURE 2. *Small platinum crucible as removed from furnace, showing results of self-sealing.* (*Natural size.*)

(n $Mg_3SiO_4.MgF_2$), forsterite (Mg_2SiO_4), sellaite (MgF_2), spinel ($MgAl_2O_4$), and glass were formed with the mica crystals. Similar impurities have been found by other investigators [8]. Several approximate weight loss determinations were made on 80-g samples, and losses of volatiles up to 8 percent were determined. A method was found to control volatilization by using platinum crucibles, and the losses were reduced to less than ½ percent. The method consisted of forming a lip on the crucible top, projecting at right angles to the crucible walls. A platinum cover was placed over the top of the crucible so that the lip and cover were flush with each other. When volatilization of the melt began, condensation or deposition of material high in SiO_2 took place at the interface between the lip and cover, sealing the crucible. On removing the crucible at room temperature, the upper side walls had crumpled inward due to the formation of a partial vacuum (fig. 2). Using the sealed crucible technique, all but glass and MgF_2 impurities were eliminated from the mica crystals. These were present in amounts estimated to be less than 1 percent by volume in most preparations.

2.3. Composition of Crucible

An ideal crucible might be considered as one having the following qualifications: (a) Does not react with the melt; (b) withstands high tempera-

tures for long periods of time; (c) is easily molded into various forms; (d) can be reused or is inexpensive enough to be discarded.

One of the major problems in growing synthetic mica crystals is to find a crucible that is not attacked by the fluorine melt. Middle and associates [9] used crucibles composed largely of silica and alumina, but these crucibles were dissolved to such an extent by the melt that corrections in the batch composition had to be made. This method was found to be quite inadequate, for it was difficult to estimate the amount of crucible material dissolved.

In early experiments at the Bureau many ceramic bodies were tested for use as crucibles, but all were unsatisfactory as the mica melt readily attacked them. Carbon crucibles made from carbon electrodes showed promise as possible containers. The carbon did not react with the melt, and the resulting crystals could be easily removed from the crucible. The chief disadvantages of these crucibles were that finally divided carbon particles were disseminated throughout the melt, darkening the mica crystals and affecting adversely the electrical properties of the mica. To prevent the carbon crucibles from oxidizing at elevated temperatures, the crucibles had to be protected by placing them in a ceramic crucible packed with carbon or silicon carbide, which interfered with establishing proper thermal gradients within the crucible. Another undesirable feature of carbon crucibles was the relatively high porosity of the carbon bodies and the presence of bonding agents. None of the carbon crucibles tested were impervious to the volatile gases generated by the fluorine melts. With the presence of bonding agents such as clay, the crucible would be attacked by the melt, leaving voids and avenues of escape for gases.

Crucibles made of silicon carbide or lined with silicon carbide showed several undesirable features. In either case it was impossible to obtain a smooth surface, as the silicon carbide occurred as large individual crystals. These crystals acted as seeding centers for the crystallizing melt, destroying the possibility of obtaining good crystal orientation. Slight decomposition of the silicon carbide took place at the contact with the melt, releasing carbon particles, which colored the mica crystal grey.

Platinum crucibles were used in all the later crystallization experiments, as they did not appear to react with the fluorine melt. However there was a tendency for the crystals to adhere to the platinum, which not only made it necessary to peel the platinum from the crystalline cake but also oriented the mica crystals parallel to the platinum walls.

In order to economize, the inner wall only of the crucible was made of platinum. This consisted of foil 0.006 in. thick. Because platinum has little rigidity at temperatures above about 1,400° C, the liner was supported by various means, depending on the size of the container. For small melts of about 70 g, the foil container was supported in a bed of granular refractory material contained in an outer, cylindrical ceramic crucible. For larger melts, the platinum liner was fitted snugly into a ceramic crucible of the correct shape. Joints in the foil were welded with a blow torch on a steel mandrel (fig. 3), and care was taken to make the completed crucible leak-proof.

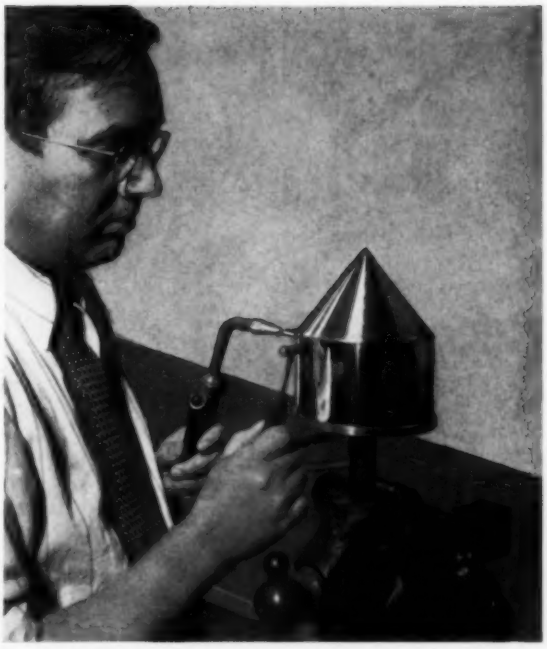

FIGURE 3. *Cylindrical crucible with conical base.*
Platinum walls being welded together on a steel mandrel.

2.4. Thermal Gradients

The disposition and steepness of temperature gradients in the crystallizing melt are of critical importance in the control of size and orientation of the mica sheets. Obviously, these are affected by the characteristics of the furnace and the shape and size of the crystallizing crucible.

As preliminary experiments indicated a melting temperature of fluorophlogopite near 1,350° C, furnaces were necessary that could produce a temperature within the crucible well above the melting temperature, say 1,500° C, in order to assure complete removal of possible nucleation centers of unmelted material. To meet this requirement, two furnaces were designed and built: (1) a platinum-wire resistance furnace for crucibles with a capacity of about 70 g (fig. 4), and (2) a Globar resistance furnace for crucibles with a capacity of about 8 kg (fig. 5).

The smaller furnace contained a cylindrical refractory core with an inside diameter of 2½ in., on which was wound the main heating element consisting of 20-gage 80-percent platinum–20-percent rhodium wire. The winding covered 9¼ in. of the core with 55 turns of the wire. A booster element made of the

FIGURE 4. *Platinum resistance furnaces for crystallization and phase determination work.*

same gage and composition wire was wound on a cylindrical core of 3-in. diameter. This element was 3-in. long, arranged coaxially with the inner core and covered the upper portion of the main element. Each winding was connected to a separate auto-transformer. The primaries of both transformers were connected to an on-off proportional program controller. Thus, the desired temperature gradient in the furnace could be maintained while the temperature in the furnace could be lowered at a predetermined rate. Experience showed that cooling rates of as low as 0.2 deg/hr could be obtained from 1,450° to 1,200° C.

The larger furnace was heated by means of Globar elements. For use with a crucible with circular section, the muffle was cylindrical with a 7-in. bore and a height of 20 in. The Globar elements were arranged in a horizontal square grid, four elements to a set, with three sets arranged vertically. The upper two sets were separated from the lower set by a horizontal baffle made of insulating refractory. In most runs, only the upper two sets were in use. These were controlled by an automatic potentiometer on an on-off control of about 15 percent of the total power, and through a platinum, platinum-rhodium thermocouple placed in the heating chamber. Temperatures could be controlled to within ± 10 deg C at 1,400° C. With the slowest cooling rates used, 0.2 deg/hr the furnace control was not sufficiently sensitive, therefore, fluctuations far exceeded the cooling rate required.

In using crucibles with elongated horizontal cross section placed in a rectangular muffle, the Globar elements were disposed parallel and close to the broad sides of the crucible and were removed from the narrow sides.

Two types of platinum-foil crucibles were used in the smaller furnace: (1) a form with cylindrical walls and a conical bottom, and (2) a form with an elongated horizontal cross section and wedge-shape bottom, similar to but smaller than that shown in

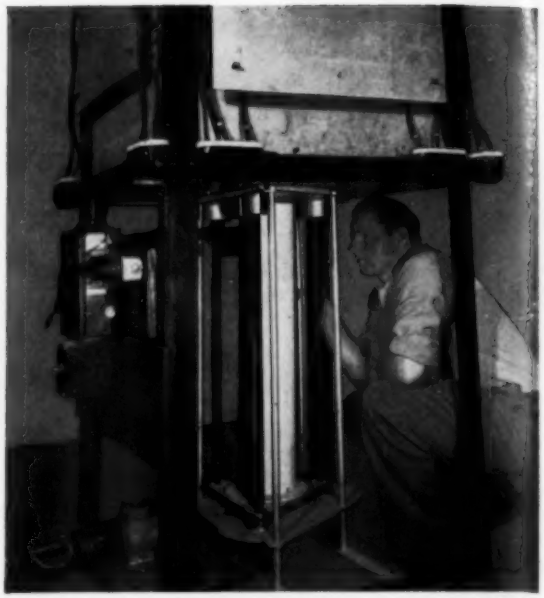

FIGURE 5. *Large Globar Crystallizing furnace with elevator lifting apparatus underneath.*

Variable speed motor at lower left lowers and raises elevator.

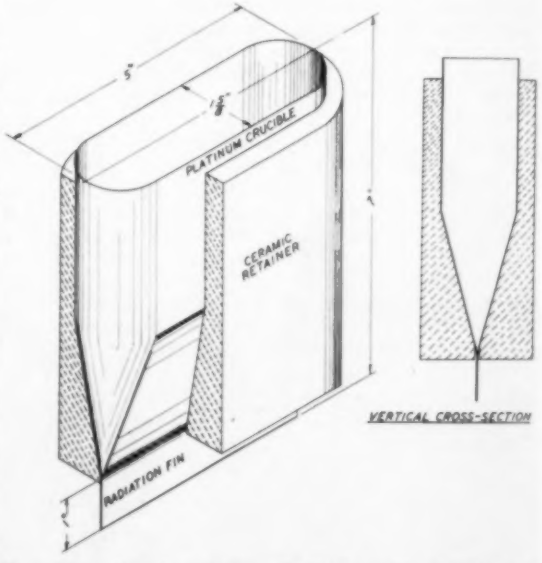

FIGURE 6. *Drawing of large elliptical crucible showing supporting ceramic container and radiation fin at base.*

figure 6. The 110 melts made in the smaller furnace provided useful information on volatilization losses, orientation control, etc., for the design of experiments in the larger furnaces. Various arrangements of cooling fins attached to the bases of both shapes

of crucible were tried in order to vary the thermal gradients (figs. 6 and 7).

The rate of cooling and the steepness of the vertical temperature gradient were varied in order to determine the effect on size of crystals and vertical orientation. The rate of cooling was varied from 15 to 0.2 deg C/hr, and the gradient from top to bottom of the crucible was varied between 15° and 90° C. In general, it was found that the slower the rate of cooling and the steeper the temperature gradient, the larger the crystals and the better the vertical orientation. Cooling rates faster than 1 deg C/hr and gradients less and 50° C provided small, randomly oriented crystals with inclusions of gas cavities (fig. 8) and with associated impurities of glass and MgF_2.

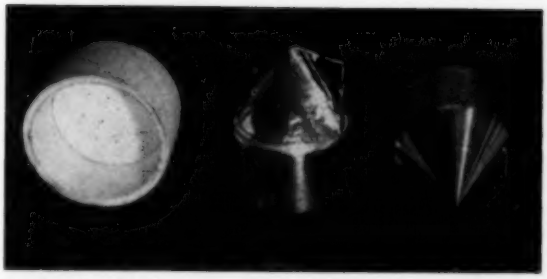

FIGURE 7. *Platinum crucible (center) showing radiation fin welded to cone portion of crucible.*

(Left) Ceramic retaining crucible; (right) steel mandrel used to shape platinum crucible.

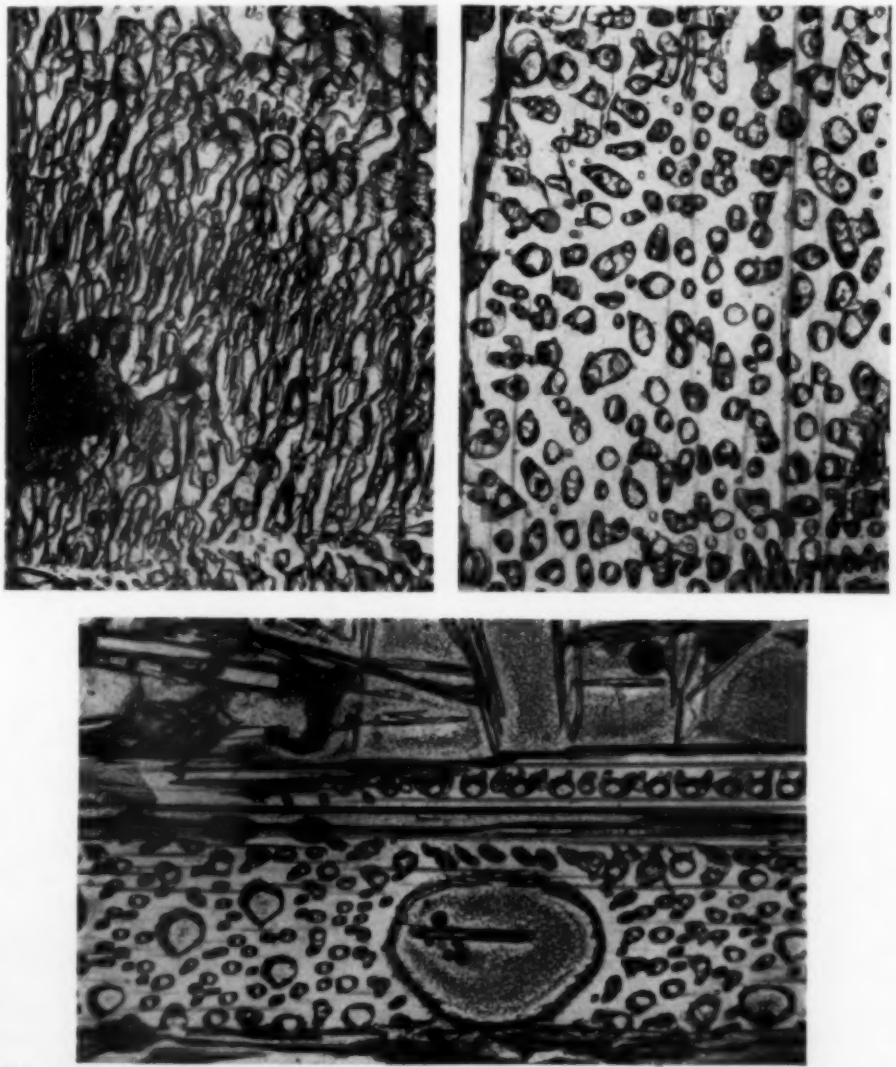

FIGURE 8.—*Thin sections of synthetic phlogopite taken at right angles to the cleavage, showing cavities in various attitudes (×40).*

FIGURE 9. *A view of the horizontal surface (one-half cake) of a large mica melt, showing good vertical orientation but lack of parallel orientation.*

FIGURE 10. *Mica crystals showing a preferred parallel orientation parallel to broad sides of small crucible.*

(A) Plan section; (B) cross section. Natural size.

In order to assure the growth of large crystals, it is necessary to reduce the number of nuclei available for new crystal formation. For this purpose, the bottoms of the crucibles were either reduced to the apex of a cone or to the trough at the base of a wedge. In the large crucible of the shape shown in figure 7, good development of vertical orientation was obtained, but the lack of horizontal orientation produced nonparallel crystals that were limited in breadth because of intersections with other growing crystals (fig. 9).

To obtain parallel lateral orientation and to prevent the intersecting growth of crystals, crucibles having the shape shown in figure 6 were used. As indicated from the small melt shown in figure 10 and the large melt shown in figure 11, a fair degree of lateral orientation was thus achieved. All of the crystallization experiments made in platinum, however, showed that both the surface of the melt and

FIGURE 11. *Mica crystals showing a preferred parallel orientation to broad sides of crucible.*

One-half surface of large melt (×1.3).

the surface against the platinum container exerted a marked effect on the orientation of the mica crystals. In one experiment made in the small furnace in platinum, the temperature gradient was deliberately reversed, and cooling took place from the top down. With the very slow rate of cooling used, 0.2 deg C/hr, a single horizontal crystal of mica formed over the entire surface of the melt, and crystallization continued until it reached a thickness of about 3 mm. Beyond this thickness, new crystals were formed predominantly parallel to the temperature gradient. In most well-crystallized melts, the crystals next to the platinum walls show a marked tendency to be parallel to the contact.

Attempts were made to obtain large crystals of mica by seeding the melt with a single mica flake at various temperatures before freezing took place. In all cases, the flakes either melted or had no effect on orientation. Pieces of corundum with known crystal orientation were introduced into melts to act as seeding centers to give a preferred orientation to the mica nuclei. There was no indication that corundum acted in orienting the mica crystals. A. Dietzel [10] claimed that a magnetic field imposed upon a crystallizing melt did have a crystal orientation effect. According to his data, the synthetic mica is slightly paramagnetic, and weak fields of about 50 to 100 gauss are sufficient to produce an orientation effect. In two experiments using a series-wound horseshoe magnet that produced about 70 gauss, no magnetic effect could be observed on a synthetic mica flake. The technique of orienting mica crystals by means of a magnetic field was thought to be impracticable, and further experiments were abandoned.

The Kyropoulos [11] technique of growing crystals was attempted with a mica melt. The essential feature of this technique is to form a single crystal by slowly withdrawing a seed from a melt. The surface of the melt is kept near but slightly above the freezing point, and crystallization takes place at the interface of the melt and the crystal. A platinum

plate 0.002 in. thick was dipped into the melt and then slowly withdrawn. Platinum has good thermal conductivity, and it was expected that a seed crystal would form at the tip of the plate, which would be below the freezing point of the melt. Trouble was experienced in keeping the melt just above freezing temperature. When the plate was dipped, either the surface of the melt would freeze completely or no crystals would form at all. This technique did not appear to offer good results unless better control of the thermal relation between the surface of the melt and the plate could be obtained.

3. Properties of Synthetic Mica

The properties of synthetic fluorophlogopite are essentially the same as its natural analogue. In thin flakes, the mica is clear and transparent. As in the natural micas, the cleavage is the most characteristic property of the synthetic mica. The cleavage occurs parallel to the (001) crystallographic plane, and in thin laminas, the flakes are elastic but less so than natural phlogopite. The mica appears to have a hardness equal to that of natural phlogopite. Its specific gravity is about 3.00, as measured on a Berman Torsion Balance. The specific gravity is troublesome to obtain, as the edges of the mica flakes are often frayed and will give erroneous results.

The optical constants of the synthetic mica were measured, using petrographic microscope techniques. The mica is negative in character, with the optical plane being parallel or nearly parallel to b(010). The optic angle 2V is about 9°, with measured indices of refraction of $\beta=1.545$, $\gamma=1.547$, and α calculated to be 1.519.

The dielectric constant and dissipation factor of six specimens were measured at the Bureau's Inductance and Capacitance Section. The measurements were made at 25° C and at three frequencies: 100, 1,000, and 100,000 cps. The values of dielectric constant at 1,000 cps vary from 5.0 to 7.0, with an average value of 6.3. As the specimens were small, ½ to ¾ in. in their longest direction, errors in measurement of dielectric constant of as much as 10 percent were to be expected. The spread in values of some 40 percent indicates a certain amount of variability in the dielectric constant of the material. The dielectric constant decreased slightly (about 2 or 3%) as the frequency was changed from 100 to 100,000 cps. Values of the dissipation factor varied from 9 to 300×10^{-4} when measured on different days. The cause for these changes with time is not known, but all of the changes were in the direction of smaller values. The average value at 1,000 cps was about 60×10^{-4}. The value of the dissipation factor seemed to decrease slightly with frequency between 100 and 100,000 cps.

The hygroscopic character of the mica or the ability of mica to absorb and retain water was determined by Donald Hubbard of the Bureau's Glass Section. In general, the method consisted of weighing the water sorbed upon exposing approximately 1.5 g of powdered mica that passed a 150 mesh standard sieve to the high (approximately 98%) humidity maintained by a saturated solution of $CaSO_4.2H_2O$. The results are expressed in water sorbed in milligrams per cubic centimeter at the end of 1 and 2 hrs. For comparison, a natural phlogopite from Argentina and three glasses have been included.

	Water sorbed in—	
	1 hour	2 hours
	mg/cm^3	mg/cm^3
Synthetic phlogopite	46	57
Argentina phlogopite	56	74
Pyrex glass	16	20
Vycor glass	11	13
No. 015 glass	88	191

Thermally, the phlogopite micas have a higher breakdown temperature than do the other micas, and this holds true for the sythetic fluorophlogopite. Several clear mica flakes were subjected to a temperature of 1,000° C for a period of 3 days. The surface of the mica had a cloudy appearance, and it was noticed that mosaic structures had formed (fig. 12). Microscopically, the thermally treated material had approximately the same optical constants as did the untreated mica, and an X-ray diffraction pattern gave essentially the same pattern as for the untreated materials.

Under the direction of B. L. Bean of this Bureau, a chemical analysis was made on selected clear flakes of synthetic mica, containing no visible impurities.

FIGURE 12. *Mosaic structure formed on surface of mica crystals after heat treatment.*

A scratch line from right to left has broken off many segments, leaving a clear area underneath (×20).

The results in weight percent are:

SiO_2	41. 87
Al_2O_3	12. 97
MgO	28. 27
F	8. 52
K_2O	10. 94
Na_2O	0. 12
Total	102. 69
Equivalent, O=F	3. 51
Total	99. 18

X-ray diffraction patterns were made of selected mica flakes, and these were compared with a natural phlogopite from Canada obtained from the U. S. National Museum. The patterns were made on a X-ray Geiger counter, using copper radiation. The synthetic and the natural patterns are essentially the same with minor differences in intensities and a small difference in *d*-spacing, as can be observed at the higher angles of 2θ (fig. 13). As mica has a highly developed cleavage, the problem of getting a random orientation of the powder grains is almost impossible, hence the intensities are not truly representative of the mica. The small difference in *d*-spacing may be due to the presence of iron in the natural sample and to the fact that the synthetic mica does not contain any (OH) ions.

Impurities were observed in all the crystallization experiments, and their presence apparently depended in part upon the loss of volatile constituents. In early crystallization experiments, using carbon and uncovered crucibles, where volatilization losses were high (about 8 to 10% by weight) impurities of forsterite, norbergite, chondrodite, and glass were present in appreciable quantities. They occurred as milky, or cloudy, patches in the plane of the mica cleavage. The orthosilicates were often inclosed in glass, or they occurred in branching structures (fig. 14). In later experiments, when volatilization was controlled by sealing the crucible, the orthosilicates were eliminated, but MgF_2 and glass remained as impurities. The glass had a mean index of about 1.51. The impurities occurred in small amounts estimated to be less than 1 percent by volume, and these were randomly scattered throughout the crystals. Mica crystals as large as 4 in.^{2} in area and free from impurities were obtained from melts in the large globar furnace. Structural defects in the form of gas bubbles were observed in those melts that were cooled quickly (greater than 1 deg C/hr).

These bubbles, or cavities, appeared to occur in planes paralleling the mica cleavage planes. It was observed that melts cooled at slower speeds contained less structural defects and fewer impurities.

FIGURE 14. *Mica flake parallel to cleavage.*

Clear mica in lower portion of photograph. Remaining area shows dendritic structures (× 30).

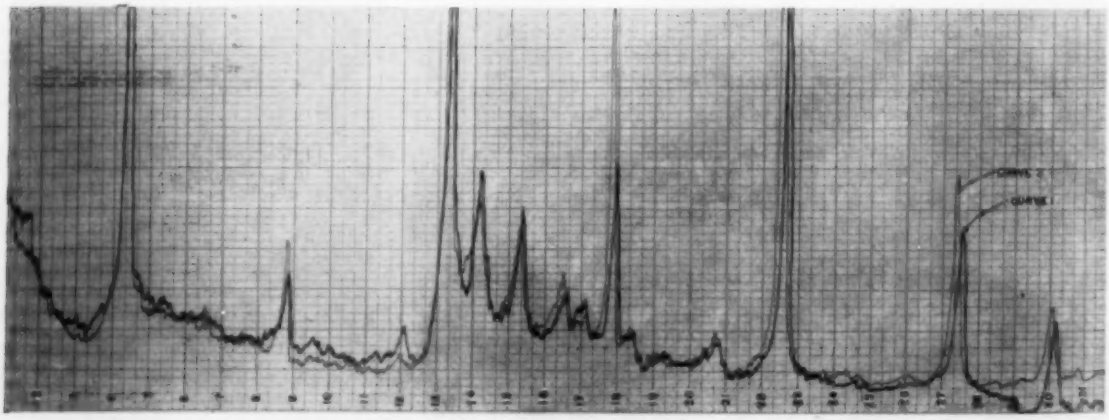

FIGURE 13. *X-ray powder diffraction patterns of natural phlogopite (1) and synthetic phlogopite (2).*

4. Summary

A synthetic fluorophlogopite mica having the approximate formula of $K_4Mg_{12}Al_4Si_{12}O_{40}F_8$ can be crystallized from a melt at atmospheric pressures. The ingredients that produced the best crystals consisted of:

	Percentage by weight
SiO_2	34. 74
Al_2O_3	11. 79
MgO	27. 99
K_2SiF_6	25. 48

This composition melts at about 1,345° C, and when it is cooled slowly in the order of magnitude of 0.3 deg C/hr, good mica crystals can be obtained. To grow large crystals it is necessary to obtain a preferred orientation of the individual crystals, otherwise growth is interrupted by intersection of one crystal with another. The disposition of the thermal gradient in a mica melt is the most important factor governing the orientation of a growing crystal, and it was found that mica crystals grow with their cleavage planes parallel to the direction of the gradient. The majority of the mica experiments were performed in closed platinum crucibles, using electric resistance furnaces.

In general, the physical, chemical, and electric properties of the synthetic fluorophlogopite, are essentially the same as those of a natural phlogopite, with the exceptions that the synthetic mica tends to be a little more brittle and does not contain (OH) ions. Thermally, it has a higher breakdown temperature, and for short periods of time can withstand temperatures of 1,200° C without noticeable changes.

5. References

[1] J. H. L. Vogt, Berg- u. hüttenmänn. Zeitung **47**, 197 (1888).
[2] F. A. Fouqué and A. M. Lévey, Compt. rend. **113,** 283 (1891).
[3] C. Doelter, Compt. rend. **2,** 178 (1888); **1,** 1 (1897).
[4] P. Hautefeville, Compt. rend. **104,** 508 (1887).
[5] L. P. de Saint-Gilles and K. Chrustschoft, Mineralog. petrog. u Mitt. **9,** 55 (1887).
[6] D. P. Grigor'ev, the preparation of artificial magnesium mica, Zentr. Mineral. Geol., p. 219 to 223 (**1934A**); the crystallization of amphibole and mica from artificial silicate melts, Zentr. Mineral. Geol., p. 117 to 123 (**1935A**); the role of fluorine, chlorine, and tungsten oxide compounds in the artificial formation of magnesium micas, Mém. soc. russe. minéral. **66,** 118 to 123 (1937); Synthesis and study of phlogopite, Compt. rend. Sci. URSS **43,** 63 to 65 (1944).
[7] E. Newman and L. W. Wells, Effect of some added material to dicalcium silicate, J. Research NBS **36,** 137 (1946) RP1696.
[8] W. Eitel, The synthesis of fluorine micas of the phlogopite group, Fiat Final Report No. **747** (1946).
[9] Bennett S. Ellefson, Crucibles for synthetic mica development, Fiat Final Report No. 1050 (1947).
[10] Paul M. Tyler, Synthetic mica research, Fiat Final Report No. 746 (1946).
[11] S. Kyropoulos, Z. anorg. chem. **154,** 308 (1926); Z. Physik **63,** 849 (1930).

Additional References on Mica Synthesis

Paul M. Tyler, Synthetic mica research, Fiat Final Report No. 746 (1946).
W. Eitel, The synthesis of fluorine mica of the phlogopite group, Fiat Final Report No. 747 (1946).
W. Eitel, Crystallochemical and microscopic investigation of synthetic phlogopites, Fiat Final Report No. 748 (1946).
W. Eitel, Regular intergrowth of synthetic phlogopite with hydrous mica, Fiat Final Report No. 749 (1946).
Rustum, Roy, Decomposition and resynthesis of the micas, J. Am. Ceram. Soc. **32,** No. 6 (1949).
Tokiti Noda, Translation of seven Japanese papers on the synthesis of fluorine micas, Tachino, translator. Section TIS Geological Survey Branch, Intelligence Division, Office of the Engineer General Headquarters, Far East Command (1945).
Chemical composition and optical properties of synthetic mica, and microscopic studies, J. Soc. Chem. Ind. (Japan) **46,** No. 8, 760 to 762 (1943).
—, Composition of fused substances from fluosilicates and mica crystallization temperature (Report No. 2); J. Soc. Chem. (Ind. (Japan) **46,** No. 10, 1082 to 1085 (1943).
—, Composition of fused substances from fluosilicates and mica crystallization temperature (Report No. 1); J. Soc. Chem. Ind. (Japan) **46,** No. 9, 921 to 923 (1943).
—Composition of fused substances from fluosilicates and mica crystallization temperature (Report No. 3) J. Soc. Chem. Ind. (Japan) **47,** No. 4, 320 to 322 (1944).
—, Synthesis of boronic phlogopite, J. Soc. Chem. Ind. (Japan) **47,** No. 6, 499 to 502 (1944).
—, Composition of fused substances from fluosilicates and mica crystallization temperature (Reports No. 4 and 5) J. Soc. Chem. Ind. (Japan) **47,** No. 7, 623 to 627 (1944).
—, Composition of fused substances from fluosilicates and mica crystallization temperature (Reports 6 and 7) J. Soc. Chem. Ind. (Japan) **48,** No. 1, 14 to 15 (1945).
D. P. Grigor'ev, The preparation of artificial magnesium mica, Zentr. Mineral. Geol., p. 219 to 223 (**1934A**).
D. P. Grigor'ev, The role of fluorine, chlorine, and tungsten oxide compounds in the artificial formation of magnesium micas, Mém. soc. russe. minéral. **64,** 347 to 354 (1935).
D. P. Grigor'ev, the crystallization of amphibole and mica from artificial silicate melts, Zentr. Mineral. Geol., p. 117 to 123 (**1935A**).
D. P. Grigor'ev, Synthesis and study of phlogopite, Compt. rend. Acad. Sci. URSS **43,** 63 to 65 (1944).
J. W. Gruner, Ammonium mica synthesized from vermiculite, Am. Mineral. **24,** 428 to 433 (1939).
J. W. Gruner, Formation and stability of muscovite in acid solutions at elevated temperatures, Am. Mineral. **24,** 624 to 628 (1939).
R. Reichmann and V. Middle, Production of synthetic mica, A Report on the synthetic mica at Siemens-Schuckert, issued in 1942.
V. Middel, Experiments on the production of synthetic mica in large experimental apparatus, Office of the Publication Board, Department of Commerce, PB32546 (1947).

WASHINGTON, December 6, 1951.

Journal of Research of the National Bureau of Standards Vol. 48, No. 5, May 1952 Research Paper 2 24

pH Response of Nonhygroscopic Glasses

Richard G. Goldman and Donald Hubbard

Electrodes prepared from glasses of low hygroscopicity, high electrical resistance, and unsatisfactory pH response in aqueous solutions have been investigated in an effort to determine if their failure to develop the full pH response is due merely to a lack of sensitivity of the indicating instrument or to a real failure of these glasses to respond to hydrogen-ion activity. By increasing the sensitivity of the indicating instrument and decreasing the thickness of the electrode membrane in order to lower the electrical resistance, many of these glasses have been shown to develop the full pH response of 59 millivolts per pH at 25° C. However, theoretical and experimental evidence indicates that glasses below a limiting hygroscopicity probably do not develop full pH response regardless of the thickness of the glass membrane, the resistance of the electrode, or the sensitivity of the indicating instrument. In fact, glass electrodes for which the thickness, electric resistance, and surface are retained essentially unaltered throughout the experiments exhibit large departures from the hydrogen electrode upon the progressive removal of water.

1. Introduction

As is well known, any silicate glass upon immersion in an aqueous solution, develops an electromotive force, which, in the case of certain glasses, varies with pH according to the Nernst equation, $\Delta E = 0.000198T\Delta$pH, over an extended range of hydrogen-ion activity. The suitability of such glasses as indicators of hydrogen-ion activity of aqueous solutions seems to be largely dependent upon adequate hygroscopicity and uniform chemical durability over as long a pH range as possible [1 to 4].[1] Glasses of adequate hygroscopicity but of very poor chemical durability exhibit substantial voltage departures (errors) from the theoretical at all pH values [2, 5 to 7]; while glasses of acceptable durability but of very low hygroscopicity also fail to develop the full pH response of 59 mv/pH at 25° C as indicated by the readings of the conventional, commercial electronic pH meters [1, 2, 5 to 8]. The present investigation was undertaken to ascertain if the failure of electrodes prepared from glasses of low hygroscopicity to exhibit the full pH response is merely the result of insufficient sensitivity of the indicating instrument or is due to an actual failure of these glasses to respond to hydrogen-ion activity. The high resistance, exceeding 1,000 megohms, of the electrodes made from the nonhygroscopic glasses would be the major contributing factor in the first case, while in the second instance the determining agent would be the absence of sufficient water in the glass to give the electrode the capacity to function as a "water electrode" [2, 9, 10] or as a "protode" [11, 12].

The problem apparently resolves itself into determining whether electronic or protonic resistance limits the proper functioning of these electrodes.[2] If a parallel exists between the electronic resistance and the voltage departures of the glass electrodes, then there is reason to believe that resistance limits their functioning; whereas, if experimental evidence points toward "sorbed water" as the only related entity, then protonic resistance is the determining factor. This latter statement is merely another way of saying that protons or hydronium ions H_3O^+ necessarily move from water site to water site within the glass.

From a practical standpoint it would be most desirable to be able to use electrodes prepared from many of the glasses of low hygroscopicity because of their superior chemical durability. Such electrodes would better survive severe operational conditions of high-acid concentrations, temperature and alkalinity.

2. Experimental Procedure

The pH response and other electrical characteristics of the experimental glass electrodes were determined on specimens of the simple Cremer-Haber type [1, 2] prepared by blowing a small tin-walled bulb on the end of a section of glass tubing. Because of their convenience of preparation and the relative simplicity of interpretation of the experimental results, mercury-filled electrodes [13] were preferred over the customary inner-solution filled type [2].

All of the routine pH and voltage measurements were obtained on a Beckman pH meter, laboratory model G, using a well-conditioned glass electrode of Corning 015, the hydrogen electrode, or the saturated calomel half cell as the reference electrode, depending on the limitations dictated by the experimental conditions.

The electrometer employed, other than the Beckman pH meter, was one assembled using the General Electric GL-5740/FP-54 Pliotron tube, which, when properly installed and operated, can readily detect currents as low as 10^{-17} amp—about 60 electrons per second. This sensitivity being far better than was feasible to handle effectively, the simple circuit recommended for the tube in measurements of currents of the order of 10^{-13} amp was modified for use in these experiments.

The hygroscopicity data were obtained by observing the increase in weight of 1.5 g of powdered glass (passed by a Tyler Standard 150-mesh sieve), exposed to the high humidity maintained by a saturated solution of $CaSO_4 \cdot 2H_2O$ under controlled conditions of temperature and time, a procedure

[1] Figures in brackets indicate the literature references at the end of this paper.
[2] It is conceivable that each is equally fundamental and that these factors parallel one another and are inseparable in the case of nonhygroscopic glasses.

previously proposed for determining the serviceability of optical glasses [14, 15].

The resistance values of the glass electrode were determined with a resistance bridge, General Radio Megohm Bridge Type 544-BS8, operating with a 500-v drop across the terminals; and also with an RCA Senior Voltohmyst, Type WV-97A, which applied only 1.5 v across the resistance under measurement. Resistance readings were obtained while the electrode was immersed in the solutions in which voltage departures appeared. The circuit was completed through the mercury column of the glass electrode and a platinum wire dipped directly into the solution. This system added an unavoidable uncertainty to the resistance readings, because it constitutes a battery whose voltage is readily affected by the oxidation-reduction potential and pH of the solution. The platinum wire and the glass electrode were held a fixed distance apart during the measurements, after which the glass electrode was replaced with a second platinum wire in order to observe the resistance offered by the solution alone. In order to reduce the electric leakage from surface conductivity, the stem of the glass electrode was treated with commercial Desicote. Organic chlorosilanes, such as Desicote, for example, dimethyl dichlorosilane, $(CH_3)_2\ SiCl_2$, react with adsorbed moisture on the surface of glass evolving HCl gas, and deposit on the glass surface a water-repellent layer of dimethylsiloxane groups approximately 10^3 molecules thick [16]. The glass electrodes were prepared from thin-walled tubing, which had a relatively low resistance per unit area. It was therefore necessary to reproduce the depth of immersion to avoid resistance variations as large as 4 megohms.

3. Results and Discussion

3.1. Instrumentation

Using the commercial Beckman pH meter, the full theoretical pH response of 59 mv/pH over the range pH 4 to 8 could be obtained with electrodes made from glasses having a hygroscopicity as low as 35 mg/cm[3]. The assembled General Electric Pliotron electrometer allowed the use of glasses of much lower hygroscopicity. For example, by careful attention to shielding and other details, the full theoretical pH response was observed with an electrode made from hard glass tubing having a hygroscopicity value of 19 mg/cm[3]. The improved sensitivity of the indicating instrument obviously effects a considerable extension of the range of usable glasses. However, instrumentation difficulties involved in obtaining adequate electric shielding and insulation became increasingly apparent. The ultimate limit to be attained by improved instrumentation, assuming perfect shielding in which all interfering charges are avoided, is the minimum noise level determined by the Brownian movement.[3] However, in the present problem the practical limit falls far short of this speculative theoretical one.

From the above evidence alone one is inclined to feel that electrodes prepared from all the glasses of very low hygroscopicity probably develop the proper pH response, but the observer is frustrated in apprehending it. In the case of electrodes made from these nonhygroscopic glasses the factors of high resistivity and low water content parallel one another, making it impossible to ascertain which one is the determining factor. Experiments designed to separate the effects of high resistance and low water content might possibly give a satisfactory answer. With the attention focused on the resistance of such electrodes, one is inclined to regard the thickness as the limiting barrier. There is some experimental evidence to support the opinion that by a sufficient reduction in the thickness, that is, by a sufficient reduction in the length of the resistive path, the full pH response of these electrodes could be realized [17, 18]. Nevertheless, the attainment of sufficiently thin films is as difficult as the other direct approaches to the problem, because of the limited strength of glass membranes thinner than 1 μ [19].

3.2. Water Content and pH Response

If one focuses attention on the water aspect of the problem concerning the response of the glass electrode to hydrogen ions, there appears to be a definite lower limit beyond which a glass electrode cannot be expected to function properly. If the glass electrode functions via the acid-base equilibria attainable through the dissociation constant of water, $[H^+]\cdot[OH^-]=K_w=10^{-14}$, then it is obvious that any glass in order to develop the full theoretical pH response must contain sufficient water to give one or more dissociated molecules at all times. It is certainly as difficult to measure these quantities of water as it is to obtain a direct answer from the instrumentation or thickness approach. But these considerations do lead to pertinent answers. If the thickness at which pH response failures appeared for electrodes made from four glasses previously investigated [18] is plotted against the hygroscopicity of the glass, a curve is obtained, figure 1, which, when extrapolated to zero thickness, indicates that electrodes from glasses having less than a certain limiting hygroscopicity (approximately 15 mg/cm[3])[4] have no proper pH function at any thickness. These data may be open to considerable criticism, but at least they do give a definite lead for additional experiments.

That nonhygroscopic glass membranes of infinitesimal thickness do not possess a satisfactory pH function is even more strikingly supported by experiments on the thickness of inhibiting films on electrode surfaces [27]. In these experiments nonhygroscopic glass layers less than 200 A (2×10^{-6}cm) thick, generated on the surface of electrodes from Corning 015 glass by acid leaching followed by heat treat-

[3] For a discussion of this limitation, see pages 251-252 of Procedures in experimental physics by John Strong (Prentice Hall, Inc., New York, N. Y., 1938).

[4] If the suggestion is accepted that the logarithm of the hygroscopicity of glass is a linear function of the departure thickness [18] then the glass exhibiting a voltage departure at zero thickness would have a hygroscopicity not greater than 8.8 mg/cm[3].

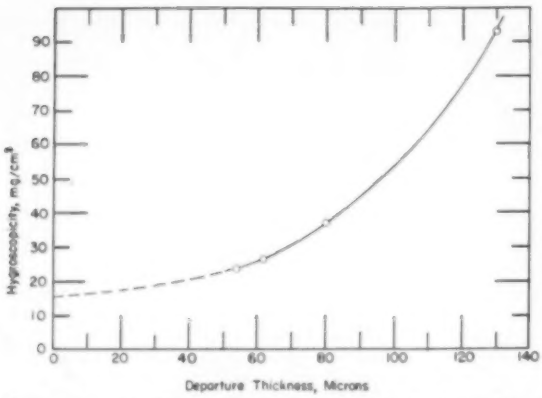

FIGURE 1. *Limiting thickness at which electrodes from glasses of various hygroscopicity values begin to show erroneous* pH *response.*

ment, caused almost complete permanent loss of pH function. Similar nonhygroscopic glass layers less than 30 A thick brought about appreciable loss of pH response.

The following experiments were designed to eliminate electric resistance as a determining factor in the observed voltage departures of the glass electrode in the "superacid" region [20, 21], and were performed in such a manner that it was hoped the only, or main, contributing variable was the progressive withdrawal of water from the electrode glass [2, 9, 10]. The voltage departures of a well-conditioned electrode of Corning 015 glass were followed well into the superacid range, using the hydrogen electrode as the reference, and any voltage departures observed were attributed to the glass electrode. This seemed a reasonable assumption because in all previous experiments in which the voltages of the glass and hydrogen electrodes have not paralleled each other, experimental evidence, such as changed chemical durability and hygroscopicity of the glass, has always indicated that the glass electrode was at fault [3 to 6]. In previous experiments in which water was withdrawn or excluded from the electrode glass by dehydration, annealing [2], and leaching followed by heat treatments [26, 27], the voltage departures introduced in each case were accompanied by variations in resistance or by surface alterations. The surface of the electrode remained unaltered throughout the present experiments, as indicated by examination of flats on Corning 015 [4] with an interferometer; at least, no alteration of the surface was detected. The usual swollen, silica-rich surface formed on this glass in acid solutions [4] was not removed, and it remained swollen over the period of the experiments in the acid solutions of high concentration. Hence, the large voltage departures cannot be attributed to any radical mechanical or chemical alteration of the electrode surface, such as is brought about by hydrofluoric acid or strongly alkaline solutions [4, 22, 23].

The data presented in table 1 and plotted in figures 2 to 6, inclusive, compare the voltage departures exhibited by a typical glass electrode with the accompanying resistance, in solutions of varying concentration for two mineral acids, H_2SO_4 and H_3PO_4, and three organic acids; HCOOH, CH_3COOH, and C_2H_5COOH. All of these voltage departures and resistance values were obtained on the same electrode, so that all the data are directly comparable. The resistance values obtained with the megohm bridge type 544–BS8 and the RCA Senior Voltohmyst are included in the plots as solid and broken lines, respectively. There is some uncertainty as to which of these instruments yields the more acceptable

TABLE 1. *Voltage departures of the glass electrode in aqueous solutions of* H_2SO_4, H_3PO_4, HCOOH, CH_3COOH, *and* C_2H_5COOH *compared with the resistance of the electrode in each of the solutions*

Solution	Departure	Resistance obtained by—	
		Bridge, 500 v	Volt-ohmyst, 1.5 v
H_2SO_4			
%	pH	mv	*Megohms*	*Megohms*
0.01	2.71	0	50	45
.1	1.7	0	50	45
1.0	0.75	0	50	46
10	0	−5	50	47
25	−0.62	−16	50	48
50	−1.49	−32	47	46
75	−2.45	−100	44	45
90	−8.1	−525	44	45
H_3PO_4				
0.01	2.4	0	44	44
.1	2.0	0	44	43
1.0	1.4	0	44	44
10	0.7	0	44	44
25	.1	0	44	43
50	−.6	−5	42	42
75	−1.1	−10	41	41
85	−1.18	−20	40	41
HCOOH				
0.01	3.2	0	48	50
.1	2.7	0	48	49
1.0	2.2	0	48	48
10	1.4	0	48	48
25	0.6	0	48	47
50	−.6	0	47	46
75	−1.6	−10	47	45
90	−2.3	−32	46	45
CH_3COOH				
0.01	2.9	0	53	46
.1	2.7	0	52	47
1.0	2.5	0	52	47
10	2.2	0	52	48
25	1.9	0	52	49
50	1.3	−5	52	49
75	0.6	−12.5	52	45
99	−2.2	−230	52	43
C_2H_5COOH				
0.01	3.2	0	51	42
.1	3.0	0	51	43
1.0	2.7	0	52	43
10	2.4	0	52	43
25	2.2	0	52	44
50	1.9	−5	52	44
75	1.1	−20	52	44
90	−0.4	−458	400	>300

data. Certainly the Voltohmyst [5] can be made to give spurious results because of the voltage developed by the battery consisting of the glass cell and the platinum electric contact.

A typical example of spurious data is shown in figure 5 for acetic acid. These are the apparent resistance values for the glass electrode obtained in the acetic acid solutions after the pH determinations had

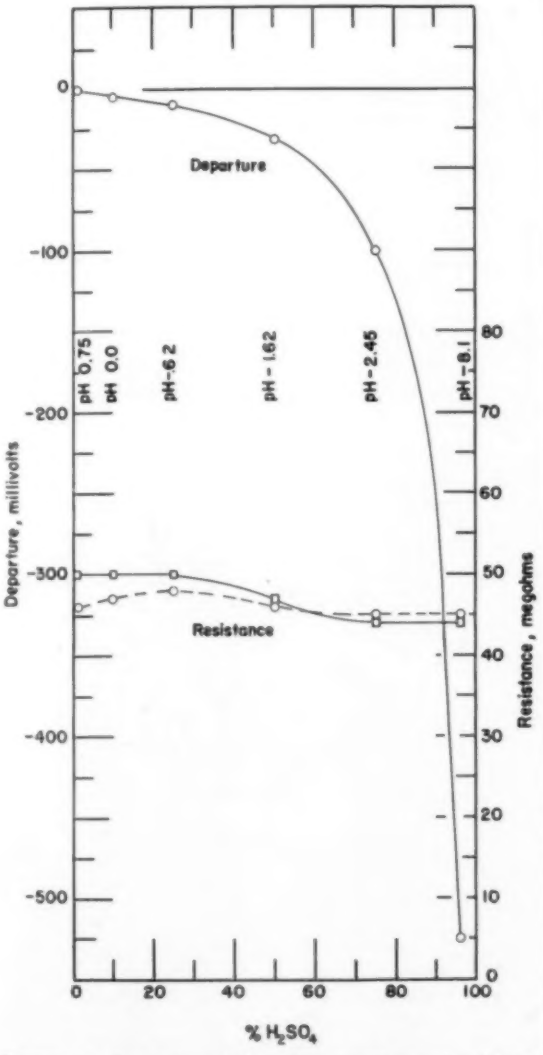

FIGURE 2. *Comparison of the voltage departure and resistance of a glass electrode (Corning 015) in various concentrations of sulfuric acid.*

——□——, Readings obtained with 500-v bridge; ——○——, readings obtained with 1.5-v voltohmyst.

[5] In order to obtain the information desired, that is, the resistance of the glass electrode in the solutions in which voltage departures were observed, it was necessary to operate this instrument in violation of the rules for its use, namely, that voltages shall not be present in the system whose resistance is to be measured

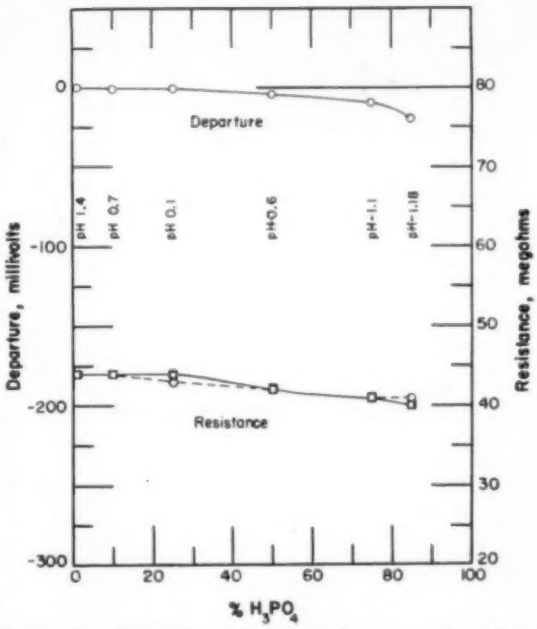

FIGURE 3. *Comparison of the voltage departure and resistance of a glass electrode (Corning 015) in various concentrations of phosphoric acid.*

——□——, Readings obtained with 500-v bridge; ——○——, readings obtained with 1.5-voltohmyst.

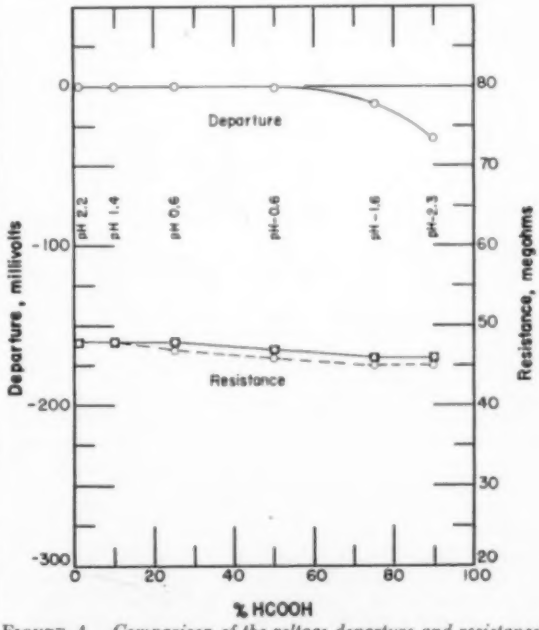

FIGURE 4. *Comparison of the voltage departure and resistance of a glass electrode (Corning 015) in various concentrations of formic acid.*

——□——, Readings obtained with 500-v bridge; ——○——, readings obtained with 1.5-v voltohmyst.

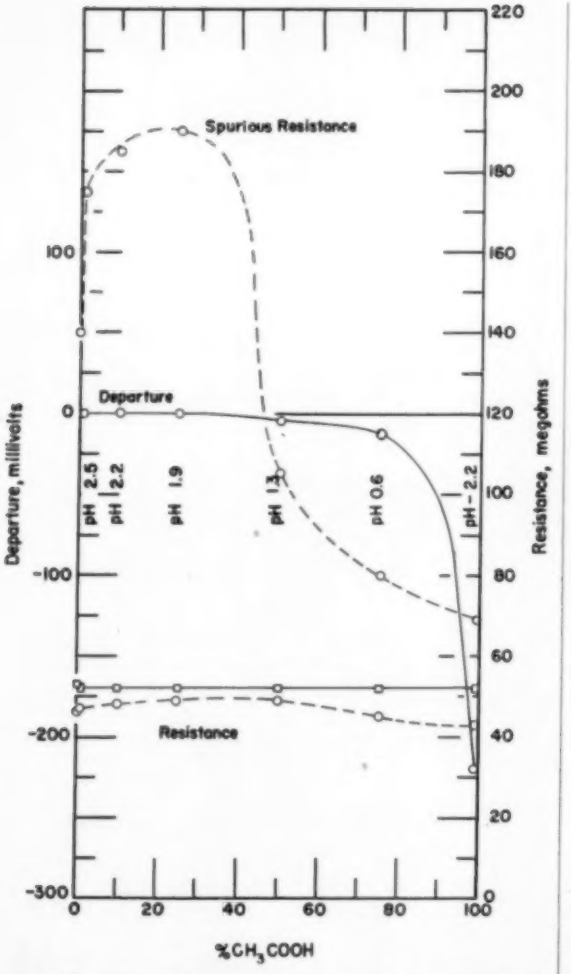

FIGURE 5. *Comparison of the voltage departure and resistance of a glass electrode (Corning 015) in various concentrations of acetic acid.*

——□——, Readings obtained with 500-v bridge; ——○——, readings obtained with 1.5-v voltohmyst.

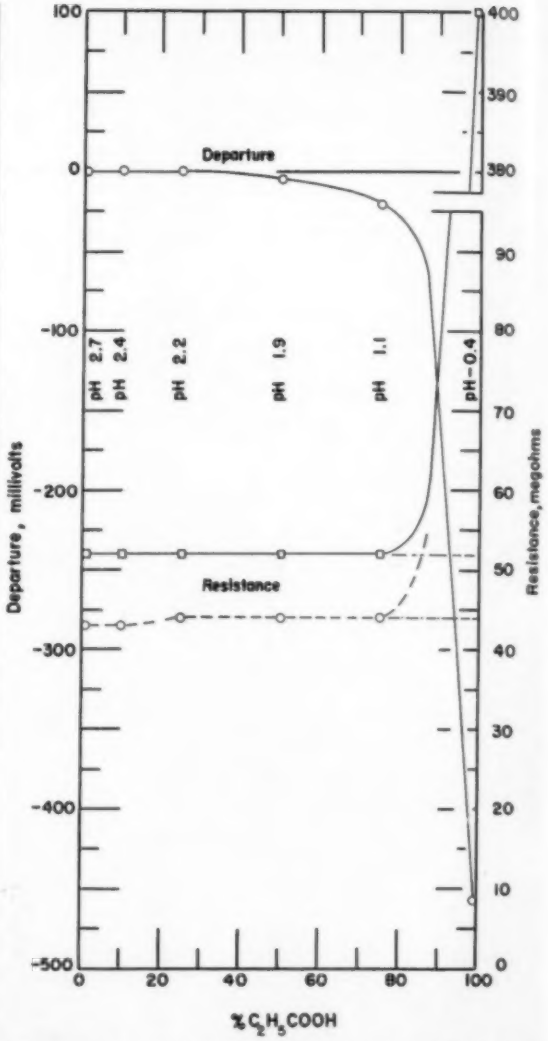

FIGURE 6. *Comparison of the voltage departure and resistance of a glass electrode (Corning 015) in various concentrations of propionic acid.*

——□——, Readings obtained with 500-v bridge; ——○——, readings obtained with 1.5-v voltohmyst.

been made, using the hydrogen electrode and the calomel half-cell. The same effect was observed after bubbling hydrogen gas through the H_2SO_4, but was not as pronounced. Voltage or polarization effects induced by the presence of hydrogen gas are presumably the reason for these high spurious resistances. It is interesting to note that the large drop in these apparent resistance values appears near 50 percent CH_3COOH, the same concentration at which marked repression in the rate of swelling had appeared in chemical-durability measurements [22]. In spite of its shortcomings, the Voltohmyst may often give more reliable readings than the resistance bridge because its low-voltage operation minimizes electrolysis and polarization. The 500 v across the terminals of the resistance bridge could conceivably cause trouble. In fact, this instrument finally terminated the resistance experiments presented in this sequence by puncturing the experimental electrode. Although the resistance bridge gave more reproducible results than did the Voltohmyst, the values obtained by the two instruments usually agreed closely, and in the cases of substantial disagreement (acetic and propionic acids) the Voltohmyst gave the lower resistance values, possibly indicating less polarization.

Figures 2 to 6 show that no general correlation

exists between the voltage departures and the corresponding resistance of the electrode in the solutions. The voltage departures follow an orderly sequence as water is withdrawn, for each series of concentrations for each of the acids, whereas the resistance of the electrode remains low and essentially constant throughout the experiments. There appears to be one notable exception to this near-constancy of the resistance in the case of propionic acid. However, this apparent increase in the resistance of the electrode turns out to be merely the resistance of the full-strength propionic acid (bp 141.1°C) superimposed on the resistance of the glass electrode.

The apparent pH values indicated by the hydrogen electrode and saturated calomel half-cell were obtained and inserted in the figures to emphasize that there was no lack of hydrogen-ion activity in any of the solutions. In other words, the failure of the glass electrode to indicate hydrogen-ion activity and to behave as a hydrogen electrode is not due to any shortage of hydrogen-ion activity of the solutions. In fact, the hydrogen-ion activity of the concentrated acid solutions is anomalously high, as indicated by the hydrogen electrode. This latter phenomenon has often raised the question: does either the glass or hydrogen electrode give any acceptable information about concentrated solutions of these strong electrolytes, especially as the hydrogen-electrode readings imply activity of hydrogen ions far in excess of that available from the full dissociation of the acid molecule? However, this anomaly is one of the unsolved problems in the theory of solutions [24].

A glance at figure 7, in which the pH values indicated by the glass and hydrogen electrodes in the sulfuric acid solutions are plotted, leaves one with the impression that the glass electrode gives a more logical answer than does the hydrogen electrode. Accepting the Wynne-Jones line of reasoning that the glass electrode responds to protons [12] rather than water activity [2, 9, 10], the pH values obtained by the glass electrode tell a more comprehendible story about the dissociation of H_2SO_4 than does the exaggerated hydrogen-ion activity indicated by the hydrogen electrode. Certainly the hydrogen electrode must be responding to some property other than hydrogen ions.

4. Summary

Experiments have been carried out that were designed to ascertain if electrodes prepared from glasses of low hygroscopicity and high electrical resistance fail to demonstrate full theoretical pH response because of the lack of sensitivity of the indicating instrument or because the glasses fail to respond to hydrogen-ion activity due to the absence of water. By means of an electrometer having greater sensitivity than the usual commercial electronic pH meters, electrodes prepared from glasses of hygroscopicity lying between 19 and 35 mg/cm³ were found to yield the full theoretical pH response, indicating that considerable use may be obtained from nonhygroscopic glasses by improved instrumentation. However, the increased resistance exhibited by electrodes prepared from glasses of still lower hygroscopicity appears to offer an insurmountable obstacle to the direct resolution of this problem.

Nevertheless, evidence was obtained by extrapolation of hygroscopicity-thickness data that indicated that electrodes from glasses below a limiting hygroscopicity would not have full pH response, even though their thickness were reduced to near zero. Further evidence showed that upon progressive removal of water from the glass, voltage departures appeared in electrodes, although the electric resistance remained low and essentially constant throughout the experiments, indicating that glasses of very low water content would not show full pH response to hydrogen-ion activity, regardless of the sensitivity of the indicating instrument. These data and conclusions seem to be compatible with the findings of earlier investigators [2, 3, 5, 6, 7, 9, 10, 25, 26], which indicate that water plays a vital role in the mechanism of the glass-electrode response to hydrogen-ion activity.

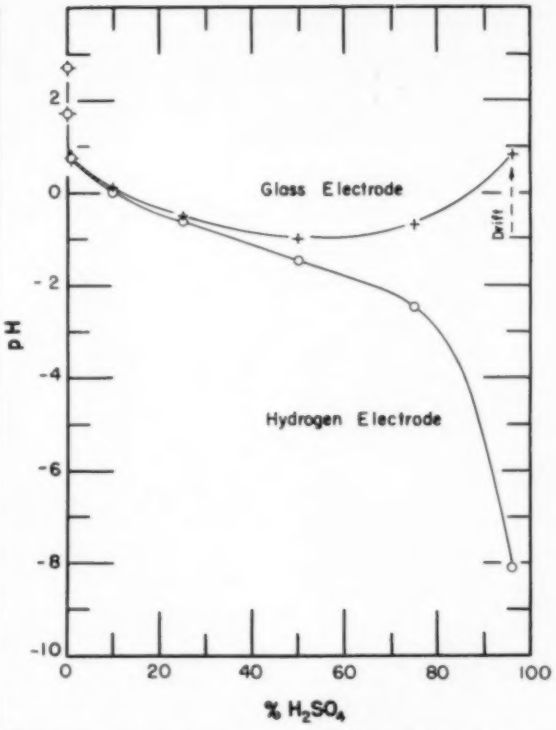

FIGURE 7. *Comparison of the* pH *values indicated by the hydrogen and glass electrodes for aqueous solutions of* H_2SO_4, *using the saturated calomel half-cell as the reference electrode.*

5. References

[1] F. Haber and Z. Klemensiewicz, On electrical interfacial potentials, Z. physik. Chem. **67,** 385 (1909).

[2] M. Dole, Glass electrode (John Wiley & Sons, Inc., New York, N. Y., 1941).

[3] W. S. Hughes, On Haber's glass cell, J. Chem. Soc. 491 (**1928**).

[4] Donald Hubbard, Edgar H. Hamilton, and Alfred N. Finn, Effect of the solubility of glass on the behavior of the glass electrode, J. Research NBS **22,** 339 (1939) RP1187.

[5] Donald Hubbard, Given W. Cleek, and Gerald F. Rynders, Electrode function (pH response), hygroscopicity, and chemical durability of Na_2O-CaO-SiO_2 glasses, J. Research NBS **44,** 247 (1950) RP2076.

[6] Donald Hubbard, Mason H. Black, and Gerald F. Rynders, Electrode function (pH response), hygroscopicity, and chemical durability of soda-lead oxide-silica glasses, J. Research NBS **45,** 430 (1950) RP2154.

[7] Donald Hubbard, Mason H. Black, Sylvanus F. Holley, and Gerald F. Rynders, Electrode function (pH response), hygroscopicity, and chemical durability of soda-potash-silica glasses, J. Research NBS **46,** 168 (1951) RP2189.

[8] Lillie B. Jenkins, Elizabeth M. Krumrine, and Donald Hubbard, Amelung glasses (early U. S. industrial 1785–1795) compared with some modern commercial galsses (1951). In preparation for publication.

[9] M. Dole, The relation between the activity of the water and the potentials of the glass electrode, J. Am. Chem. Soc. **54,** 2120 (1932).

[10] M. Dole, The theory of the glass electrode. II The glass as a water electrode, J. Am. Chem. Soc. **54,** 3095 (1932).

[11] Theodore Shedlovsky, Electromotive force from proton exchange reactions, National Academy of Science Annual Meeting (1951); National Bureau of Standards, NBS Circular 524 (in press).

[12] W. F. K. Wynne-Jones, The glass electrode, Office of Naval Research, London. European Scientific Notes **5,** 217 (1951).

[13] M. R. Thompson, A metal-connected glass electrode, BS J. Research **9,** 833 (1932) RP511.

[14] Donald Hubbard, Hygroscopicity of optical glass as an indicator of serviceability, J. Research NBS **36,** 365 (1951) RP1706.

[15] Donald Hubbard, Hygroscopicity and electrode function (pH response) of glasses as a measure of serviceability, J. Research NBS **36,** 511 (1951) RP1719.

[16] J. E. Stanworth, Physical properties of glass (Oxford University Press, London, 1950).

[17] H. Kahler and F. DeEds, J. Am. Chem. Soc. **53,** 2998 (1931).

[18] J. J. Diamond and Donald Hubbard, The thickness of glass electrodes, J. Research NBS **47,** 443 (1951) RP2270.

[19] D. A. MacInnes and M. Dole, Test of a new type of glass electrode, Ind. Eng. Chem. Anal. Ed. **1,** 57 (1929).

[20] D. A. MacInnes and D. Belcher, Further studies on the glass electrode, J. Am. Chem. Soc. **53,** 3315 (1931).

[21] G. Buchbock, A property of the glass electrode, Z. physik. Chem. **156A,** 232 (1931).

[22] Donald Hubbard and Gerald F. Rynders, Voltage anomalies of the glass electrode and the chemical durability of the glass, J. Research NBS **39,** 561 (1947) RP1848.

[23] Donald Hubbard and Richard G. Goldman, Heterogeneous equilibria at the glass electrode-solution interface, NBS, publication pending.

[24] G. N. Lewis and Merle Randall, Thermodynamics and free energy of chemical substances (McGraw-Hill Book Co., Inc., New York, N. Y., 1923).

[25] H. Yoshimura, Effect of water on the potential of the glass electrode, Bul. Chem. Soc. Japan **12,** 359 (1937).

[26] Donald Hubbard and Gerald F. Rynders, Effect of annealing and other heat treatment on the pH response of the glass electrode, J. Research NBS **40,** 105 (1948) RP1859.

[27] Donald Hubbard and Gerald F. Rynders, Thickness of inhibiting films on glass electrode surfaces, J. Research NBS **41,** 163 (1948) RP1915.

WASHINGTON, February 1, 1952.

Journal of Research of the National Bureau of Standards Vol. 48, No. 5, May 1952 Research Paper 2325

Wavelengths of Rotational Lines in the Water-Vapor Bands at 0.93 and 1.13 Microns

C. C. Kiess

The infrared water-vapor bands at 0.93 and 1.13 microns have been photographed with the grating spectrographs of the National Bureau of Standards. These bands appear in absorption in the continuous spectrum of white-light sources, part or all of the optical path being in air. They appear also in emission in the spectra of flames containing hydrogen and oxygen compounds. In relatively short light-paths, the rotational lines of these bands are sharp and show little or no tendency toward diffuseness, even in air for which the relative humidity is 90 percent. Their wavelengths may be measured with accuracy on high-dispersion spectrograms. Wavelengths, estimated intensities, and wave numbers, as derived from the spectrograms, are presented. The wavelengths are recommended for use in calibrating infrared spectrometers.

1. Introduction

Among the outstanding features in the near infrared solar spectrum are the bands due to absorption by the water vapor in the earth's atmosphere. Between 9000 A and the limit photographically attainable at 13500 A there are several bands that make up the groups of lines designated by the symbols ρ, σ, τ, and Φ on Langley's normal map of the solar spectrum [1].[1] These, and other absorption features, beyond the visible limit in the red, have been observed frequently ever since the discovery of the infrared region of the spectrum by Sir William Herschel in 1800 [2]. However, it was not until 70 years later that their telluric origin was established by Lamansky [3], who observed their fluctuations in intensity with altitude of the sun and humidity of the atmosphere. Subsequently, this behavior of the bands was verified when Abney and his collaborators made the first photographs of the near infrared spectrum of the sun. In 1883 Abney and Festing [4] reported that at a high altitude on a dry day the banded absorption between 9420 and 9800 A nearly disappeared from the sun's spectrum. At such times, according to these authors, the strengths of the bands, as they were observed on humid days, could be restored to the solar spectrum by placing a water-cell in front of the slit of the spectrograph. Control observations of an artificial source through cells of water 3 and 12 inches thick revealed the same "water bands". But these observers were reluctant to attribute them to the absorption of water vapor because the "Fraunhofer lines in the band are irregularly distributed through the band . . . and do not spread out as the darkness of the band increases". However, it is known now that the absorptions of liquid water and its vapor are not the same, and therefore the general or continuous darkness, observed in Abney and Festing's experiments with the water-cells, is not to be confused with the selective absorption of the vapor.

Although the origin of the bands in the absorption of water vapor was long suspected the fact was established beyond doubt only in 1918 by Hettner [5], who observed the radiant energy from a Nernst glow lamp through a column of water vapor. He placed the maxima of the bands at 0.94μ and 1.128 μ, respectively, noting that previously Fowle [6] had detected a depression at 1.13 μ in the Φ band of the solar spectrum. Except for the photographic method of Abney, which apparently was not successful in the hands of later investigators, the only way of studying the bands was with radiometric devices of various kinds. Observations of this kind, with the low dispersions employed, usually delineate the outline of the bands without yielding much information about their finer structure.

The first photographic recording of the ρ, σ, τ bands, since the days of Abney, was made more than 30 years ago by Meggers [7]. With the plane grating spectrograph of the Johns Hopkins University, Meggers photographed the sun's spectrum from 6800 to 9600 A on ordinary plates sensitized with dicyanin. A few years later Burns [8], and then Brackett [9], again by using plates sensitized with dicyanin, were able to extend the sun's spectrum to nearly 9900 A. Both these observers noted the variable intensity of some of the strong lines near 9300 A and suggested that terrestrial water vapor was very probably the cause of their appearance and behavior.

About 25 years ago, when new photosensitizers became available, it was possible to record spectra photographically with high dispersion; first out to 11000 A, later out to 13000 A, with the same precision as that used for the shorter wavelength regions. At the National Bureau of Standards [10] the work of extending our knowledge of the infrared emission spectra was undertaken on about 50 chemical elements. One of the first fruits of these new investigations was the recognition of the water-vapor absorption bands superimposed on the continuum that usually accompanies the emission lines and bands in the spectra of arcs between metallic electrodes. Their nuisance value in a study of emission-line spectra was soon felt when it was realized that errors of wavelength and intensity afflicted all lines that were blended partially or almost completely with the absorption lines. Therefore, it became important

[1] Figures in brackets indicate the literature references at the end of this paper.

to determine the wavelengths and intensities of these lines so that their effect on nearly coincident atomic and molecular emission lines could be estimated.

In recent years, however, the importance of these bands has been felt in other branches of spectroscopy. In the investigation with infrared spectrometers of various flames containing hydrogen and oxygen compounds, these bands and others, due to the H_2O molecule, appear in emission with intensities proportional to the temperature of the flame. In experiments on the absorption of liquids and vapors, they appear as sharp absorption lines in the continuous spectrum of the source, if the spectrometer is filled with air containing moisture. These facts have led to the suggestion by Plyler [11] that the bands be used as standards in the calibration of infrared spectrometers, particularly of grating spectrometers in which the shortward regions of overlapping orders can be used to calibrate the longward first-order spectrum, in which reliable standards are still lacking. The allocation of the lines to the P, Q, and R branches of the bands in the vibration-rotation spectrum of the H_2O molecule was first carried through by Mecke and collaborators [12], who interpreted the spectrum on the basis of the unsymmetrical rotator. The wavelengths used by them for the bands at 0.93 and 1.13 μ are those measured by Lueg and Hedfeld [13]. This earlier work on the analysis of the bands was later revised and extended by Benedict [14].

2. Experimental Details

In order to secure spectrograms of the water-vapor bands unaffected by atomic and molecular emission features, several exposures were made to a Point-o-lite lamp, a very convenient source of continuous radiation. Two sets of observations were made, the first early in December 1934 when the air in the laboratory was dry (the recorded relative humidity being between 20 and 25%); the second in July and August 1935, when high relative humidities were recorded (90% on the July date, 50 to 57% on the August dates). To obtain the spectrograms, two 6-in. concave gratings of 21-ft. radius were used: one was a Rowland grating with 20,000 lines per inch, the other a Wood grating with 15,000 lines per inch. Each grating was set up in a Wadsworth mounting, in which the total light path source-to-collimator-to-grating-to-plate was approximately 11 m. The Rowland grating, with a dispersion of 3.4 A/mm in the first order, was used only for the band at 0.93 μ, whereas the Wood grating, dispersion 4.8 A/mm, was used for both bands. In juxtaposition to the water-vapor spectrum, each plate received exposures to the iron arc to supply standards for the wavelength reductions. The desired order of spectrum for each exposure was secured by inserting appropriate colored-glass filters in the light path between the source and the slit. For recording the spectra, plates coated with Eastman I–M and I–Q emulsions were used. Immediately before exposure, each plate was hypersensitized in an ammonia bath according to the procedure described by Burka [15]. The bands are illustrated in figure 1.

3. Discussion and Results

Visual inspection of the spectrograms reveals only slight differences among those taken on dry and humid days. The latter show a few more very faint lines than do the plates taken when the air was relatively dry; but there is no indication of broadening and blending of the band lines such as occur on the solar spectrograms. The wavelengths measured on the different plates for the individual lines are in very close agreement. Therefore, the values adopted for entry in the first columns of tables 1 and 2 are the unweighted averages of the different measurements. For all the lines in table 1, except a few of the faintest, the wavelengths are the means of four measurements. Similarly, the values of nearly all the lines of table 2 are the means of three measurements. In the third column of each table are given the vacuum wave numbers of the lines as interpolated from Kayser's *Tabelle der Schwingungszahlen*. For

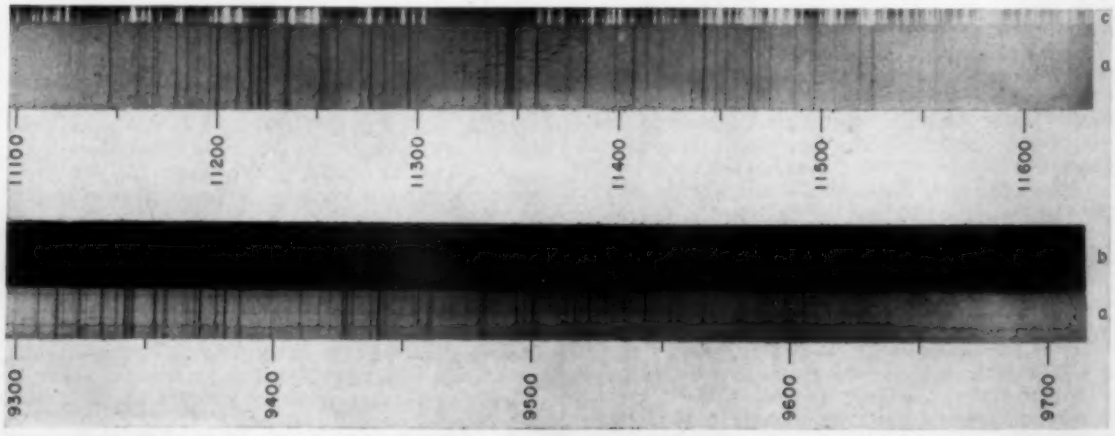

FIGURE 1. *Infrared bands of water-vapor: (a) water-vapor; (b) Fe arc, 2d order; (c) Fe arc, 3d order.*

TABLE 1. *Wavelengths, intensities, and wave numbers in the band at 1.13 μ*

Wavelength	Intensity and notes	Wave number	Wavelength	Intensity and notes	Wave number	Wavelength	Intensity and notes	Wave number	Wavelength	Intensity and notes	Wave number
A		cm^{-1}	*A*		cm^{-1}	*A*		cm^{-1}	*A*		cm^{-1}
11620. 26	1	8603. 30	11446. 62	12	8733. 81	11312. 35	1	8837. 47	11197. 08	10	8928. 44
11600. 99	1	8617. 59	11440. 47	50	8738. 50	11298. 81	5	8848. 05	11192. 01	4	8932. 49
11586. 66	4	8628. 25	11434. 68	10	8742. 92	11294. 42	50	8851. 50	11190. 85	7	8933. 41
11575. 25	2	8636. 76	11419. 03	5	8754. 90	11290. 11	2	8854. 88	11189. 12	5	8934. 79
11562. 19	1	8646. 51	11412. 27	10	8760. 02	11286. 85	12	8857. 43	11187. 26	5	8936. 28
11554. 71	7	8652. 11	11405. 83	30	8765. 04	11282. 14	12	8861. 13	11186. 16	20	8937. 16
11546. 74	1	8658. 08	11397. 41	1	8771. 52	11275. 75	40	8866. 15	11180. 75	25	8941. 49
11541. 64	1	8661. 90	11396. 36	2	8772. 32	11271. 02	15	8869. 87	11172. 16	10*d*?	8948. 36
11537. 38	3	8665. 13	11382. 23	20	8783. 21	11265. 06	1	8874. 56	11169. 73	15	8950. 31
11533. 95	<1	8667. 67	11373. 84	1	8789. 69	11259. 31	20	8879. 09	11165. 80	3	8953. 46
11524. 25	12	8674. 97	11373. 26	1	8790. 13	11254. 57	12	8882. 84	11165. 02	1	8954. 08
11523. 19	10	8675. 77	11358. 00	15	8801. 95	11253. 13	4	8883. 98	11163. 79	2	8955. 07
11517. 23	12	8680. 27	11357. 76	25	8802. 13	11252. 47	5	8884. 50	11163. 06	1	8955. 65
11509. 96	2	8685. 75	11349. 62	7	8808. 45	11251. 15	40	8885. 54	11162. 29	5	8956. 27
11505. 37	2	8689. 21	11348. 48	2	8809. 33	11248. 26	1	8887. 82	11160. 36	2	8957. 82
11497. 37	<1	8695. 26	11346. 30	20	8811. 02	11242. 04	<1	8892. 74	11159. 35	1	8958. 63
11495. 12	20*d*?	8696. 96	11345. 04	5	8812. 00	11240. 67	<1	8893. 82	11155. 38	<1	8961. 82
11493. 10	3	8698. 49	11343. 78	18	8812. 98	11235. 17	25	8898. 18	11152. 03	4	8964. 51
11492. 08	<1	8699. 26	11343. 26	1	8813. 38	11233. 98	5	8899. 12	11148. 91	20*d*?	8967. 03
11485. 52	5*d*?	8704. 23	11342. 54	4	8813. 95	11233. 30	7	8899. 66	11147. 97	1	8967. 78
11483. 78	<1	8705. 55	11338. 13	15	8817. 37	11224. 92	25	8906. 30	11136. 05	2	8977. 38
11473. 12	15	8713. 64	11337. 31	<1	8818. 01	11222. 92	1	8907. 88	11134. 37	2	8978. 73
11471. 64	1	8714. 76	11334. 29	2	8820. 36	11221. 40	5	8909. 09	11128. 23	<1	8983. 68
11470. 20	7	8715. 86	11333. 31	6	8821. 12	11221. 14	20	8909. 30	11126. 97	1	8984. 70
11467. 50	10	8717. 91	11332. 30	5	8821. 90	11217. 40	7	8912. 27	11120. 62	<1	8989. 83
11463. 69	40	8720. 81	11329. 64	2	8823. 97	11216. 54	20	8912. 96	11112. 03	2	8996. 79
11456. 30	10	8726. 43	11326. 99	<1	8826. 05	11210. 62	18	8917. 66	11109. 40	1	8998. 92
11451. 47	15	8730. 11	11321. 64	7	8830. 22	11201. 12	15	8925. 22	11106. 00	1	9001. 68
						11200. 84	15	8925. 45	11102. 89	2	9004. 20

TABLE 2. *Wave lengths, intensities, and wave numbers in the band at 0.93 μ*

Wave length	Intensity and notes	Wave number	Wave length	Intensity and notes	Wave number	Wave length	Intensity and notes	Wave number	Wave length	Intensity and notes	Wave number
A		cm^{-1}	*A*		cm^{-1}	*A*		cm^{-1}	*A*		cm^{-1}
9782. 45	<1	10219. 60	9568. 96	1	10447. 59	9461. 33	6	10566. 44	9357. 53	4	10683. 65
9757. 65	1	10245. 56	9566. 63	7	10450. 14	9460. 01	10	10567. 92	9354. 29	20	10687. 35
9749. 32	<1	10254. 31	9565. 07	3	10451. 84	9456. 16	10	10572. 22	9353. 58	1	10688. 16
9743. 56	1	10260. 38	9563. 89	1	10453. 13	9454. 67	1	10573. 88	9353. 04	<1	10688. 78
9715. 32	<1	10290. 20	9562. 75	<1*d*?	10454. 38	9454. 08	1	10574. 54	9345. 48	15	10697. 43
9701. 41	<1	10304. 95	9557. 31	3	10460. 33	9445. 98	1	10583. 61	9344. 16	5	10698. 94
9680. 37	1	10327. 35	9556. 11	<1	10461. 64	9444. 47	<1	10585. 30	9343. 52	2	10699. 67
9670. 66	<1	10337. 72	9553. 43	4	10464. 58	9443. 32	5	10586. 60	9342. 61	20	10700. 72
9662. 30	1	10346. 67	9548. 74	<1	10469. 71	9441. 06	10	10589. 13	9339. 37	8	10704. 43
9659. 81	<1	10349. 33	9544. 35	3	10474. 53	9440. 66	10	10589. 58	9338. 44	<1	10705. 49
9645. 62	1	10364. 56	9543. 93	7	10474. 99	9437. 73	7	10592. 87	9337. 12	<1	10707. 00
9640. 73	<1*w*	10369. 81	9540. 90	1	10478. 32	9430. 62	5	10600. 85	9336. 03	<1	10708. 26
9637. 50	1*w*	10373. 29	9535. 94	2*w*	10483. 77	9428. 23	20	10603. 54	9334. 51	3	10710. 00
9626. 42	1	10385. 23	9528. 43	1	10492. 03	9426. 87	18	10605. 08	9333. 55	10	10711. 10
9622. 72	1	10389. 22	9525. 06	1	10495. 74	9421. 81	1	10610. 77	9331. 51	1	10713. 44
9621. 25	1	10390. 81	9522. 27	15	10498. 82	9417. 66	3	10615. 44	9327. 74	2	10717. 77
9620. 01	<1	10392. 15	9519. 31	2	10502. 09	9410. 42	4	10623. 61	9325. 46	5*d*?	10720. 39
9618. 17	1	10394. 14	9516. 99	8	10504. 65	9398. 97	1	10636. 55	9324. 19	1	10721. 85
9615. 50	<1	10397. 03	9501. 73	3	10521. 52	9387. 02	1	10650. 09	9323. 19	1	10723. 00
9615. 03	1	10397. 53	9500. 92	12	10522. 42	9386. 65	3	10650. 51	9319. 07	2	10727. 74
9610. 05	1	10402. 92	9497. 44	5	10526. 27	9381. 14	15	10656. 76	9316. 84	5	10730. 31
9605. 12	1*w*	10408. 26	9494. 31	10	10529. 74	9379. 60	<1	10658. 51	9316. 24	2	10731. 00
9592. 53	1	10421. 92	9493. 44	1	10530. 70	9377. 67	12	10660. 71	9315. 96	<1	10731. 33
9591. 23	1	10423. 34	9481. 67	15	10543. 78	9371. 45	20	10667. 78	9315. 15	1	10732. 26
9590. 14	1	10424. 52	9480. 27	5	10545. 33	9369. 39	6	10670. 13	9309. 44	5	10738. 84
9589. 06	1	10425. 69	9479. 19	<1	10546. 53	9366. 41	4	10673. 52	9308. 09	4*d*?	10740. 40
9581. 12	3	10434. 33	9474. 47	1	10551. 79	9364. 83	3*w*	10675. 32	9303. 76	1	10745. 39
9579. 94	1*w*	10435. 62	9469. 39	2	10557. 45	9358. 65	5	10682. 37	9300. 88	<1	10748. 72
9571. 31	<1	10445. 03	9468. 64	1	10558. 29	9357. 81	5	10683. 33	9300. 35	<1	10749. 33

the band at 0.93 μ, they were read directly from the table; for the 1.15-μ band, they were interpolated by the procedure described by H. D. Babcock [16].

The second columns of tables 1 and 2 contain the intensities of the band lines as based on visual estimates. A comparison of these estimates for the fainter lines with those made by Babcock and Moore [17] for the same lines in the solar spectrum shows that on the average those marked <1, 1, and 2 correspond, respectively, to the solar estimates 25, 40, and 50. For the stronger lines, no reliable correlation with the solar intensities is feasible because of blending; but it is evident from the above comparison that the fainter members of the bands cannot be expected to appear in the laboratory spectra. The letters *w* and *d* after the intensities of some of the lines indicate that they are wide, probably unresolved pairs or pairs on the verge of resolution.

In the solar spectrum, the water-vapor lines are greatly widened owing to the long light path in the earth's atmosphere, so that most of them are affected by blending with other lines of terrestrial or solar origin. However, for some of the fainter lines the effects of blending are very slight or absent. The wavelengths measured for such lines in the solar and in the laboratory spectra, as given in tables 1 and 2, are in very good agreement. On the other hand, a comparison of the wavelengths recorded in this paper with those published by Lueg and Hedfeld show marked differences. These investigators followed an experimental procedure essentially the same as that described in this paper. However, their wavelengths for the stronger lines in the 1.13-μ band are, on the average, 0.16 A shorter than those of table 1, whereas those they give for the 0.93-μ band are longer than the wavelengths of table 2 by 0.16 A. The cause of the discrepancy between the two sets of measurement is not apparent.

4. References

[1] S. P. Langley, Ann. Astrophys. Observ. Smithsonian Inst. **1,** 200 (1900).
[2] W. Herschel, Phil. Trans. Roy. Soc. London **90,** 284 (1800).
[3] S. Lamansky, Ann. Physik [II] **146,** 200 (1872).
[4] W. de W. Abney and E. R. Festing, Proc. Roy. Soc. (London) **35,** 80 (1883).
[5] G. Hettner, Ann. Physik [IV] **55,** 492 (1918).
[6] F. E. Fowle, Astrophys. J. **35,** 151 (1912).
[7] W. F. Meggers, Astrophys. J. **47,** 1 (1918).
[8] K. Burns, Lick Observ. Bul. **10,** 64 (1920).
[9] F. S. Brackett, Astrophys. J. **53,** 121 (1921).
[10] W. F. Meggers and C. C. Kiess, BS J. Research **9,** 309 (1932) RP473.
[11] E. K. Plyler, J. Research NBS **48,** 221 (1952) RP2309.
[12] R. Mecke, Z. Physik. **81,** 313 and 445 (1933).
[13] P. Lueg and K. Hedfeld, Z. Physik. **75,** 512 (1932).
[14] W. S. Benedict, Phys. Rev. **74,** 702, 703, and 1246 (1948); NBS Report 1123 to Office of Naval Research.
[15] S. M. Burka, J. Franklin Inst. **189,** 25 (1920).
[16] H. D. Babcock, Phys. Rev. **46,** 382 (1934).
[17] H. D. Babcock and C. E. Moore, Carnegie Institution of Washington, Publication No. 579 (1947).

WASHINGTON, January 10, 1952.

Journal of Research of the National Bureau of Standards Vol. 48, No. 5, May 1952 Research Paper 2326

Comparative Strengths of Four Organic Bases in Benzene[1]

Marion Maclean Davis and Hannah B. Hetzer

Spectrophotometric studies have shown that the reaction of the base 1,3-di-*o*-tolylguanidine with the acidic indicator dye bromophthalein magenta E (tetrabromophenolphthalein ethyl ester) in benzene at 25° C, like the reactions of 1,3-diphenylguanidine and 1,2,3-triphenylguanidine with the same indicator, can be represented by the following two equations:

$$\underset{\text{(colorless base)}}{B} + \underset{\text{(yellow acid)}}{HA} \rightleftharpoons \underset{\text{(magenta salt)}}{BH^{+}.A^{-}}$$

$$BH^{+}.A^{-} + B \rightleftharpoons \underset{\text{(blue salt)}}{(BHB)^{+}A^{-}}$$

For ditolylguanidine, the equilibrium constants K_1 and K_2 for the first and second reactions, respectively, are estimated to be 1.1×10^{6} and 6.4. These values are compared with values for K_1 and K_2 previously found for di- and triphenylguanidine and the value of K_1 found for triethylamine.

The values for K_1, which measure the relative tendencies of the bases to form salts with the indicator acid in benzene, would be expected to parallel the ionic dissociation constants of the bases in water. However, the parallelism is not good. Diphenylguanidine and ditolylguanidine, which are presumed to be weaker bases in water than triethylamine, are much more reactive in benzene. The results demonstrate how misleading the aqueous dissociation constants may be as a gage of the relative reactivities of bases in a nonaqueous solvent such as benzene. Steric and solvation effects are discussed.

1. Introduction

Hantzsch and his coworkers were the first to demonstrate that acids that appear equally strong in aqueous solutions (for example, perchloric, hydrochloric, and nitric acids) display markedly different intrinsic strengths in organic solvents like chloroform and ether [1].[2]

In their work, two kinetic methods and a static method were used in measuring the differences in strength. In the kinetic methods the differences in acidic strength were measured by the differing effects of the acids on the rate of inversion of cane sugar and on the rate of decomposition of diazoacetic ester. In the static method the relative strength of the acid was measured by the extent of salt-formation with an indicator dye or, what is in effect the same, by the stability of the salt upon dilution with an inert solvent. *p*-Dimethylaminoazobenzene is a yellow base that combines with acids to form fairly stable red salts; upon dilution with an "indifferent" solvent, such as chloroform or benzene, the salts decompose into the constituent acid and base to an extent that varies with the strength of the acid. This indicator was found suitable for comparisons of the strengths of weak or moderately strong acids. More weakly basic indicators (for example, dibenzalacetone and crystal violet) were used in the case of very strong acids, whose salts with dimethylaminoazobenzene were not measurably dissociated into the constituent acid and base even at very high dilutions. With the optical instruments then available, it was possible to make only roughly quantitative comparisons of acidic strengths. However, Hantzsch considered that in principle a *chemical* method, such as the indicator method, provides the most valid criterion of relative acidic strengths. Hantzsch also maintained that for many acids the strength, as measured by chemical reactivity, is diminished rather than increased by dilution with water. According to his views, water has a "leveling effect" on the strengths of acids because it combines with an acid, just as does a base, to form an "oxonium salt"; ionization, while a very important phenomenon, is a secondary effect that does not provide a scale of universal validity for the comparison of intrinsic acidic strengths. Hantzsch's methods and conclusions drew severe criticism, notably from von Halban[2]. However, as rigid application of the ionization theory of acidity and basicity has given way to the Brønsted-Lowry and Lewis concepts and as an increasing number of investigators have turned their attention to nonaqueous systems, it has become increasingly evident that Hantzsch's chemical criterion of tendency toward salt-formation is fundamentally sound. Moreover, it is not in violent conflict with earlier views, as is sometimes supposed, but is in harmony with the concepts of acids, bases, and salts that have been most widely accepted during the development of chemistry as a science [3].

While the ionization theory of acidity and basicity was dominant, the custom developed of applying a common term, pH, to aqueous solutions irrespective of whether the solute was an acid, a base, or a neutral salt. Later it became common practice to calculate

[1] Presented in part at the XIIth International Congress of Pure and Applied Chemistry, New York, N. Y. (Sept. 1951). The work was facilitated by a grant from the Office of Naval Research.

[2] Figures in brackets indicate the literature references at the end of this paper.

997319—52——3

the "acidity constant" for basic as well as for acidic compounds [4]. Thus, in the case of ammonia, the earlier representation of its strength by an ionization constant (approximately 1.8×10^{-5}) was succeeded by the use of the acidity constant (approximately 5.7×10^{-10}) for its "conjugate ion", the ammonium ion. The custom of expressing the strengths of both acids and bases in terms of acidity constants is perhaps one reason why the comparative strengths of acids have been studied more extensively than the comparative strengths of bases, not only in water but also in nonaqueous solvents. The neglect of bases has also resulted from the greater difficulties in their handling and purification.

Too few studies have been made for any estimate of a general leveling effect of water on the strengths of basic compounds,[3] although one would expect to find that the intrinsic strengths of bases, like those of acids, are masked to some extent by water. Trotman-Dickenson [5] has proposed a type of leveling effect as the reason why three separate equations, rather than a single equation, were required to express the relation between the catalytic power of a group of aniline bases for the decomposition of nitramide in anisole and the aqueous dissociation constants of the bases—one equation held for primary amines, a second held for secondary amines, and the third one held for tertiary amines. According to Trotman-Dickenson's views, the ionic dissociation of amines in water is promoted by greater solvation of the cations as compared with solvation of the free amines. The solvation is considered to involve hydrogen bonding, the hydrogen of the bond being one of the ammonium hydrogens; stabilization by solvation will thus be greater for secondary ammonium ions than for tertiary ammonium ions, and greatest of all for primary ammonium ions. As a result, the dissociation constants measured in water (or in other hydrogen-bonding solvents) will indicate too great a strength for primary and secondary amines compared with that of tertiary amines; consequently, in experiments employing all three types of amines as catalysts in solvents of little or no hydrogen-bonding capacity, the proton-accepting powers of the amines cannot be related to the aqueous dissociation constants by a single equation.

Experiments performed with indicator dyes at this Bureau [6, 7, 8] have provided other evidence of a leveling effect of water on bases. When an indicator dye is used in aqueous solutions to measure the pH, changes in color do not depend on the *nature* of the acid or base added, but only on the strength and on the quantity. For example, in water bromophenol blue is yellow at a pH of 3.0 and purple blue at a pH of 4.6, whatever the acid or base added. However, in benzene the color produced on the addition of a base is not the same for all bases but depends on its nature, as well as on its strength and on the quantity employed [7]. The different colors obtained in benzene, which were described in the references cited, were attributed to different kinds of hydrogen bonding between bases and indicators. The absence of the differences in aqueous solutions is evidence that in water, in place of hydrogen-bonded complexes of different colors, all of the bases form hydrated cations.

Evidence of a third kind may be cited to show that the aqueous dissociation constants of bases provide only an imperfect guide to their behavior in media other than water. H. C. Brown and coworkers, in an exhaustive study of steric factors [9], have shown that the relative capacities of amines to combine in the gaseous phase with acids of the Lewis type (for example, trialkyl derivatives of boron)[4] depend on the "steric requirements" of the amine and the acid and not merely on the polar effect of substituents. Thus, when both the acid and the base are highly "hindered" (that is, have large steric requirements, owing to the presence of bulky substituents), the proportion of addition compound formed is less than when the acid is one of small steric requirements, such as the proton. In extreme cases, the acid and base fail to combine to any measurable extent.

From these few examples, it is clear that the behavior of a base is a function of its environment, from a qualitative as well as a quantitative standpoint. In view of the mounting industrial importance of organic bases, their numerous applications in catalyzing reactions, and their vital role in medicine, it is fortunate that they are becoming the subject of an increasing number of investigations.

The investigations of bases performed at this Bureau have had as their main purpose the development of methods for measuring acidity and basicity in organic solvents, particularly in the so-called "inert solvents" like benzene and other hydrocarbons.[5] An incidental, but essential, part of the studies is finding out how bases of various classes behave in such solvents and the reasons for any unexpected phenomena. In one phase of the investigations, spectrophotometric studies have been made of reactions in which one of the reactants was an indicator dye. Some preceding publications [6 to 8] have dealt with the reactions of different organic bases with an acidic indicator dye named "bromophthalein magenta E" (the ethyl ester of tetrabromophenolphthalein). The most recent publication [8] was concerned with the reactions of 1,3-diphenylguanidine and 1,2,3-triphenylguanidine with this indicator. Previously [6] it had been found that arylguanidines such as these show the same pattern of behavior with the indicator as that of tertiary aliphatic amines (R_3N). Spectrophotometric evidence was presented [8] that the reaction

[3] In this paper, as in our previous papers, the term "base" refers chiefly to the neutral molecules of organic compounds that may be regarded as derivatives of ammonia, although the term, as broadly defined by both Brønsted and G. N. Lewis, covers other types of substances, including many compounds containing oxygen, anions, and even certain cations.

[4] There appears to be a growing tendency in this country to employ the term "acid" in the general sense advocated by G. N. Lewis [10], treating the hydrogen acids as a special class of Lewis acids. Bell [11] has presented the viewpoint of those who wish to retain the Brønsted-Lowry definition of an acid, that is, to restrict the term "acid" to hydrogen acids (proton-donors), and who recommend that the term "acceptor" (or "acceptor molecule") be applied to the remaining Lewis acids. However, as Bell has said [11], " . . . questions involved in the use of the terms acid and base are concerned essentially with convenience and consistency, and not with any fundamental differences in the interpretation of experimental facts."

[5] Recently there has been much interest in uncovering basic properties of benzene itself. However, benzene is an exceedingly weak base compared with water [12], and water in turn is much weaker as a base than the nitrogen compounds with which these studies are concerned. In such studies, benzene behaves as an inert, or differentiating, solvent, not as a leveling solvent [6 to 8].

of bases of this type with a monobasic, nonassociated acid HA in a solvent such as benzene can be represented by the equations

$$R_3N + HA \rightleftharpoons R_3NH^+.A^- \quad (1)$$

$$R_3N + R_3NH^+.A^- \rightleftharpoons (R_3NHNR_3)^+A^-. \quad (2)$$

In the first step ("primary reaction") the proton of the acid HA is displaced toward the nitrogen of the base R_3N (although not transferred completely), yielding a salt $R_3NH^+.A^-$ (or S_1), which is, in effect, a highly polar addition compound. This reaction is analogous to the addition of a base R_3N to a Lewis acid such as sulfur dioxide or a trialkyl boron. The "secondary reaction" (eq 2) involves rupture of the hydrogen bond between N and A and the formation of a new hydrogen bond between two nitrogen atoms. The secondary salt, $(R_3NHNR_3)^+A^-$ (or S_2), may be regarded as consisting of "ion pairs." [6]

Upon application of a comparable sequence of reactions to the ionization of an acid (eq 3 to 5) and of an amine (eq 6 to 8) in aqueous solutions, one obtains

$$\underset{\text{base}}{H_2O} + HA \rightleftharpoons H_2OH^+.A^- \quad (3)$$

$$\underset{\text{base}}{H_2O} + H_2OH^+.A^- \rightleftharpoons (H_2OHOH_2)^+ + A^- \quad (4)$$

$$2H_2O + HA \rightleftharpoons (H_2OHOH_2)^+ + A^- \quad (5)$$

$$R_3N + HOH \rightleftharpoons R_3NH^+.OH^- \quad (6)$$

$$\underset{\text{base}}{H_2O} + R_3NH^+.OH^- \rightleftharpoons (R_3NHOH_2)^+ + OH^- \quad (7)$$

$$R_3N + 2H_2O \rightleftharpoons (R_3NHOH_2)^+ + OH^- \quad (8)$$

The over-all reactions (eq 5 and 8) differ from the "classical" and Brønsted-Lowry formulations of such reactions in the following respects: (1) An additional molecule of water is involved; (2) the hydrogen ion is represented as being doubly hydrated; (3) the substituted ammonium ion is represented as being hydrated. The assumptions made in regard to hydration are in accordance with a variety of experimental evidence previously set forth [8]. Recent investigations by Rodebush have given further support to the proposed representation of the hydrogen ion as being doubly hydrated in aqueous solutions.[7]

We do not mean to imply, of course, that eq 3 to 5 and 6 to 8 are to be regarded as complete descriptions of the processes by which acids or amines become ionized in water. The behavior of water is so complex that no theory yet proposed accounts satisfactorily for all of its properties. However, such formulations are advantageous in several respects. In the first place, they bring out clearly that the fundamental step in the reaction of any hydrogen acid HA (water included) with a base is the formation of an addition compound. The formation of this addition compound involves *displacement* of the proton toward a molecule of the base, but for complete removal of the proton from the acid HA a second molecule of a base seems to be required [8]. The reactions involved in the ionization of acids or amines are thus seen to be manifestations of the tendency of the proton to form a bridge between electronegative atoms such as oxygen and nitrogen, new hydrogen bonds forming as previously formed hydrogen bonds are broken. Secondly, the cations formed in the over-all reactions (eq 5 and 8) are represented more accurately than in the classical formulation or in the Brønsted-Lowry formulation, in view of the evidence that in aqueous solutions the proton is associated with at least two molecules of water and water molecules are coordinated with any hydrogen atoms attached to an ammonium nitrogen.

Furthermore, our concept of the fundamental, or "primary", reaction (eq 3 and 6) as an addition reaction provides a means of harmonizing the Brønsted-Lowry and Lewis definitions of acids. At the same time, our concept of the "secondary" reaction (eq 4 and 7) that may occur when the acid in question is a hydrogen (Brønsted-Lowry) acid emphasizes the distinctive behavior of the hydrogen acids that has its origin in the ability of the proton to form a bond between electronegative atoms. While the proposed formulations help to clarify the points of similarity and dissimilarity in the behavior of hydrogen acids and other compounds regarded as acids by Lewis, they do not impede the development of quantitative relationships among the hydrogen acids in aqueous solutions, as the over-all reactions (eq 5 and 8) differ from the Brønsted equations only in that an additional molecule of the solvent appears in our equations.

Finally, it should be clear from a consideration of eq 1 through 8 that the proper measure of the reactivity of an acid HA in a nonionizing medium such as benzene is the *association* constant for its reaction with some reference base (eq 1), and not a dissociation constant. The primary reaction measures the tendency of the proton to undergo displacement from A^- toward a base, and this tendency would be expected to parallel the tendency in aqueous solutions for the proton to be separated completely from A^- by conversion to a hydrated cation. Likewise, the proper measure of the reactivity of a base such as R_3N in a nonionizing medium is the association constant for its reaction with some reference acid. To be explicit, a primary acid-base association constant in benzene and other essentially inert solvents corresponds to an ionic dissociation constant in water, whereas we should expect to find inverse relationships between acid-base dissociation

[6] Among various investigations that provide additional support for this two-step formulation are other spectrophotometric studies [6, 13], measurements of the variation of dielectric constant with concentration [14], conductance titrations [15], and studies of the properties of electrolytic solutions in nonaqueous solvents [16, 17].

[7] W. H. Rodebush, at the Symposium on Hydrogen Bonds held by the Division of Physical and Inorganic Chemistry of the American Chemical Society at Cleveland, Ohio, on April 9, 1951, stated that recent infrared studies have indicated that the hydrated proton should be represented as $H_5OHOH_2^+$ rather than as H_3O^+. Our eq 3 to 8 ignore possible hydration of the anions A^- and OH^-.

constants in benzene and ionic dissociation constants in water.

For two reasons the constant K_1 for the primary reaction is the proper criterion of reactivity in benzene rather than the constant K_2 for the secondary reaction (or the product K_1K_2): (1) In the secondary reaction both reactants vary when the nature of R_3N varies. (2) Under favorable conditions K_1 can be measured with precision, but it is more difficult to ascertain the value of K_2 [8]. However, when the solvent (for example, water) plays the dual role of acid (eq 6) and of excess base (eq 7), the first objection does not hold. Furthermore, in such a solvent the criterion of reactivity is of necessity the overall reaction, as the primary and secondary reactions cannot be studied separately.[5]

In previous papers we have described the spectrophotometric determination of equilibrium constants for the primary reaction of bases with reference acids such as bromophthalein magenta E [6, 8], picric acid [13], and trinitro-*m*-cresol [13] in benzene. Of these three acids, bromophthalein magenta E is the most generally useful. In the determination of relative strengths, the reactions being compared must not proceed too far toward completion, and picric acid is too strong to serve as a reference acid for most of the aliphatic amines. Also, the positions and intensities of the absorption bands in reactions involving bromophthalein magenta E are such as to permit measurements of greater precision than can be attained with picric acid or trinitro-*m*-cresol. A dilute solution of bromophthalein magenta E (in the range of concentrations 10^{-5} *M* to 10^{-4} *M*) has a yellow color, which shifts through tones of orange and red as minute, accurately measured increments of a base of the type R_3N are added until a sufficient excess of the base has been added to drive the reaction essentially to completion, whereupon the color becomes magenta. From measurements of the absorption of such solutions at suitable wavelengths, the association constants are readily calculated. (The secondary reaction indicated by eq 2 occurs when a very large excess of base is added and is recognized by a shift in color from magenta toward blue.)

In this paper studies of the reaction of 1,3-di-*o*-tolylguanidine, $CH_3C_6H_4\overset{1}{N}H(C=\overset{2}{N}H)\overset{3}{N}HC_6H_4CH_3$, with bromophthalein magenta E in benzene at 25° C are described. Ditolylguanidine is one of the arylguanidines that react with bromophthalein magenta E in the same way as tertiary aliphatic amines (R_3N). One purpose of the studies was to check a provisional measurement of the association constant for the primary reaction [6]. A second object was to attempt to measure the constant for the secondary reaction. In the final portion of the paper the association constant for the primary reaction is compared with the constants previously found for the reaction of bromophthalein magenta E in benzene with triethylamine, 1,3-diphenylguanidine, and 1,2,3-triphenylguanidine, and the relationship between the association constants in benzene and published ionization constants for the same bases in water is discussed.

[5] It will be clear from the discussion that attempts to express the strength of bases in inert solvents like benzene in terms of "acidity constants", as is common practice for aqueous solutions, would lead to confusion.

2. Equipment and Procedure

As in preceding studies of the reaction of bromophthalein magenta E with bases [6, 8], the data were obtained with a Beckman Model DU quartz photoelectric spectrophotometer. However, the data given in this paper for ditolylguanidine were obtained with a recently purchased instrument, and the storage battery was operated from a power supply unit.[9] The cell compartment, which was constructed of copper and brass parts in the Instrument Shop of the Bureau, was very similar to the thermostated air bath previously used [8, 18] except for a different arrangement for circulation of water through the bottom, side walls, and top. The outside of the compartment was plated with chromium over nickel; the interior was treated electrochemically to produce an optical black finish.[10] In use, the temperature of the compartment varied from 25° C by less than ±0.1 deg C, while the temperature of the room was automatically controlled to stay between 24° and 27° C but was usually between 24.5° and 25.5° C. The stock solutions were kept in the constant-temperature bath which controlled the temperature of the cell compartment. In other respects the equipment and procedure were as previously described.

The following terminology and symbols are used in the discussion and the figures: C_s,C_a, and C_b are the initial concentration of the salt, acid, and base respectively, in moles per liter; [*S*], [*A*], and [*B*] are the molar concentration of the salt, acid, and base, respectively, in an equilibrium mixture; S_1 is the primary salt, and S_2 is the secondary salt. T_s (transmittancy of the solute) $= T_{soln}/T_{solv}$; A_s (absorbancy of the solute) $= -\log_{10} T_s$; a_M (molar absorbancy index) $= A_s/bM$, where b is the length in centimeters of the absorption cell, and M is the concentration of the solute in moles per liter of solution.

3. Materials

The purification of the benzene and the preparation and purification of bromophthalein magenta E were described previously [6]. A commercial grade of di-*o*-tolylguanidine, the neutralization equivalent of which indicated the presence of 1.1 percent of inert impurity, was recrystallized twice from 95-percent ethanol, washed with benzene, air-dried overnight, then dried in a vacuum oven at approximately 66° C. After recrystallization, the melting point was 175.8° to 176.3° C, and the titration of three successive samples gave the following values for the

[9] Manufactured by the Fisher Scientific Company.

[10] The cell compartment and accessory cell holders were constructed by Vernon L. Mix, who, together with Raymond Davis and E. R. Smith, made many helpful suggestions. The electroplating was done in the Electrodeposition Section of the Bureau.

purity, expressed as percentage: 99.87, 100.01, 99.99. In the titrations, samples weighing approximately 0.5 to 0.7 g were dissolved in redistilled 95-percent ethanol and titrated with approximately 0.1-*N* standard aqueous hydrochloric acid, with an aqueous mixture of methyl red sodium salt and alphazurine [19] as indicator.

4. Data and Discussion

4.1. The Primary Reaction of Bromophthalein Magenta E with 1,3-Di-o-tolylguanidine

The progressive changes in spectral absorption that accompany the primary reaction of bromophthalein magenta E (2.5×10^{-5}-*M* in benzene, 5-mm absorption cells) with ditolylguanidine are illustrated in figure 1. The absorption curves were measured over the wavelength region extending from 320mμ to the longest wavelength at which there was measurable absorbancy.[11] Curve A is for the indicator without added base, and curves 1 to 3 are for its mixtures with approximately 7.3×10^{-6}-*M*, 1.45×10^{-5}-*M*, and 2.18×10^{-5}-*M* ditolylguanidine, respectively. When the concentration of ditolylguanidine was progressively increased in the range from 2.5×10^{-4}*M* (10 moles of base to 1 mole of indicator) to 10^{-3}*M* (40 moles of base to 1 mole of indicator), the successive absorption curves showed no measurable difference. The curve for the solution that contained 6.25×10^{-4}-*M* ditolylguanidine (25 molar equivalents) was adopted as the limiting curve for the primary reaction and is shown as S_1 in figure 1 and subsequent figures.

Well-marked isosbestic points occur near 355 and 455mμ just as in the reactions of bromophthalein magenta E with other bases of this type [6, 7] and, as is usual, are regarded as satisfactory evidence of the absence of side reactions.

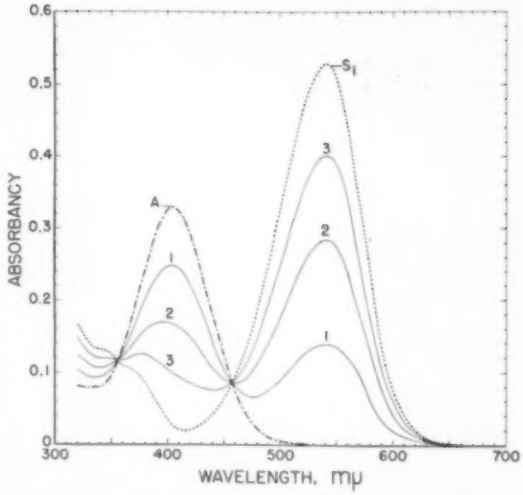

FIGURE 1. *Changes in absorbancy accompanying the primary reaction of bromophthalein magenta E, 2.5×10^{-5}-M in benzene, with di-o-tolylguanidine.*

A, BPM-E without added base; 1 to 3, with approximately 7.3×10^{-6}-*M*, 1.45×10^{-5}-*M*, and 2.18×10^{-5}-*M* base, respectively; S_1, with 6.25×10^{-4}-*M* base (limiting curve).

The data used in the calculation of the primary association constant and the calculated values are presented in table 1. The association constant is the equilibrium constant corresponding to eq 1, which, with a different choice of symbols, is the same as

$$\text{A (acid)} + \text{B (base)} \rightleftarrows \text{S}_1 \text{ (primary salt)}. \qquad (9)$$

From measurements at 540 mμ, the calculated association constant (K_1 or $K_{assn.}$) is 1.1×10^6; from measurements at 405 mμ, the value is 1.0×10^6. In a parallel series of measurements with different stock

[11] Absorption in this region is ascribed to the indicator and its magenta salt. A benzene solution of ditolylguanidine in a 5-mm absorption cell does not show measurable absorption at wavelengths longer than approximately 390 to 400 mμ, even at a concentration as great as 0.02-*M*. The absorption due to ditolylguanidine is probably shifted slightly toward shorter wavelengths when it combines with bromophthalein magenta E to form the magenta salt. When the concentration of ditolylguanidine in the solution was 1.25×10^{-4}-*M* or greater, the same quantity was placed in both absorption cells; when the concentration was smaller, benzene was used in the reference cell.

TABLE 1. *Experimental data and association constant for the primary reaction of bromophthalein magenta E with 1,3-di-o-tolylguanidine in benzene*

C_A[a]	From measurements at—					
	540 mμ					405 mμ
	A_o[b]	$[S_1]$[a]	$[A]$[a, c]	$[B]$[a]	$K_{assn.}$	$K_{assn.}$
1.25×10^{-5}	0.2482	1.174×10^{-5}	1.326×10^{-5}	0.076×10^{-5}	1.16×10^6	0.85×10^6
1.5	.2914	1.378	1.122	.122	1.01	.90
1.75	.3309	1.565	0.935	.185	0.90	.81
1.875	.3546	1.677	.823	.198	1.03	.96
2.0	.3732	1.765	.735	.235	1.02	.95
2.125	.3957	1.871	.629	.254	1.17	1.03
2.25	.4112	1.944	.556	.306	1.14	0.99
2.5	.4428	2.094	.406	.406	1.27	1.11
2.75	.4656	2.202	.298	.598	1.35	1.07
3.0	.4773	2.257	.243	.743	1.25	1.10
Limiting value	.5287	2.500				
				AVG.	1.13×10^6	0.98×10^6

[a] In moles per liter of solution.
[b] Calculated from the average of 10 readings of the transmittancy.
[c] $C_B=2.5\times10^{-4}$ mole per liter. 5-mm cells.

solutions and slightly different concentrations of ditolylguanidine, the same values were obtained. The value for 540 mμ is probably the better, as any errors are likely to be greater at 405 mμ where *two* limiting values have to be determined (one for the indicator, as well as one for the salt). The changes in absorption are also greater at 540 mμ and correspond to a more suitable range of absorbancies. There is evidence that ditolylguanidine, like other bases, is adsorbed to a very small extent on glass (probably in a monomolecular layer); the error caused by such adsorption (or actual salt-formation with silicic acid groups in the glass) would vary with the extent of contact of the various solutions with fresh glass surfaces during their preparation and would be greatest for the solutions that contain the smallest concentrations of ditolylguanidine. (For this reason the data obtained for concentrations of ditolylguanidine less than $1.25\times10^{-5}M$ were not included in the computation of $K_{assn.}$) The association constant could be measured with greater precision if ditolylguanidine combined less readily with bromophthalein magenta E; even at the "limiting" concentration for the reaction, the ditolylguanidine is less than 10^{-3}-M in concentration. However, we believe that when all conceivable sources of error are taken into account, the value obtained for the association constant is well within ±10 percent of the correct value. The provisional value 0.63×10^{5}, found in earlier exploratory studies [6] probably indicates that a small amount of inert material was present in the sample of ditolylguanidine used at that time. The ditolylguanidine had been recrystallized twice from benzene (a method of purification that had proved satisfactory for diphenylguanidine), but its purity was not checked by titration. Later it was found for a different sample of ditolylguanidine that a satisfactory neutralization equivalent could be obtained by recrystallization of the commercial material from ethanol, but not by recrystallization from benzene.

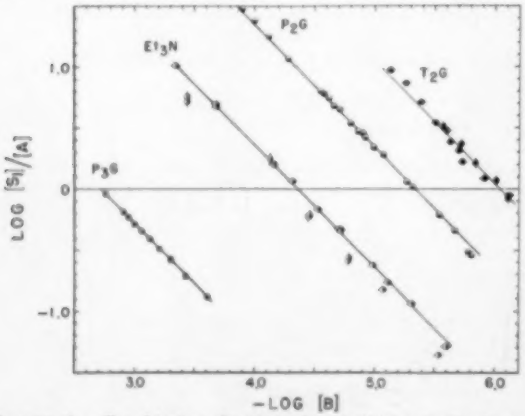

FIGURE 2. *Graphical evaluation of association constants for the primary reaction of bromophthalein magenta E with bases in benzene.*

P_3G, 1,2,3-triphenylguanidine; Et_3N, triethylamine; P_2G, 1,3-diphenylguanidine; T_2G, 1,3-di-o-tolylguanidine.

Graphical evaluation of the association constant is shown in figure 2. The association constant for the primary reaction in logarithmic terms can be expressed by the equation

$$\log[S_1]/[A]-\log\ [B]=\log\ K_{assn.} \qquad (10)$$

In figure 2, log $[S_1]/[A]$ is plotted against $-\log[B]$. The theoretical curve is a straight line of slope -1. Log $K_{assn.}$ is the intercept on the horizontal axis for log $[S_1]/[A]=0$. The solid circles near the line marked T_2G indicate the values obtained for the primary reaction of bromophthalein magenta E with ditolylguanidine. The values from the two parallel experiments are distinguished by the vertical or horizontal lines through the solid circles. The symbols P_3G, Et_3N, and P_2G indicate previous results [6, 8] for the reaction of bromophthalein magenta E with triphenylguanidine, triethylamine, and diphenylguanidine, respectively; the corresponding association constants were found to be 525, 2.3×10^{4}, and 2.2×10^{5}.[12]

4.2. The Secondary Reaction of Bromophthalein Magenta E with Di-o-tolylguanidine

As mentioned earlier, the secondary reaction of bromophthalein magenta E in benzene with bases of this type (eq 2) is indicated by a shift in the color of the solution from magenta toward blue. In the reaction of 2.5×10^{-5}-M bromophthalein magenta E with ditolylguanidine, the rate of change with increasing concentration of the base was smaller than in the case of the reaction of bromophthalein magenta E with diphenylguanidine. Furthermore, the measurements could not be extended to such high concentrations of the base, because ditolylguanidine is less soluble in benzene than diphenylguanidine.[13] In figure 3 is shown the change in the absorption curve that accompanied an increase in the concentration of ditolylguanidine from 6.25×10^{-4}-M (curve S_1) to 0.02178-M (curve 2). Enlarged sections of these two curves in the wavelength range 500 to 600 mμ and a portion of the curve for a solution that contained 0.01-M ditolylguanidine are shown in figure 4. The three curves in figure 4 intersect near 547.5 mμ; curves for solutions that contained intermediate concentrations of ditolylguanidine had the same isosbestic point. Study of the curves reveals that as the absorption near 540 mμ decreases, the most marked increase in absorption occurs near 585 mμ, which is probably the approximate location of the head of the main

[12] The association constant 2.3×10^{4} obtained for the reaction of triethylamine with bromophthalein magenta is a provisional value but is thought to be very close to the true value, although the measurements were made before the thermostated cell compartment had been obtained. Preliminary measurements with bromophthalein magenta E are indicated by the circles intersected by vertical lines; the remaining circles, with horizontal intersecting lines, indicate a more complete series of measurements with bromophthalein magenta B (the *n*-butyl ester of tetrabromophenolphthalein), performed under somewhat better controlled conditions. We believe that under the most favorable experimental conditions the association constant would be found to be exactly the same for the reaction of triethylamine with bromophthalein magenta E as for its reaction with bromophthalein magenta B.

[13] A 0.022-M solution of ditolylguanidine is near the limit of solubility in benzene at 25° C, while 0.07-M diphenylguanidine and 0.25-M triphenylguanidine were prepared without difficulty.

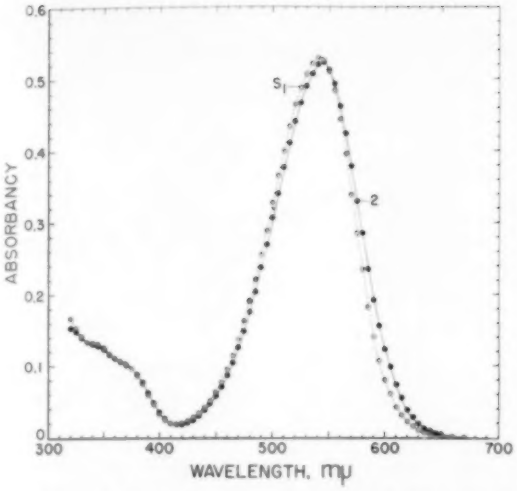

FIGURE 3. *Changes in absorbancy accompanying the secondary reaction of bromophthalein magenta E, 2.5×10^{-5}-M in benzene, with di-o-tolylguanidine.*

S_1, BPM–E with 6.25×10^{-4}-*M* base (limiting curve for primary reaction); 2, with 0.02178-*M* base.

absorption band of the secondary salt, S_2. When several solutions in this series were tested after standing for about a month, the absorption curves were the same as those obtained within an hour or two after preparation of the solutions.

As previously found for diphenyl- and triphenylguanidine [8], further shifts in the absorption curves toward longer wavelengths occur when the concentration of both the indicator and the base are greatly increased. The changes are illustrated in figure 5. The shapes of the curves indicate that an absorption curve with a strong band near 585 mμ is changing to a curve with a strong band in the vicinity of 600 mμ. We believe this change to be caused by aggregation of molecules of the secondary salt. When an attempt was made to prepare a solution with 0.003–*M* indicator (bromophthalein magenta B) and 0.006–*M* base, it was evident that the limit of the solubility of the salt had been exceeded.

An over-all picture of the primary and secondary reactions is presented in figure 6. The changes in absorbancy at two wavelengths, 580 mμ (curve 1a) and 590 mμ (curve 1b) are plotted against the square root of the concentration of ditolylguanidine (which is again expressed as molar equivalents of the indicator). With minute additions of the base, the absorption at first increases rapidly; this is the region of the primary reaction. At intermediate concentrations, there is no measurable change. At high concentrations of the base, the absorption again shows a measurable, although slow rise; this is the region of the secondary reaction. Dotted lines 2a and 2b show corresponding changes in the secondary reaction of bromophthalein magenta E with *diphenyl*guanidine; the rate of change is

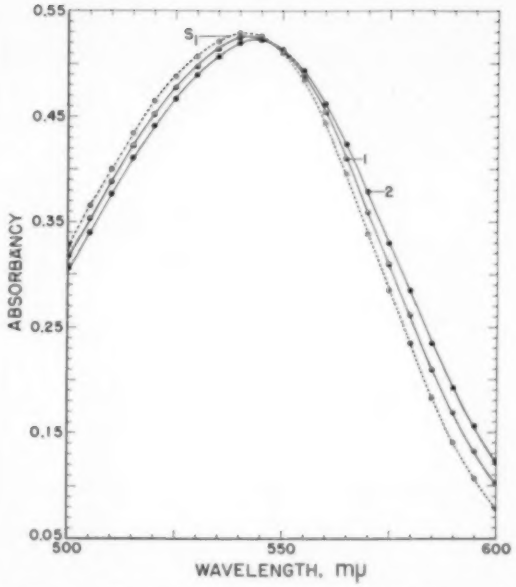

FIGURE 4. *Changes in absorbancy accompanying the secondary reaction of bromophthalein magenta E, 2.5×10^{-5}-M in benzene, with di-o-tolylguanidine.*

S_1, BPM–E with 6.25×10^{-4}-*M* base (limiting curve for primary reaction); 1, with 0.01-*M* base; 2, with 0.02178-*M* base. Curves S_1 and 2 are enlarged sections of curves S_1 and 2 in figure 3.

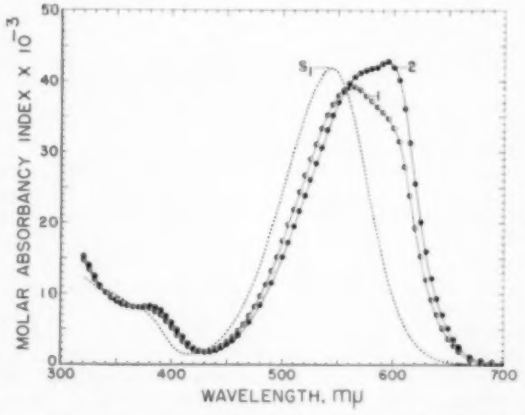

FIGURE 5. *Changes in the molar absorbancy of benzene solutions with variation in the concentration of both bromophthalein magenta E and di-o-tolylguanidine.*

S_1, 2.5×10^{-5}-*M* BPM–E with 6.25×10^{-4}-*M* base; 1, 1.25×10^{-5}-*M* BPM–E with 0.011-*M* base; 2, 2.0×10^{-5}-*M* BPM–E with 0.004-*M* base.

clearly appreciably greater for diphenylguanidine than for ditolylguanidine. If data for 540 mμ had been plotted on this figure, they would have shown a steeper rise in the region of the primary reaction, a plateau in the same region as those in curves 1a and 1b, and a very slow decrease in absorbancy in the region of the secondary reaction.

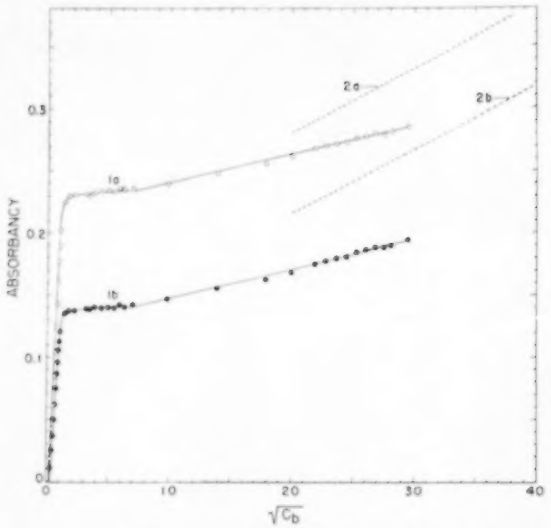

FIGURE 6. *Changes in absorbancy at two wavelengths accompanying the primary and secondary reactions of 2.5×10^{-5}–M bromophthalein magenta E with 1, di-o-tolylguanidine and 2, diphenylguanidine in benzene.*

5-mm cells. a, 580 mμ; b, 590 mμ. C_b is the concentration of the base expressed as molar equivalents of BPM–E; $[B]\cong C_b$.

From what has been said, it is obvious that the limiting curve for the secondary reaction of bromophthalein magenta E with di-*o*-tolylguanidine could not be obtained experimentally. In the previous experiments with diphenylguanidine [8], it was possible to work at higher concentrations of the base, and, as already mentioned, the absorbancy at the longer wavelengths changed more rapidly with increase in the concentration of base as the magenta primary salt was converted to the blue secondary salt. By trial and error a limiting value was found that gave a series of 10 values of K_2 in very good agreement, with the average value 15.5. Because the increments in absorbancy, which of course had to be measured on steep portions of the curves (see figs. 3 and 4), were so much smaller in the case of ditolylguanidine in the limited range of concentrations that could be studied, it was not possible to estimate the limiting value with as high a degree of certainty. However, it is reasonable to assume, for a rough approximation, that for two such closely related bases as diphenyl- and ditolylguanidine the limiting value of the absorbancy for the secondary salt would be the same. On the assumption of the same limiting value (0.680) for the two secondary salts, the values in table 2 were calculated. The method of calculation was the same as that described in [8]. The values thus obtained for the secondary association constant K_2, given in the last column, range from 5.9 to 6.8, with the average value 6.4.

A graphical evaluation of the secondary association constant K_2 is shown in figure 7. The symbols T_2G, P_2G, and P_3G have the same significance as in figure 2, as also do the horizontal and vertical lines through the solid circles. The construction of figure 7 is analogous to that of figure 2. Figure 7 indicates how close all the values for diphenylguanidine are to a straight line of the theoretical slope −1. There is much greater uncertainty about the value of the K_2 for the reaction of triphenylguanidine with bromophthalein magenta E [8]. However, the tendency for the secondary reaction to occur appears to be in the reverse order of the magnitude of the primary association constant.

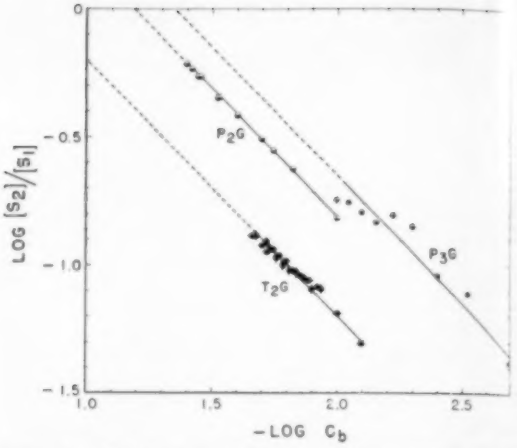

FIGURE 7. *Graphical evaluation of equilibrium constants for the secondary reaction of bromophthalein magenta E with bases in benzene.*

T_2G, 1,3-di-o-tolylguanidine; P_2G, 1,3-diphenylguanidine; P_3G, 1,2,3-triphenylguanidine.

TABLE 2. *Experimental data and association constant for the secondary reaction of bromophthalein magenta E with di-o-tolylguanidine in benzene*

C_b[a]	A_s[b]	ΔA_s[c]	$z-A_s$[d]	$-\log (S_2/S_1)$	$-\log C_b$[e]	K_2[e]
0.008	0.2553	0.0209	0.4247	1.308	2.097	6.2
.010	.2614	.0270	.4186	1.190	2.000	6.5
.012	.2661	.0317	.4139	1.087	1.921	6.8
.013	.2701	.0357	.4099	1.060	1.886	6.7
.014	.2716	.0372	.4084	1.041	1.854	6.5
.015	.2732	.0388	.4068	1.021	1.824	6.4
.016	.2762	.0418	.4038	.985	1.796	6.5
.017	.2779	.0435	.4021	.966	1.770	6.4
.018	.2802	.0458	.3998	.941	1.745	6.4
.019	.2794	.0450	.4006	.950	1.721	5.9
.0198	.2818	.0474	.3982	.924	1.703	6.0
.02178	.2857	.0513	.3943	.886	1.662	6.0
Avg.						6.4

[a] Initial molar concentration of di-o-tolylguanidine. $[B]\cong C_b$.
[b] Absorbancy at 580 mμ, calculated from the average of 10 readings of the transmittancy.
[c] $\Delta A_s = A_s - 0.2344$; 0.2344 is the limiting value found for the primary salt at 580 mμ when 2.5×10^{-5}–M in 5-mm cell.
[d] z, the assumed limiting value for the secondary salt (S_2) at 580 mμ = 0.680; $\Delta A_s/(z-A_s) = S_2/S_1$.
[e] $K_2 = S_2/(S_1 C_b)$.

4.3. Discussion

The values given in section 4.1 for the primary association constants (K_1 or $K_{assn.}$) for the reaction of bromophthalein magenta E in benzene with the

bases discussed in this paper place the bases in the following order of increasing strength: (1) triphenylguanidine, (2) triethylamine, (3) diphenylguanidine, (4) di-*o*-tolylguanidine. It is of interest to compare the relative association constants for the four bases in benzene with their ionic dissociation constants K_b in water. This comparison can be made from figure 8, in which log $K_{diss.}$ (log K_b) in water is plotted against log $K_{assn.}$ in benzene.[14] For each axis, the lowest values are those nearest the origin. Therefore, if the tendency toward salt-formation in benzene paralleled the extent of ionization in water, the values for the four bases should fall on or close to a line of positive slope. It is obvious that they do not do so. (In fact, for the three strongest bases one might suspect an inverse relationship.) The figure also shows clearly that the values vary over a greater range in benzene than in water.

One of the purposes of studies such as these is to ascertain the causes of any lack of uniformity in the behavior of bases with different acids and in different solvents, in order that acid-base behavior may be predicted as well as understood. Although a complete interpretation of our data must await the accumulation of knowledge from more extensive experimentation, it is possible to draw some tentative conclusions. The first point to consider, however, is the possibility that any of the constants are unreliable. As to the association constants determined in benzene, we believe that any conceivable errors in the values would not affect their relative order of magnitude. There is also probably no question about the relative magnitudes of the aqueous ionization constants for triethylamine, diphenylguanidine, and triphenylguanidine. The aqueous dissociation constant for di-*o*-tolylguanidine was determined by Metz [20], who also measured the ionization constant for diphenylguanidine and adopted for it a value slightly greater than that for ditolylguanidine (although slightly lower than the accepted value). Metz did not claim high accuracy for his measurements, and his values for different concentrations are not in close agreement. From a scrutiny of his data no conclusion appears warranted other than that diphenyl- and di-*o*-tolylguanidine are of about the same basicity in water. Perhaps the same value (−4.0) should have been used for both bases in the construction of figure 8. However, a more precise measurement of the basicity of di-*o*-tolylguanidine in water is desirable.

The effects of substituents on the basicity of guanidine have been studied by Davis and Elderfield [21], Hall and Sprinkle [22], Wheland and coworkers [23], and Angyal and Warburton [24]. The high basicity of guanidine, which approaches that of sodium and potassium hydroxides [21, 22] has been explained by the resonance hypothesis [25, p. 212]; that is, the guanidinium ion, because it resonates among three equivalent structures, is more stable than guanidine, which resonates among three structures of which only two are equivalent. Replacement of one or more of the hydrogens by alkyl groups has almost no effect on the strength in water [21, 23, 24]. However, the basicity in water is progressively weakened as phenyl groups are introduced in the 1-, 1,3-, and 1,2,3-positions [22].[15] On the resonance hypothesis, a reduction in the basicity by the introduction of phenyl groups is to be expected, because phenyl derivatives of guanidine are also derivatives of aniline, and the nitrogen atoms will be involved in resonance with the benzene rings just as in aniline [25, p. 206].[16] The greater reactivity of di-*o*-tolylguanidine, as compared with diphenylguanidine, with the acid bromophthalein magenta E in benzene may result from the effect of the ortho methyl substituents in reducing the aniline type of resonance. As just noted, the aniline type of resonance would have a base-weakening effect; steric inhibition of this resonance should have a base-strengthening effect. If this line of reasoning is correct, still greater reactivity should be found for compounds such as 1,3-dimesitylguanidine, in which the aniline groups have substituents in all ortho positions. Strong bases are needed for titrations of weak acids in nonaqueous solvents, and various derivatives of guanidine are worthy of attention in this connection. Although the only available value for di-*o*-tolylguanidine [20] is of too provisional a character to justify a final decision as to the relative basicities of diphenylguanidine and di-*o*-tolylguanidine in water, the similarity of Metz's results for the

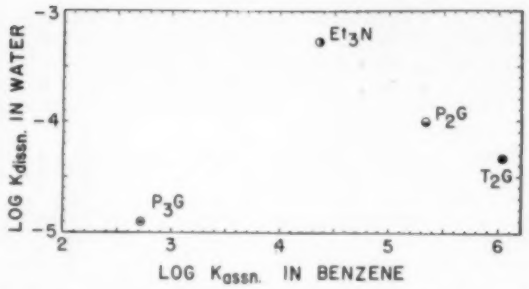

FIGURE 8. *Comparative strengths of bases as measured by association with bromophthalein magenta E in benzene and by ionic dissociation constants in water.*

P_3G, 1,2,3-triphenylguanidine; Et_3N, triethylamine; P_2G, 1,3-diphenylguanidine; T_2G, 1,3-di-*o*-tolylguanidine.

[14] The values for log $K_{diss.}$ in water were taken from the publications indicated in [6], table 2. For triethylamine, diphenylguanidine, ditolylguanidine, and triphenylguanidine, in the order named, these values are −3.28, −4.0, −4.33, and −4.9. (The value for ditolylguanidine was obtained at 18° C, the other values at 25° C.)

[15] The numbering of substituents conforms to the following formula for the parent compound, guanidine: $H_2^1N.C(=NH).NH_2^3$. The statement by Dewar [26] that 1,2,3-triphenylguanidine is a very strong base in comparison with 1-phenyl- and 1,3-diphenylguanidine is erroneous, as shown by the data in [22], which are in harmony with the relative effectiveness of the three bases when used as accelerators in the vulcanization of rubber [27].

[16] As already mentioned in this paper, 1,3- and 1,2,3-arylguanidines react in the same way as trialkylamines with bromophthalein magenta E in benzene. On the other hand, commercial samples of 1-arylguanidines and 1-, 1,1-, and 1,3-alkylguanidines resemble dialkylamines in their behavior with BPM–E in benzene. These observations suggest that in the first-mentioned group of guanidines the positive charge on the cation is concentrated on one of the nitrogen atoms, although in the second group the positive charge is spread over at least two of the nitrogen atoms. (For a description and discussion of the behavior of BPM–E with di- and trialkylamines [6, p. 256–7].

two bases suggests that solvation by water may have a leveling effect on the basicities. Nevertheless, for the three guanidines considered in this paper (diphenyl-, triphenyl-, and di-*o*-tolyl-) there appears to be at least a rough proportionality between the basicities in benzene and water.

In the introduction, two factors (solvation [5] and steric effects [9]) that may affect the strength of bases were discussed briefly. A more detailed discussion will show that the behavior of triethylamine is strikingly dependent on its environment. For some years it has been known [28] that when the hydrogen atoms in ammonia are replaced successively by ethyl groups, the first and second ethyl groups increase the basicity in water, but that the basicity is then markedly reduced by the third ethyl group. That is, the order of basic strengths in water is $NH_3 < Et_3N < EtNH_2 < Et_2NH$.[17]

The base-strengthening effect of the first and second alkyl groups is commonly regarded as a polar ("positive inductive") effect, and if no opposing factor were in operation, a third group should increase the basicity still further rather than decrease it.

The relative order of basicities found in water does not hold under all conditions. For example, Rimbach and Volk [29] studied the partition of nitric acid between the optically active base, cinchonidine, and a large number of optically inactive aliphatic and aromatic amines [18] in aqueous ethanol (97.5% ethanol by volume). A smaller number of bases was studied in 99.5-percent methanol. In some cases equilibrium was approached by adding cinchonidine to the nitrate of the inactive base, and in other cases the inactive base was added to cinchonidine nitrate; the results from the two methods did not differ significantly. From these measurements, the comparative strengths, or "avidities", of the various optically inactive bases were estimated. In every series of primary, secondary, and tertiary amines the mono-derivative was found to be the strongest and the tri-derivative the weakest. More recently, Brown and Taylor [30, 31] have observed that with hydrogen chloride (gaseous) as the reference acid the order of basicity of the ethylamines (as shown by their tendency to combine with the acid) is the same as in water. However, with trimethylboron as the reference acid, the order is altered to $Et_3N < NH_3 < Et_2NH < EtNH_2$, and with tri-*t*-butyl-boron there is a further change in order to $Et_3N < Et_2NH < EtNH_2 < NH_3$. Thus, it appears that the order of strengths varies with the steric requirements of the reference acid, and that as these requirements increase the steric requirements of the base become more vital.

Brown [9, 31 to 33] has suggested reasons why the ethylamines behave as hindered amines toward a rather bulky acid like trimethylboron. His detailed explanation may be summarized as follows: In *ethylamine* it seems likely that there are three stable configurations of the ethyl group, in one of which the methyl group is close to the free electron pair of the nitrogen atom. This configuration would be prohibited in an addition compound with trimethylboron, and the restriction of motion of the ethyl group would cause a certain amount of strain in the addition compound that would be relieved by dissociation of the compound. In an addition compound of *diethylamine* with trimethylboron there is only one possible configuration of the ethyl groups. The addition compound has almost no freedom of motion and is therefore under appreciable strain. Consequently it has a low degree of stability. In *triethylamine* one of the ethyl groups is adjacent to the free electron pair of the nitrogen. The amine cannot combine with trimethylboron without undergoing changes in the normal bond angles that result in a crowding of the ethyl groups. This explains why the addition compound is highly strained and extremely unstable.

The large steric requirements of triethylamine are evident not only in the instability of its addition compound with trimethylboron but in its relatively low rates of reaction with alkyl iodides in nitrobenzene solution [33]. In the reactions of amines with alkyl halides to give tetraalkylammonium halides, the first step is thought to be the formation of an addition compound ("activated complex") of the amine and the alkyl halide. On this hypothesis it is easy to see why the rate of formation of the tetraalkylammonium halide will be decreased if the steric requirements of the reactants are such as to impede the formation of the intermediate complex. Very recently Toy [34] has reported that the synthesis of tetraalkyl dithionopyrophosphates, by the action of a tertiary amine on a mixture of water and dialkyl thionochlorophosphate, appears to involve intermediate formation of a complex of the dialkyl thionochlorophosphate and the tertiary amine. With an unhindered amine a high yield of the desired product can be obtained, but with triethylamine and other hindered amines the yields are greatly reduced, in consonance with the experience of Brown and his coworkers in their studies of addition reactions.[19]

Brown has stated [32] that the ability of hindered amines such as triethylamine "to react with aqueous acids is not noticeably affected because of the low steric requirements of the proton." It should be borne in mind, however, that in water, as in other media, *the proton does not have an independent existence.* If it is not part of some neutral molecule, it is associated with molecules of solvent, and the steric requirements of various protogenic molecules and ions when reacting with bases are not equally great. As noted in one of our earlier publications ([6, p. 232]), the reactive proton in a molecule of bromophthalein magenta E probably forms a bridge between the phenolic oxygen and a neighboring bromine atom, so that the molecules do not undergo intermolecular

[17] The same order of strengths holds when the alkyl substituent is methyl, *n*-propyl, or isobutyl [28].

[18] These included all of the methyl, ethyl, *n*-propyl, isobutyl, isoamyl, and benzylamines.

[19] (Note added after completion of the manuscript.) Some Japanese workers [35] have studied the separation of various amines by distillation from aqueous or alcoholic solutions after partial neutralization of the hydrochlorides (hydrobromides) by alkali. Separation of aliphatic amines by ion-exchange resins was also studied. The investigators failed to find a correlation between the order of distillation, adsorbability by resins, and aqueous dissociation constants of amines, and commented that such examples of discrepancies between the apparent and true basicities have often been noticed. Their observations lend further support to the conclusions reached in this paper.

association. There is no apparent reason for classifying bromophthalein magenta E as a hindered acid, but its steric requirements may be enough greater than those of the hydrated proton to account for lowered reactivity with a base as highly hindered as triethylamine. Furthermore, in benzene stabilization of the cation by solvation does not occur.

An earlier observation ([6, p. 256]) as to the behavior of bromophthalein magenta E when dissolved in some hindered alcohols seems pertinent to the present discussion. The magenta color of the solutions suggested that the indicator acid forms an addition compound with a hindered alcohol, but does not undergo ionization to form its blue anion, as it does in unhindered alcohols like ethanol. The explanation proposed was that the hydrogen bridge in the addition compound is shielded by hydrocarbon radicals in the alcohol, so that further solvation of the proton (necessary for ionization, according to the views presented in the introduction to this paper) is impeded. If this explanation is correct, it should follow that when BPM–E has combined with a reactive but highly hindered amine (eq 1), the addition compound S_1 will be less susceptible to attack by excess base than when the amine is not hindered. In support of this prediction, qualitative tests of the reaction of BPM–E with several aliphatic amines in benzene have indicated a greater tendency for the secondary reaction (eq 2) to occur when the amine contains one or more methyl groups than when the smallest substituent is an ethyl group. These considerations lead to the conclusion that while a hydrogen acid and an organic base may be sufficiently reactive and unhindered to form an addition compound S_1, it will not necessarily follow that S_1 will undergo ionization when an excess of the same base is added. Ionization may result, however, if a base of low steric requirements is added to the system. Such ideas are helpful in understanding why the addition of a very minute quantity of water has been found in some cases to have a marked effect on the ionization of acids and bases in nonaqueous solvents.

The results reported in this paper are of immediate practical interest in demonstrating how misleading the aqueous dissociation constants may be as a gage of the relative reactivities of bases in a nonaqueous solvent such as benzene. It could not have been predicted that diphenyl- and ditolylguanidine, which seem to be decidedly weaker than triethylamine in water, would be so reactive with bromophthalein magenta E in benzene. Although very limited in scope, the results indicate that water has a leveling effect on the strengths of bases as well as on those of acids, and that steric factors are important in the reactions of bases with protogenic acids as well as in their reactions with Lewis acids.

It can be predicted that when the strengths of a series of bases are compared in different media, a greater number of irregularities will be observed than in a similar comparison of the strengths of hydrogen acids. Although hydrogen acids may differ somewhat in steric requirements and their behavior may be modified by intramolecular hydrogen bonding, they have more in common from a structural standpoint than do the organic bases, which may owe their basicity to nitrogen, oxygen, or various other atoms, as well as vary over a wider range in their steric requirements.

5. References

[1] A. Hantzsch, Z. Elektrochem. **29,** 221 (1923); **30,** 194 (1924); see also L. P. Hammett, J. Am. Chem. Soc. **50,** 2666 (1928).
[2] H. von Halban, Z. Elektrochem. **29,** 434 (1923); **30,** 601 (1924).
[3] P. Walden, Salts, acids, and bases: Electrolytes: Stereochemistry (McGraw-Hill Book Co., Inc., New York, N. Y., 1929).
[4] J. N. Brønsted, Chem. Rev. **5,** 231 (1928).
[5] A. F. Trotman-Dickenson, J. Chem. Soc. (London) 1293 (1949).
[6] M. M. Davis and P. J. Schuhmann, J. Research NBS **39,** 221 (1947) RP1825.
[7] M. M. Davis, P. J. Schuhmann, and M. E. Lovelace, J. Research NBS **41,** 27 (1948) RP1900.
[8] M. M. Davis and H. B. Hetzer, J. Research NBS **46,** 496 (1951) RP2219.
[9] H. C. Brown, Science **103,** 385 (1946); see also [30 to 33] in this paper.
[10] G. N. Lewis, J. Franklin Inst. **226,** 293 (1938).
[11] R. P. Bell, Quarterly Rev. Chem. Soc. (London) **I,** 113 (1947).
[12] S. J. O'Brien, C. L. Kenny, and R. A. Zuercher, J. Am. Chem. Soc. **61,** 2504 (1939).
[13] M. M. Davis and E. A. McDonald, J. Research NBS **42,** 595 (1949) RP1997.
[14] A. A. Maryott, J. Research NBS **41,** 7 (1948) RP1897.
[15] A. A. Maryott, J. Research NBS **38,** 527 (1947) RP1794.
[16] W. F. K. Wynne-Jones, J. Chem Soc. (London) 795 (**1931**).
[17] C. A. Kraus, J. Phys. Chem. **43,** 231 (1939); see also discussion by M. Kilpatrick and K. Fajans, J. Phys. Chem. **43,** 288 (1939).
[18] E. E. Sager and I. J. Siewers, J. Research NBS **45,** 489 (1950) RP2162.
[19] H. Fleisher, Ind. Eng. Chem., Anal. Ed. **15,** 742 (1943).
[20] L. Metz, Z. Elektrochem. **34,** 292 (1928).
[21] T. L. Davis and R. C. Elderfield, J. Am. Chem. Soc. **54,** 1499 (1932).
[22] N. F. Hall and M. R. Sprinkle, J. Am. Chem. Soc. **54,** 3469 (1932); see also N. F. Hall, J. Am. Chem. Soc. **52,** 5115 (1930).
[23] B. Neivelt, E. C. Mayo, J. H. Tiers, D. H. Smith, and G. W. Wheland, J. Am. Chem. Soc. **73,** 3475 (1951).
[24] S. J. Angyal and W. K. Warburton, J. Chem Soc. (London) 2492 (**1951**).
[25] L. Pauling, The nature of the chemical bond (Cornell Univ. Press, Ithaca, N. Y., 2d ed., 1940).
[26] M. J. S. Dewar, The electronic theory of organic chemistry, p. 95 (Oxford Univ. Press, New York, N. Y., 1949).
[27] G. D. Kratz, H. H. Young, Jr., and I. Katz, Ind. Eng. Chem. **41,** 399 (1949).
[28] G. Bredig, Z. phys. Chem. **13,** 289 (1894).
[29] E. Rimbach and H. Volk, Z. phys. Chem. **77,** 385 (1911).
[30] H. C. Brown, J. Am. Chem. Soc. **67,** 503 (1945).
[31] H. C. Brown and M. D. Taylor, J. Am. Chem. Soc. **69,** 1332 (1947).
[32] H. C. Brown and S. Sujishi, J. Am. Chem. Soc. **70,** 2878 (1948).
[33] H. C. Brown and N. R. Eldred, J. Am. Chem. Soc. **71,** 445 (1949).
[34] A. D. F. Toy, J. Am. Chem. Soc. **73,** 4670 (1951).
[35] Kyosuke Tsuda and Tetsuro Matsumoto, J. Pharm. Soc. Japan **67,** 107, 236 (1947); Kyosuke Tsuda, Tetsuro Matsumoto, and Takahiro Nakamura, J. Pharm. Soc. Japan **67,** 115 (1947); Kyosuke Tsuda and Takahiro Nakamura, J. Pharm. Soc. Japan **67,** 117 (1947). Through Chem. Abstracts **45,** 9465 (1951).

WASHINGTON, February 7, 1952.

The $3\nu_3$ Bands of Carbon Disulfide and Carbon Dioxide

Norman M. Gailar and Earle K. Plyler

The $3\nu_3$ bands of carbon disulfide and carbon dioxide are described. This band of CS_2 is complex, containing two transitions from excited states and two transitions attributed to the isotopic molecule $CS^{32}S^{34}$ in addition to the primary transition 000→003 of CS_2^{32}. A multiple-reflection cell of 6-meter path length, 20-cm optics, and negligible loss of aperture is described. Molecular constants are checked for CO_2 and found for CS_2. These latter constants are $B_0=0.1089$ cm$^{-1}\pm0.0004$, $\alpha_3=0.0007$ cm$^{-1}\pm0.00003$, $X_{33}=-5.2$ cm^{-1}, and $X_{23}=-3.3$ cm^{-1}.

The infrared absorption spectrum of carbon dioxide is well known. Carbon disulfide, however, although of similar structure, has received much less study. This is probably due to the difficulty of resolving the fine structure of its spectrum, caused by the large moment of inertia of this molecule. In order to resolve the fine structure, several requirements must be met. A spectrometer capable of resolving to 1 or 2 tenths of a wave number in the region of the spectrum must be used, and a path of sufficient length to permit measurable absorption must be devised.

Both conditions being obtainable in the Radiometry laboratory of the Bureau, the $3\nu_3$ band of CS_2 has been studied, along with the analogous band of CO_2. This latter band has been observed under low resolution by Barker and Wu [1] and under higher resolution by Goldberg, Mohler, Pierce, and McMath,[2] but they did not report the band origin.

The spectrometer used was a 15,000-line-per-inch grating spectrometer with a lead-sulfide detector. This instrument, previously described,[3] was capable of resolving to better than 0.1 cm^{-1} in the 2.2-μ (CS_2) region and to better than 0.2 cm^{-1} in the 1.4-μ (CO_2) region.

A multiple-reflection absorption cell was used to obtain a long path length. In designing the cell a major consideration was to avoid the loss of aperture when small mirrors were used. The cell was designed for use in the spectral region beyond the photographic. This prevents the use of a long exposure time to compensate for any loss of aperture. In order to keep slit widths at a minimum and resolution at a maximum, the path length was kept to 6 m. With this path length it was possible to design a cell with negligible loss of aperture and still use small-diameter optics. A cell of long, variable path-length and somewhat different optics has been described by White.[4]

Figure 1 is a schematic drawing of the cell with a central ray traced through the system. The lines representing this ray are numbered according to the number of the transversal of the cell they represent. The source, S, is placed off-axis and farther from the spherical mirror, M_1, than the radius, R, of this mirror. The radius of curvature of this mirror is 102 cm, and it has a diameter of 18 cm. Light from the source follows line 1 to M_1, line 2 to mirrors M_2 and M_3, line 3 back to M_1, etc. The plane mirrors, M_2, M_3, M_4, M_5, and M_6, are so arranged as to cause the final image of the source to be focussed on the entrance slit of the spectrometer. These plane mirrors were adjusted with the aid of a photocell, assuring maximum transmission of energy. Points X_1 and X_2 are the points where the image of the source is focussed the first and second times. M_5 is placed considerably off-axis so that M_6 can reflect the light out of the cell without intercepting light going to M_1 or M_2. At no time is the off-axis condition as great as 8°. An aluminum tube 1 m long and 20 cm inside diameter forms the body of the cell.

An original record obtained on the recorder is shown in figure 2. The water absorption bands in this region distorted the CO_2 lines, and thus the various constants could not be calculated with the utmost accuracy. Table 1 shows the wavelength and vacuum wave number of the lines of this spectrum.

TABLE 1. *Wavelengths and wave numbers of the $3\nu_3$ band of CO_2*

J	R branch		P branch	
	Wavelength	Wave number	Wavelength	Wave number
	A	cm^{-1}	A	cm^{-1}
0	14336.3	6973.39	-------	-------
2	14333.4	6974.80	-------	-------
4	14330.5	6976.21	14344.6	6969.35
6	14327.8	6977.53	14348.4	6967.51
8	14325.0	6978.89	14351.9	6965.81
10	14322.6	6980.06	14355.7	6963.97
12	14320.4	6981.13	14359.5	6962.12
14	14318.2	6982.20	14363.8	6960.04
16	14316.2	6983.18	14368.1	6957.69
18	14314.6	6983.96	14372.6	6955.78
20	14312.9	6984.79	14377.2	6953.55
22	14311.5	6985.47	14382.0	6951.23
24	14310.1	6986.16	14387.0	6948.82
26	14308.9	6986.74	14392.3	6946.26
28	14307.9	6987.23	14397.5	6943.75
30	14307.0	6987.67	14403.0	6941.10
32	14306.4	6987.96	14408.4	6938.49
34	-------	-------	14414.1	6935.75
36	-------	-------	14420.0	6932.91

[1] E. F. Barker and T. Y. Wu, Phys. Rev. **45**, 1 (1934).
[2] L. Goldberg, O. Mohler, A. Pierce, and R. McMath, Phys. Rev. **78**, 74 (1950).
[3] Earle K. Plyler and Norman Gallar, J. Research NBS **47**, 248 (1951) RP2249.
[4] John U. White, J. Opt. Soc. Am. **32**, 285 (1942).

In analyzing the structure of the $3\nu_3$ band of CO_2, use was made of the well-known combination differences for linear molecules [5]

$$R(J-1)-P(J+1)=4B''(J+1/2), \quad (1)$$

$$R(J)+P(J)=2\nu_0+2B'+2(B'-B'')J(J+1). \quad (2)$$

Here B′ is the upper and B'' the lower-state rotational constant, ν_0 the band origin, J the rotational quantum number of the lower state of the transition, and P and R are the short and long wave-number branches, respectively. These relations yield $\nu_0=6972.4$ cm^{-1}, $\alpha_2=0.0032$ cm^{-1}, $B_0=0.3900$ cm^{-1}. These values are in good agreement with those reported by Benedict, Herman, and Silverman.[6] Using the value of 2349.3 cm^{-1} for ν_3 as reported by Herzberg (footnote 5), $X_{33}=-12.6$ cm^{-1}. The value of 22.5 cm^{-1} for X_{33} given by Benedict, Herman, and Silverman (footnote 6) is a *typographical* error and was intended to read 12.5 cm^{-1}.

The $3\nu_3$ band of CS_2 is presented in figure 3. Here five different band heads can be seen. The major

[5] G. Herzberg, Infrared and Raman spectra of polyatomic molecules, chapters III, IV (D. Van Nostrand Co., New York, N. Y., 1945).
[6] W. S. Benedict, Robert C. Herman, and Shirleigh Silverman, J. Chem. Phys. 19, 1325 (1951).

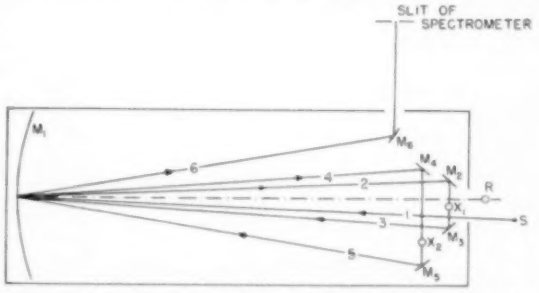

FIGURE 1. *Schematic drawing of multiple reflection absorption cell.*

The lettered components are described in the text.

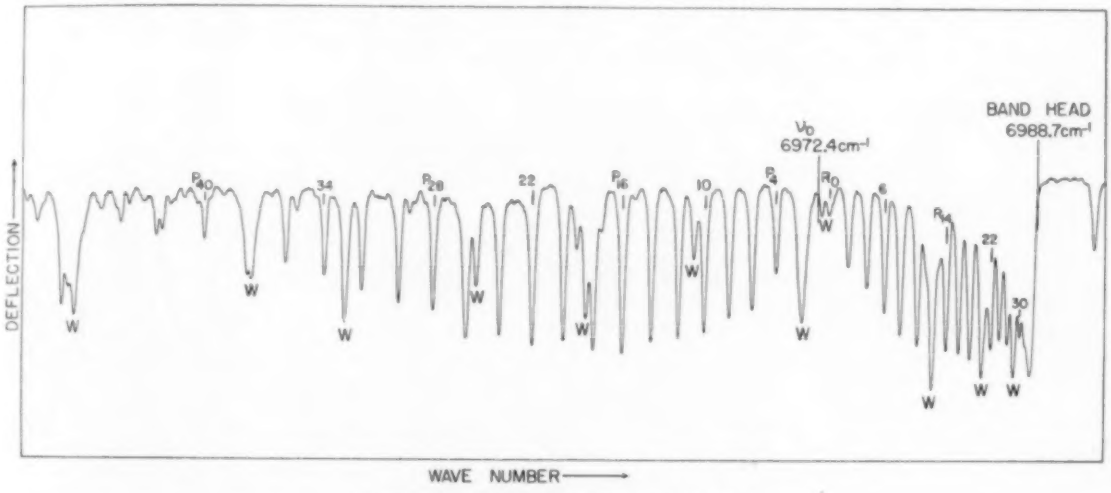

FIGURE 2. *The $3\nu_3$ absorption band of* CO_2.

Some lines are labeled with the J values of the transition. Wavelengths and vacuum wave numbers of all the lines are found in table 1. Lines labeled W are water absorption lines.

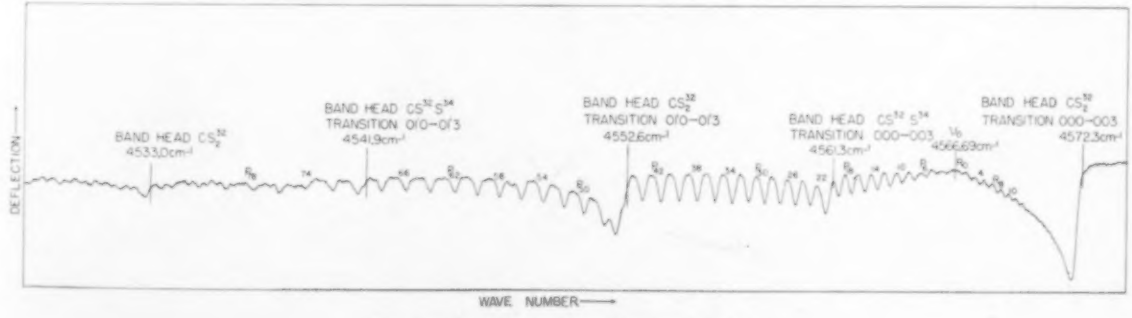

FIGURE 3. *The $3\nu_3$ absorption band of* CS_2.

Some lines are labeled with the J values of the transition. Wavelengths and vacuum wave numbers of all the lines are found in table 2.

band head and the rotational structure are of the 000→003 transition and occur at about 572.3 cm^{-1}. At 4561.3 cm^{-1} is the band head for the same transition for the isotopic molecule $CS^{32}S^{34}$. The band head of the transition $01^10 \rightarrow 01^13$ occurs at 4552.6 cm^{-1}, and the head for the same transition for the isotopic molecule occurs at 454 1.9 cm^{-1}. A very weak band head can be seen at 4533.0 cm^{-1}. This can be attributed to the pair of transitions $02^00 \rightarrow 02^03$ and $02^20 \rightarrow 02^23$. The band head of the transition 100→103 is expected to occur at approximately this position and may be superimposed at 4533.0 cm^{-1}.

The scarcity of lines in the R branch of the principal transition prevented the use of the combination differences (eq 1 and 2). Instead, the absorption lines were fitted to the equation

$$\nu = \nu_0 + (B' + B'')m + (B' - B'')m^2, \qquad (3)$$

(see footnote 5) in order to determine ν_0, B' and B''. These symbols have the same meanings as in eq 1 and 2. $m = J+1$ for the R branch, and $m = -J$ for the P branch. A least-square fit to this equation yielded $\nu_0 = 4566.69$ cm^{-1}, $B_0 = 0.1089$ cm^{-1}, and $\alpha_3 = (B'' - B')/3 = 0.007$ cm^{-1}. Table 2 contains the J and m values, the wavelengths, and vacuum wave numbers of the lines of this spectrum, and the wave numbers calculated from eq 3.

The location of the band origins can be calculated to a good first approximation by assuming that the differences, $\nu_{\text{band head}} - \nu_0$, remain constant. This is shown by considering eq 3. A band head is expected when $d\nu/dm = 0$ or when $m = -(B' + B'')/2(B' - B'')$. Substituting this value of m into eq 3, $\nu_{\text{band head}} - \nu_0 = -(B' + B'')^2/4(B' - B'')$ for the difference between the band head and the band origin. Comparing this difference for two transitions $(\nu_{\text{band head}} - \nu_0)_{000 \rightarrow 003} - (\nu_{\text{band head}} - \nu_0)_{01^10 \rightarrow 01^13} = -(B_{003} + B_{000})^2/4\,(B_{005} - B_{000}) + (B_{01^13} + B_{01^10})^2/4\,(B_{01^13} - B_{01^10})$. Expressing these $4B'$s in terms of the equation $B(v) = B_e = \sum_i \alpha_i (v_i + (d_i)/2)$ see footnote 5) and noting that $B_e \gg \alpha_i$, to a good approximation, we find $(\nu_{\text{band head}} - \nu_0)_{000 \rightarrow 003} - (\nu_{\text{band head}} - \nu_0)_{01^10 \rightarrow 01^13} < B_e$.

Since B_e is approximately 0.1 cm^{-1}, it is seen that the difference between band head and band origin is equal for the transitions 000→003 and $01^10 \rightarrow 01^13$ to within experimental error.

Using this relation, ν_0 for $01^10 \rightarrow 01^13$ is found to be 4546.7 cm^{-1}. Taking the value of ν_0 for 000→001 of 1532.5 cm^{-1} as measured at the Bureau on a prism spectometer, it is found that $X_{33} = -5.2$ cm^{-1} and $X_{23} = -3.3$ cm^{-1}.

TABLE 2. *Wavelengths band wave numbers of the ν_3 band of CS_2*

J	m	Wavelength	Wave number observed	Wave number calculated
		A	cm^{-1}	cm^{-1}
$R18$	19	21875.73	4570.02	4570.04
16	17	21876.91	4569.78	4569.76
14	15	21878.37	4569.48	4569.46
12	13	21879.78	4569.18	4569.15
10	11	21881.47	4568.83	4568.82
$R8$	9	21883.11	4568.48	4568.47
6	7	21884.81	4568.13	4568.10
4	5	21886.69	4567.74	4567.72
2	3	21888.47	4567.36	4567.32
$P4$	−4	21895.98	4565.79	4565.80
6	−6	21898.16	4565.35	4565.32
8	−8	21900.60	4564.84	4564.83
10	−10	21903.10	4564.32	4564.33
12	−12	21905.58	4563.80	4563.81
$P14$	−14	21908.19	4563.26	4563.27
16	−16	21910.88	4562.70	4562.71
18	−18	21913.71	4562.10	4562.14
20	−20	21916.46	4561.54	4561.55
22	−22	.....	.....	4560.95
$P24$	−24	21922.46	4560.28	4560.33
26	−26	21925.40	4559.60	4559.69
28	−28	21928.65	4559.00	4559.02
30	−30	21931.89	4558.32	4558.36
32	−32	21935.16	4557.64	4557.68
$P34$	−34	21938.52	4556.95	4556.97
36	−36	21941.98	4556.23	4556.25
38	−38	21945.56	4555.48	4555.52
40	−40	21949.21	4554.73	4554.76
42	−42	21952.84	4553.98	4553.99
$P44$	−44	21956.63	4553.19	4553.21
46	−46	.....	.....	4552.41
48	−48	21964.16	4551.63	4551.59
50	−50	21968.24	4550.78	4550.75
52	−52	21972.30	4549.94	4549.90
$P54$	−54	21976.44	4549.07	4549.03
56	−56	21980.76	4548.20	4548.14
58	−58	21985.11	4547.30	4547.24
60	−60	21989.50	4546.38	4546.32
62	−62	21994.11	4545.43	4545.39
$P64$	−64	21998.66	4544.49	4544.44
66	−66	22003.44	4543.50	4543.47
68	−68	22008.69	4542.42	4542.49
70	−70	22012.96	4541.54	4541.49
72	−72	22018.38	4540.53	4540.47
$P74$	−74	22023.48	4539.46	4539.44
76	−76	22028.26	4538.38	4538.39
78	−78	22033.47	4537.36	4537.32
80	−80	22038.88	4536.20	4536.24
82	−82	22044.36	4535.07	4535.14
$P84$	−84	22049.99	4533.91	4534.02

WASHINGTON, JANUARY 21, 1952.

Journal of Research of the National Bureau of Standards Vol. 48, No. 5, May 1952 Research Paper 2328

On Cauchy-Riemann Equations in Higher Dimensions[1]

E. Stiefel[2]

The n linear partial differential equations with constant complex coefficients

$$l_j \equiv \sum_{i,k}^{n} a_{jk}^{i} \frac{\partial u_k}{\partial x_i} = 0,$$

$(j=1, \ldots, n)$ are said to form a system of generalized Cauchy-Riemann equations, if there exist constants f_{jk}^{h} such that

$$\Delta u_j \equiv \sum_{h,k}^{n} f_{jk}^{h} \frac{\partial l_k}{\partial x_h}.$$

It is proved that such systems exist for $n=1,2,4,8$ only. In the cases $n=2,4$ there are three essentially inequivalent systems; $n=8$, only two. If the coefficients are required to be real, there exist only the classic system of two equations, the two systems of Dirac-Fueter equations, and two systems of eight equations.

If two real functions u_1, u_2 of the real variables x_1, x_2 satisfy the Cauchy-Riemann equations

$$\frac{\partial u_1}{\partial x_1} - \frac{\partial u_2}{\partial x_2} = 0, \qquad \frac{\partial u_2}{\partial x_1} + \frac{\partial u_1}{\partial x_2} = 0, \tag{1}$$

they are harmonic, that is, from (1) follows Laplace's equation by differentiation:

$$\Delta u_1 = \frac{\partial^2 u_1}{\partial x_1^2} + \frac{\partial^2 u_1}{\partial x_2^2} = 0, \qquad \Delta u_2 = \frac{\partial^2 u_2}{\partial x_1^2} + \frac{\partial^2 u_2}{\partial x_2^2} = 0. \tag{2}$$

Introducing the left sides of the Cauchy-Riemann equations

$$l_1 = \frac{\partial u_1}{\partial x_1} - \frac{\partial u_2}{\partial x_2}, \qquad l_2 = \frac{\partial u_2}{\partial x_1} + \frac{\partial u_1}{\partial x_2}, \tag{3}$$

we observe that this statement is an immediate consequence of the relations

$$\Delta u_1 = \frac{\partial l_1}{\partial x_1} + \frac{\partial l_2}{\partial x_2}, \qquad \Delta u_2 = \frac{\partial l_2}{\partial x_1} - \frac{\partial l_1}{\partial x_2}, \tag{4}$$

that is to say, that the Laplacians of u_1, u_2 are linear combinations of the derivatives of the left sides of the Cauchy-Riemann equations.

In 1939 Olga Taussky-Todd[3] studied the following general problem. Let $u_1, u_2, \ldots, u_n$ be functions of the independent variables $x_1, x_2, \ldots, x_n$. Is it possible to find a system of n linear partial differential equations with constant coefficients

$$l_j \equiv \sum_{i,k}^{n} a_{jk}^{i} \frac{\partial u_k}{\partial x_i} = 0, \tag{5}$$

in such a way that

$$\Delta u_j = \sum_{h,k}^{n} b_{jk}^{h} \frac{\partial l_k}{\partial x_h}, \tag{6}$$

the b_{jk}^{h} again being constant coefficients? If a set of functions $u_1, u_2, \ldots, u_n$ satisfies (5), it follows then from (6) that they are harmonic. So we may say that (5) are *Cauchy-Riemann equations in n-dimensional space* and generate a *theory of functions* in this space reasonably *related to potential theory*. O. Taussky proved that this problem can only be solved in spaces of dimension $n=2^m$. In this paper the better result is established that *n must be 1, 2, 4, or 8* and moreover all Cauchy-Riemann systems (5) will be classified. In our discussion we admit that the x_h, u_k and the coefficients in (5), (6) are complex. We will use methods of representation theory introduced by Wigner and Eckmann[4] for the solution of problems of an analogous type, but we shall simplify matters a little by dealing with algebras instead of groups.

1. Introducing the n-row matrices

$$A_i = (a_{jk}^{i}), \; B_h = (b_{jk}^{h}), \quad i,h = 1,2, \ldots, n, \tag{7}$$

and the vectors

$$l = (l_1, l_2, \ldots, l_n), \qquad u = (u_1, u_2, \ldots, u_n), \tag{8}$$

relations (5), (6) can be written

$$l = \sum_{i=1}^{n} A_i \frac{\partial u}{\partial x_i}, \quad . \quad \Delta u = \sum_{h=1}^{n} B_h \frac{\partial l}{\partial x_h}. \tag{9}$$

Inserting the second equation into the first we get

$$\Delta u = \frac{\partial^2 u}{\partial x_1^2} + \frac{\partial^2 u}{\partial x_2^2} + \ldots + \frac{\partial^2 u}{\partial x_n^2} = \sum_{h,i} B_h A_i \frac{\partial^2 u}{\partial x_h \partial x_i}. \tag{10}$$

[1] This work was performed on a National Bureau of Standards contract with the University of California at Los Angeles, and was sponsored (in part) by the Office of Naval Research.

[2] University of California, Los Angeles, Cal., and Eidgenössische Technische Hochshcule, Zurich, Switzerland.

[3] O. Taussky, An algebraic property of Laplace's differential equation, Quart. J. Math. **10**, 99 (1939).

[4] B. Eckmann, Gruppentheoretischer Beweis des Satzes von Hurwitz-Radon über die Komposition quadratischer Formen, Comment Math. Helv. **15**, 358 (1942).

This identity holds for every vector u. Comparing coefficients it turns out that

$$B_iA_i=I, \quad B_hA_i+B_iA_h=0, \qquad i\neq h, \tag{11}$$

I being the n-row unit matrix. Thus the matrix B_i is the inverse of A_i, and our question is reduced to the problem of constructing n matrices A_i of n rows satisfying the relation

$$A_h^{-1}A_i+A_i^{-1}A_h=0, \qquad i\neq h, \tag{12}$$

2. In order to solve this problem we observe that (12) is invariant under a general equivalence transformation

$$A_i\to SA_iT, \qquad i=1,2,\ldots,n, \tag{13}$$

where S, T are two matrices with nonvanishing determinants. We do not distinguish between two Cauchy-Riemann systems (5) related to each other by such a transformation but call them essentially equal. Using this equivalence, we may transform by (13) one of our matrices—say A_n—into the unit matrix. For $h=n$ we have then

$$A_i+A_i^{-1}=0 \quad \text{or} \quad A_i^{-1}=-A_i \quad \text{or} \quad A_i^2=-I$$

and for $h=1, 2, \ldots, n-1$ this gives

$$A_hA_i+A_iA_h=0.$$

Thus we may restrict ourselves to the problem of constructing $(n-1)$ matrices $A_1, A_2, \ldots, A_{n-1}$ having the property

$$A_i^2=-I, \quad A_hA_i+A_iA_h=0, \qquad i\neq h. \tag{14}$$

If we have only these special systems under consideration the general equivalence transformation (13) will be restricted to a similarity transformation

$$A_i\to SA_iS^{-1}, \tag{15}$$

because the unit matrix must be left invariant. Matrices of the type (14) have been studied at first by Hurwitz [5] in the special case where the A_i are real and orthogonal.

3. From the basic relations (14) it follows that the 2^{n-1} matrices

$$\left.\begin{array}{l} I,\ A_1,\ A_2,\ \ldots,\ A_{n-1}, \\ A_1A_2,\ A_1A_3,\ \ldots,\ A_{n-2}A_{n-1}, \\ A_1A_2A_3,\ \ldots,\ A_{n-3}A_{n-2}A_{n-1}, \\ \ldots \\ A_1A_2,\ \ldots,\ A_{n-1}, \end{array}\right\} \tag{16}$$

this is to say, all products with increasing subscripts of the factors, form a matrix algebra of order 2^{n-1}. Indeed, the product of two matrices of the set (16) is (up to the sign) again a matrix of the set. Let us now consider the abstract associative algebra H of order 2^{n-1} over the complex field given by the basic elements

$$\left.\begin{array}{l} 1,\ e_1,\ e_2,\ \ldots,\ e_{n-1}, \\ e_1e_2,\ e_1e_3,\ \ldots,\ e_{n-2}e_{n-1}, \\ e_1e_2e_3,\ \ldots,\ e_{n-3}e_{n-2}e_{n-1}, \\ \ldots \\ e_1e_2,\ \ldots,\ e_{n-1}, \end{array}\right\} \tag{17}$$

and the multiplication rules

$$e_i^2=-1, \qquad e_he_i+e_ie_h=0, \qquad i\neq h. \tag{18}$$

Thus our problem is finally to construct a representation of the algebra H by n-row matrices. In order to do this we use the following well-known theorems of representation theory:

Theorem I. *There is—up to similarity transformation (15)—only a finite number m of irreducible representations, where m is the order of the center of the given algebra H. Any representation is the sum of irreducible representations.*

Theorem II. *Let f be the degree of a representation (number of rows of the representing matrices). Then the degrees $f_1, f_2, \ldots, f_m$ of the irreducible representations satisfy the relation*

$$f_1^2+f_2^2+\ \ldots\ +f_m^2=\text{order of } H=2^{n-1}.$$

4. Let us discuss first the case that the number n of Cauchy-Riemann eq (5) is even. Then the last element $(e_1e_2\ \ldots\ e_{n-1})$ of the sequence (17) commutes with $e_1, e_2, \ldots, e_{n-1}$ and is therefore a center element of the algebra H. It is not difficult to show that the elements 1 and $(e_1e_2\ \ldots\ e_{n-1})$ span the center of H, that is to say that the general center element is of the form $\alpha+\beta(e_1e_2\ \ldots\ e_{n-1})$, where α, β are complex numbers. The order of this center being $m=2$, we learn from theorem I, that our algebra H has exactly two irreducible representations, D_1 and D_2. They are related in the following way. If D_1 is given by

$$D_1: \qquad 1\to I, \qquad e_i\to E_i, \tag{19}$$

(E_i being the representing matrices) then D_2 is given by

$$D_2: \qquad 1\to I, \qquad e_i\to -E_i. \tag{20}$$

In order to prove this let us observe that if the E_i satisfy the basic relations (14)

$$E_i^2=-I, \qquad E_hE_i+E_iE_h=0,$$

[5] A. Hurwitz, Über die Komposition der quadratischen Formen, collected papers 2, 641 (1933).

the same is true for the matrices $(-E_i)$. Hence, if (19) is a representation, then (20) is another. Furthermore, if D_1 is irreducible, the same is true for D_2 and, finally, D_1, D_2 are not similar. Indeed, the center element $(e_1e_2 \ldots e_{n-1})$ is represented in D_1 by the matrix $E_1E_2 \ldots E_{n-1}$, which must be a multiple cI of the unit matrix, since it commutes with the whole irreducible set of representing matrices. In D_2 the representing matrix is

$$-E_1E_2 \ldots E_{n-1}=-cI.$$

But (cI) and $(-cI)$ are not similar because, certainly, $c\neq 0$. This finishes our proof.

This discussion shows, in particular, that D_1 and D_2 have the same degree f. From theorem II we have

$$2f^2=2^{n-1} \quad \text{and so} \quad f=2^{\frac{n-2}{2}}. \tag{21}$$

As stated in section 3, our basic problem is to find a representation D of the algebra H by n-row matrices. From theorem I it follows that D must be the sum of the representations D_1, D_2, each of them perhaps repeated several times. So the degree n of D is a multiple of f:

$$n=k\cdot 2^{\frac{n-2}{2}}. \tag{22}$$

But this is only possible for $n=2,4,8$, and the multiplicities k are 2, 2, 1, respectively. In the cases $n=2,4$ we have for D the three inequivalent possibilities

$$D_1+D_1, \qquad D_1+D_2, \qquad D_2+D_2 \tag{23}$$

and in the case $n=8$ the two possibilities D_1, D_2.

5. The case of odd n is rather trivial because the center of H in this case is formed only by the multiples of the unity element. So we have only one irreducible representation. Its degree f is given by

$$f^2=2^{n-1}, \qquad f=2^{\frac{n-1}{2}},$$

and the wanted representation D must be a multiple of this unique irreducible representation:

$$n=k\cdot 2^{\frac{n-1}{2}}.$$

This leads to $n=1$.

Collecting the results we get the theorem:

A system of n Cauchy-Riemann equations of the type (5), (6) is only possible for $n=1,2,4,8$. In the cases $n=2,4$, there are three inequivalent systems, in the case $n=8$, only two.

6. In this section we establish the Cauchy-Riemann systems explicitly and discuss especially the real ones.

(a) In the case $n=2$ the degree f of the irreducible representation D_1 is $f=1$ according to (21). So D_1, D_2 may be given by

$$D_1: \quad e_1\to i, \qquad D_2: e_1\to -i, \tag{24}$$

i being the imaginary unit. Our first possibility (23) $D=D_1+D_1$ is then

$$e_1\to\begin{pmatrix} i & 0\\ 0 & i\end{pmatrix}=A_1, \qquad A_2=I \tag{25}$$

and yields the Cauchy-Riemann system (5)

$$i\,\frac{\partial u_1}{\partial x_1}+\frac{\partial u_1}{\partial x_1}=0, \qquad i\,\frac{\partial u_2}{\partial x_1}+\frac{\partial u_2}{\partial x_2}=0 \tag{26}$$

consisting of two separate equations for u_1 and u_2. Hence, we may restrict ourselves to the single equation

$$i\,\frac{\partial u}{\partial x_1}+\frac{\partial u}{\partial x_2}=0, \tag{27}$$

which expresses the fact (if x_1, x_2 are real variables) that u is a complex analytic function of x_1-ix_2. By differentiation of (27) it follows of course $\Delta u=0$. The two other possibilities (23) may be established by changing i into $(-i)$ in one or both equations (26).

In order to find the real Cauchy-Riemann systems—that is to say real representations of H—we must form the sum of one of our irreducible representations and its complex conjugate representation. Taking into account that D_1 and D_2 are complex conjugates, we have finally only the unique real representation $D=D_1+D_2$ and only one real Cauchy-Riemann system, which is, of course, the system (1).

(b) For $n=4$ the representation D_1 may be given by the so-called Pauli-matrices

$$D_1: \quad e_1\to E_1=\begin{pmatrix} 0 & i\\ i & 0\end{pmatrix}, \quad e_2\to E_2=\begin{pmatrix} 0 & -1\\ 1 & 0\end{pmatrix},$$

$$e_3\to E_3=\begin{pmatrix} i & 0\\ 0 & -i\end{pmatrix} \tag{28}$$

with

$$e_1e_2e_3\to\begin{pmatrix} -1 & 0\\ 0 & -1\end{pmatrix}. \tag{29}$$

D_2 is obtained by changing the sign of those matrices The Cauchy-Riemann system corresponding to $D=D_1+D_1$ splits again into the equations

$$\left.\begin{aligned} i\,\frac{\partial u_2}{\partial x_1}-\frac{\partial u_2}{\partial x_2}+i\,\frac{\partial u_1}{\partial x_3}+\frac{\partial u_1}{\partial x_4}=0\\ i\,\frac{\partial u_1}{\partial x_1}+\frac{\partial u_1}{\partial x_2}-i\,\frac{\partial u_2}{\partial x_3}+\frac{\partial u_2}{\partial x_4}=0\end{aligned}\right\} \tag{30}$$

for u_1, u_2 alone and the same equations for u_3, u_4. In this case, however, D_1 and D_2 are *not* conjugate complex, but D_1 is similar to its own conjugate complex and the same is true for D_2. This follows from the fact that in D_1 the center-element $e_1e_2e_3$ is represented by a real matrix according to (29). So we have two nonequivalent real Cauchy-Riemann systems corresponding to the representations D_1+D_1 and D_2+D_2. They are R. Fueter's equations for

right and left regular functions of a quaternion variable, and they are closely related to Dirac's equations in quantum mechanics. The first system may be derived from our equations (30) in the following way. Let x_1, x_2, x_3, x_4 be real variables and u_1, u_2 complex functions:

$$u_1 = v_1 + iv_2, \qquad u_2 = v_3 + iv_4.$$

Splitting the eq (30) into their real and imaginary parts we get the four equations wanted for v_1, v_2, v_3, v_4. The second system follows in the same way if we replace (30) by the equations corresponding to $D_2 + D_3$.

(c) The case $n=8$ is entirely different from the previous cases, because we found in section 4 that the representation D solving our problem is either D_1 or D_2 and hence irreducible. Thus the Cauchy-Riemann systems of this case will not split into systems of fewer equations. We omit the computation of the matrices of D_1, which is closely related to the socalled Cayley numbers building a nonassociative algebra and mention only the result that those matrices may be constructed as real matrices. They yield two Cauchy-Riemann systems.

As a final result we have the following statement: *The only generalized real Cauchy-Riemann systems are* 1. *the classic system of two equations*; 2. *the two systems of Dirac-Fueter equations, each system having four equations*; *and* 3. *two systems of eight equations.*

Los Angeles, December 4, 1951.